5-2014

A Study in Conjugated Polymers: From Solution Properties of P3HT to Synthesis of Highly Functionalized Conjugated Polymers; Moving Toward Block Copolymers and Beyond

Justin Taylor Roop
University of Tennessee - Knoxville, jroop2@utk.edu

To the Graduate Council:

I am submitting herewith a dissertation written by Justin Taylor Roop entitled "A Study in Conjugated Polymers: From Solution Properties of P3HT to Synthesis of Highly Functionalized Conjugated Polymers; Moving Toward Block Copolymers and Beyond." I have examined the final electronic copy of this dissertation for form and content and recommend that it be accepted in partial fulfillment of the requirements for the degree of Doctor of Philosophy, with a major in Chemistry.

Jimmy W. Mays, Major Professor

We have read this dissertation and recommend its acceptance:

Gajanan S. Bhat, Brian K. Long, Sheng Dai

Accepted for the Council:

Carolyn R. Hodges

Vice Provost and Dean of the Graduate School

(Original signatures are on file with official student records.)

A Study in Conjugated Polymers: From Solution Properties of P3HT to Synthesis of Highly Functionalized Conjugated Polymers; Moving Toward Block Copolymers and Beyond

A Dissertation Presented for the
Doctor of Philosophy
Degree
The University of Tennessee, Knoxville

Justin Taylor Roop
May 2014

ACKNOWLEDGEMENTS

A project with the magnitude of the one contained within the covers of this dissertation could never be accomplished without the help of many people. Firstly, I want to give glory to my savior, Jesus Christ who equipped me to do the work put before me. Additionally, I want to thank my advisor, Professor Jimmy Mays and Dr. Kunlun Hong for their guidance and support throughout my graduate work. They have given of their time to share their knowledge and experience with me. I am indebted to them for this. Others I would like to thank include Dr. Xiang Yu, Dr. Xiaojun Wang, Andrew Goodwin, Dr. Vikram Srivastava, Chris Hurley, Sachin Bobade, Weiyu Wang, all other members of the Mays group past and present, Adam Imel, Dr. Craig Barnes, Dr. Richard Mayes, Dr. Michael Peretich, Dr. Josh Abbott, and Dr. Youjun He.

I also could not be here today without the love and support that has been unwavering from my beautiful wife, Tiffani. She has believed in me and encouraged me at all times. Additionally, my sons, Nathaniel and Samuel have provided more than enough incentive to keep pushing forward. Their love was the same when I came home from the lab whether the results that day had been favorable or discouraging. These three people are why I do what I do every day.

ABSTRACT

Conjugated polymers have been the focus of intense research for more than a decade now, and advances in this field are beginning to materialize in the production of high-efficiency opto-electronic materials that may led to the generation of energy without the need for fossil fuels. However, these current materials have not been shown to be capable of reaching efficiency levels high enough to be competitive with the silicon-based solar cells that are the standard today. We embarked on a journey in this work to help the next step in conjugated polymer research be attained. We have done just that through a fundamental study of dilution solution properties of these materials in addition to the synthetic pathway we have cleared so that highly functionalized conjugated polymers may be synthesized that will lead to block copolymers with tailored properties. These materials will revolutionize the field of organic photovoltaics and organic field transistors. The synthetic method for the generation of functionalized conjugated polymers described here represents an approach that can used to impart any number of functionalities onto the conjugated polymer chains which will lead directly to block copolymer systems. We have shown this ability through the synthesis of a diblock copolymer with promise of a miktoarm star block copolymer in this work. The versatility of the method developed

here allows for other combinations of polymers and molecular architectures to be attainable in like manner. This work serves to provide other means by which these useful polymers may reach their maximum potential.

TABLE OF CONTENTS

LIST OF TABLES

LIST OF FIGURES

List of Schemes

CHAPTER 1

INTRODUCTION

Abstract: Conjugated polymers have shown great promise in the field of organic electronic materials. Specifically, they have captured the attention of researchers due to their expected use in the production of light-weight solar cells that are more cost-efficient than the silicon-based solar cells that presently dominate the market. In this chapter, we introduce P3HT and the most common synthetic methods for its production. Additionally, we discuss structural parameters of the polymer that must be understood and controlled in order to reach maximum efficiencies. Finally, we introduce the research in this field that will be detailed throughout this dissertation.

Introduction to Conjugated Polymers

In the late 1970s, Shirakawa MacDiarmid, and Heeger made a discovery that would lead to their winning the Nobel Prize. They reported that a conjugated polymer, polyacetylene, was conductive in the oxidized state [1-3]. That single breakthrough has led to an abundance of research in this field involving many different π-conjugated polymers [4-19]. Such polymeric materials have also shown the ability to absorb and emit light leading to the expectation that their applications could be extended to many fields. In fact, it is estimated that the conductive polymers market may reach $1.6 billion in the US alone by 2017[20]. The impact such materials could have on commercial applications is massive and far-reaching. However, in the more than 35 years since Shirakawa, MacDiarmid, and Heeger published their ground-breaking work, conjugated polymers have failed to take over commercial optoelectronic applications.

A long period of this stagnation can be attributed to less-than-optimal synthetic procedures. For more than 20 years, researchers attempted to synthesize conjugated polymers via transition-metal-catalyzed step-growth methods that provided very little control over the connectivity of the repeat units of the polymer chains. This approach led

to polymers with very poor performance. All of this changed, however, in 2004 when McCullough [21, 22] and Yokozawa [23] independently developed a "living" chain-growth approach to the synthesis of well-defined poly(3-hexylthiophene). This approach would come to be known as catalyst-transfer polycondensation (CTP) and has been shown to be an effective synthetic route for other conjugated polymers as well. This approach allows for the control of molecular weight and produces polymeric materials with a high degree of regioregularity and narrow polydispersities. All of these factors are important for device applications and will be discussed further below.

Once this new and improved synthetic approach was established, the hope for conjugated polymers to reach their potential in the field of optoelectronics again seemed very real. Such potential device applications include sensors, light emitting diodes, electrochromic devices, field effect transistors, and polymer solar cells [24-26]. One polymer in particular, poly(3-hexylthiophene) (P3HT), has garnered a large portion of the attention directed toward development of organic solar cells to replace their inorganic counterparts that are the current standard. This attention has been based on P3HT's high hole mobility, environmental stability, chemical processability, and relatively efficient light absorption in the visible range of the solar spectrum [27]. The hole mobility, as well as other favorable properties of these materials,

originates from and are influenced by the π-stacking, regioregularity of the polymer chain, molecular weight, and polydispersity of the sample [28-31]. However, as a p-type semiconductor, P3HT cannot reach performance levels suitable for applications alone and needs to be a part of copolymer or polymer blend systems. It is for these reasons that the major focus of this dissertation will be fundamental understanding of block copolymer systems incorporating P3HT.

Introduction to the Role of Conjugated Polymers in Organic Solar Cells

Conjugated polymers make up the electron donor portion of the active layer of an organic solar cell. The electron acceptor portion of the active layer is typically a fullerene-based material. Together, they comprise the portion of the solar cell where the exciton is generated and separated so that the electron and hole can travel to their respective electrodes. Figure 1.1 was taken from Scharber and Sariciftci's recent review article and shows two arrangements for polymer-based solar cells [6]. Figure 1.1a is a representation of a standard polymer solar cell arrangement. In this setup, the substrate is coated with a transparent anodic material such as indium tin oxide (ITO) which provides a bridge between the anode and active layer. On top of the ITO layer is a hole

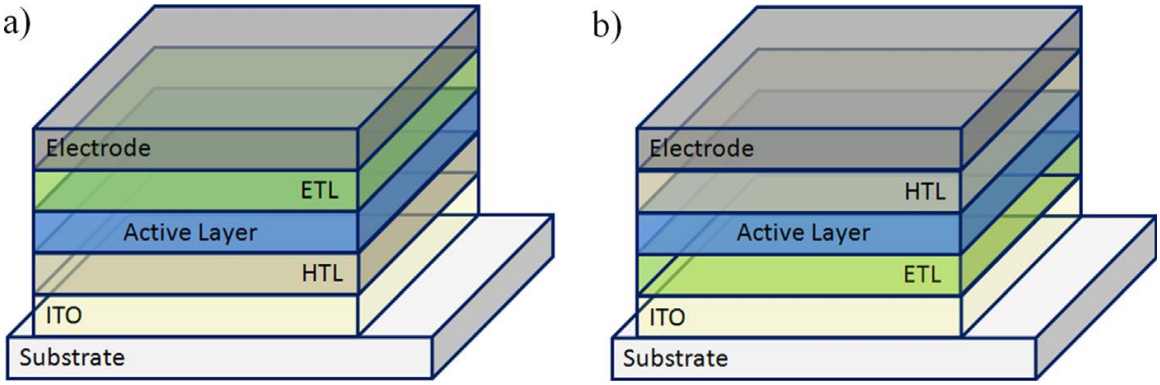

Figure 1.1: Two possible designs for polymer solar cells. a) is the standard design and b) is the inverted design [6]

transport layer (HTL), typically comprised of poly(3,4-ethylenedioxythiophene) and poly(styrenesulfonate) (PEDOT:PSS). Next comes the active layer with the makeup as mentioned above. On top of the active layer is the electron transport layer (ETL) which is typically made up of zinc oxide or titanium oxide. Finally, on top is the cathode which is made of calcium, barium, or aluminum.

In the inverted architecture, the substrate is coated with a cathode material followed by the ITO, ETL and the active layer. On top of the active layer is the HTL and anode. The anode is typically comprised of silicon or gold, and the other layers have the same composition in both designs. The inverted architecture possesses an advantage over the standard, it is more stable in ambient conditions due to the absence of a low work function electrode.

Introduction to the Synthetic Methods Used to Produce P3HT in this Research

Grignard Metathesis (GRIM) Polymerization – Introduction to Two Types

Developed independently and simultaneously, McCullough and Yokozawa's GRIM polymerization revolutionized the field of conjugated

polymer synthesis [21, 32]. In contrast to previous methods, GRIM provides a quasi-living polymerization that enables the synthesis of well-defined polythiophenes with controlled molecular weights and narrow polydispersities[33]. The quasi-living title has been given to synthesis of P3HT due to the ability to predict and control molecular weight through adjustment of the monomer to catalyst ratio. Additionally, it has been shown that chain extension of P3HT or block copolymer synthesis is possible by sequential addition of monomers [33]. Narrow polydispersities can be achieved by limiting polymerization time. It has been observed in the work reported herein that polymerization times beyond 15 minutes does not significantly increase the size of the polymer chains but does broaden the PDI of the material. The quasi-living nature of the polymerization procedure has been further demonstrated by the ability to sequentially add conjugated monomers in order to produce fully-conjugated block copolymers [34, 35]. The two types of GRIM as well as advantages/disadvantages of each are discussed below.

In McCullough's version of the GRIM reaction 2,5-dibromothiophene is refluxed in THF with a Grignard reagent leading to exchange between the Grignard and at least one of the bromines on the thiophene ring. It is desirable that only one bromine be exchanged during this step, and in order to produce a high degree of regioregularity, the exchange reaction should take place at the 5-position. Figure 1.2

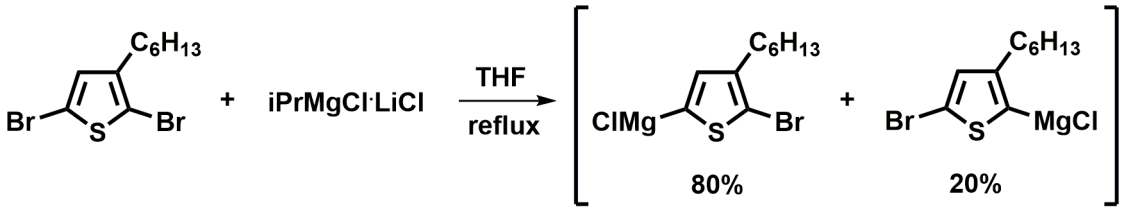

Figure 1.2: Reaction schematic depicting the Grignard exchange reaction with 2,5-dibromo-3-hexylthiophene that leads to an isomeric mixture of the active 3-hexylthiophene monomer

shows the Grignard exchange reaction with 2,5-dibromo-3-hexylthiophene leading to the typical isomeric mixture of active thiophene monomers. The 5-position is the favored location for the exchange reaction to occur, and over-conversion of the monomer by exchange occurring at both the 5- and 2-positions can be limited by controlling the stoichiometric ratio of thiophene to Grignard reagent. The location of Grignard exchange reaction in McCullough's method of GRIM using a 3-substituted-2,5-dibromothiophene is driven mainly by sterics. The substituent at the 3-position limits access of the Grignard reagent to the bromine located at the 2-position of the thiophene ring. However, the bromine located at the 5-position of the thiophene ring is not hindered and is therefore the favored site for the Grignard exchange reaction to occur. In order to further exploit this phenomenon, a Grignard reagent with a bulky R-group, such as ^{t}BuMgCl, is typically used. With this approach, an isomeric mixture of (2-bromo-3-hexylthiophen-5-yl)magnesium bromide and (5-bromo-3-hexylthiophen-2-yl)magnesium brominde is typically obtained in a ratio of about 4 to 1 respectively. Figure 1.3 displays the three types of linkages that can occur between two 3-hexylthiophene monomers during propagation of the polymer chain. The presence of the undesired isomer can lead to regio-defects in the polymer chain as its reaction with a propagating HT-P3HT chain results in a head-head linkage. Such regio-defects can lead to a decrease

in the performance of device applications. However, the undesired isomer typically does not participate in the propagation of the polymer chain, again due to sterics, and is simply removed with the other unreacted monomers during the post-polymerization purification process. This behavior is evidenced by the fact that P3HT samples synthesized using McCullough's version of the GRIM reaction display a degree of regioregularity comparable to P3HT samples produced using other synthetic approaches which do not contend with isomeric mixtures of activated Grignard monomers.

One such alternate approach is the GRIM polymerization method developed by Tsutomu Yokozawa's group at Kanagawa University about the same time as McCullough's group was developing their method [23]. The initiation, propagation, and termination steps are the same for both McCullough's and Yokozawa's versions of the GRIM polymerization. The difference between the two approaches lies in the monomer that is used. Where McCullough's method is carried out using 2,5-dibromo-3-alkylthiophene, Yokozawa's method requires the use of 2-bromo-3-alkyl-5-iodothiophene. The advantage this approach possesses over McCullough's method is that the increased reactivity of the iodine, as compared to the bromine, on the thiophene ring effectively eliminates the isomeric mixture after Grignard exchange. This is possible because the Grignard exchange reaction with the iodine on the thiophene ring can be

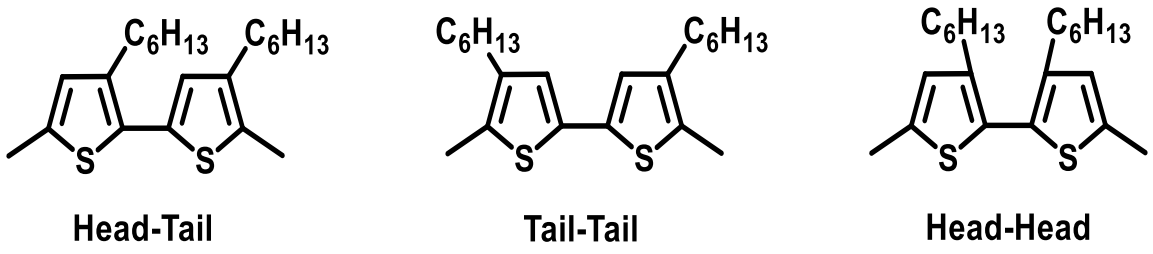

Figure 1.3: The three possible linkages for two 3-hexylthiophene monomers. Head-Tail is considered regioregular with the other two linkages considered to be defects.

carried out at room temperature or even at temperatures as low as 0ºC. In order for bromine on the thiophene ring to undergo the Grignard exchange reaction in a timely manner energy must be added to the system. This energy is added via reflux conditions. Therefore, when 2-bromo-3-alkyl-5-iodothiophene is reacted with a Grignard reagent such as ispropylmagnesium chloride at room temperature or below, the exchange reaction will occur nearly exclusively at the desired 5-position. Not only does this change in monomer of Yokozawa's method result in a much more desirable isomeric mixture of active monomer, it also reduces the energy required to synthesize the polythiophene by eliminating the need to reflux the solvent. This savings in energy would serve to increase the appeal of this method from an industrial vantage point.

Yokozawa's method, however, is not without its drawbacks. Although there are advantages to using 2-bromo-3-alkyl-5-iodothiophene in terms of the polymerization process, this monomer is inferior in some respects to its 2,5-dibromo-3-alyklthiophene counterpart. The synthesis of 2,5-dibromo-3-alkylthiophene is achieved by reacting 3-alkylthiophene with 2 equivalents of N-bromosuccinimide (NBS) as described in Scheme 1.1. The reaction is quenched with water and sodium thiosulfate before being extracted with diethyl ether and dried over magnesium sulfate overnight. The organic layer of the extraction may contain a mixture of the following three species: unreacted 3-alkylthiophene, 2-bromo-3-

alkylthiophene, and the desired 2,5-dibromo-3-alkylthiopene. After solvent is removed *in vacuo*, the desired product can be easily isolated via distillation under reduced pressure. This distillation is very straightforward due to the large difference in molar mass of each of the species in the mixture which results in very different boiling points for the different thiophenes. Once purified, the monomer can be stored at -23°C for an indefinite amount of time. A portion of a 100 gram bottle of 2,5-dibromo-3-hexylthiophene that was received in March 2011 remains stable at the time of this writing. It has been stored in the freezer the entire time, and GC/MS analysis shows it to still be 100 percent pure.

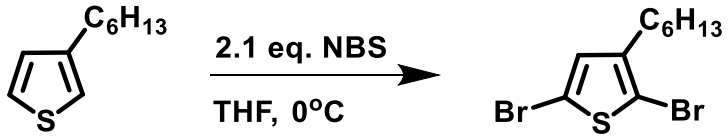

Scheme 1.1: Synthetic procedure for the synthesis of 2,5-dibromo-3-hexylthiophene from 3-hexylthiophene

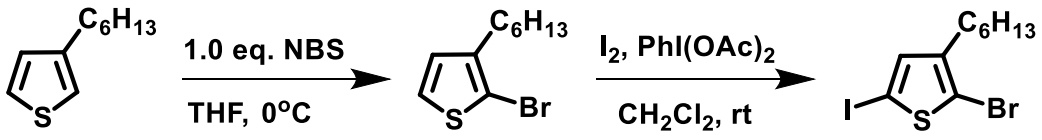

Scheme 1.2: Synthetic procedure for the synthesis of 2-bromo-3-hexyl-5-iodothiophene from 3-hexylthiophene

Conversely, 2-bromo-3-hexyl-5-iodothiophene requires more steps to synthesize and purify. Starting again from 3-alkylthiophene, a single equivalent of NBS serves to brominate the 2-position. Purification of 2-bromo-3-alkylthioiphene is identical to the purification process described above for 2,5-dibromo-3-alkylthiophene. Iodation of the 5-position is carried out by reacting 2-bromo-3-alkylthiophene with iodobenzene diacetate and iodine. This reaction schematic can be seen in Scheme 1.2. After reaction, the solution is again quenched, extracted, and dried. Purification of 2-bromo-3-alkyl-5-iodothiophene requires column chromatography using a silica gel column and hexanes as eluent. These extra steps in the synthetic procedure add nearly two days to the time required to prepare thiophene monomer for GRIM polymerization. In addition, 2-bromo-3-alkyl-5-iodothiophene is not very stable and cannot be stored for more than a month before degradation begins to affect the integrity of the monomer.

Over the course of all the research described within this dissertation, both monomers were synthesized and polymerized at some point. While they each have their advantages, McCullough's method was chosen over Yokozawa's method to synthesize a portion of the polymers for the solution properties study described below. This decision was based primarily on the stability of the monomer which allowed polymerizations to be performed over a period of time without the need to

spend days repeatedly synthesizing and purifying small batches of monomer.

Introduction to Nickel-Catalyzed Dehydrobrominative Polycondensation (Mori's Method)

More recently, Atsunori Mori's group has developed a more atom-efficient method for the synthesis of well-defined P3HT [36, 37]. This approach allows for all of the same controls over molecular weight and regioregularity as the GRIM methods described above, but it starts with a thiophene monomer which possesses only a single bromine atom. They have shown that 2-bromo-3-alkylthiophene can be converted to the Grignard-possessing active thiophene monomer in a single step via reaction with 2,2,6,6-tetramethylpiperidinylmagnesium chloride lithium chloride complex solution (TMPMgCl·LiCl) [36, 37]. Using only the solvent from the Grignard complex, this reaction occurs in very high yield at room temperature. Once the TMPMgCl·LiCl has reacted, solvent and catalyst can be added to initiate polymerization. The polymerization proceeds in the same manner as the GRIM counterparts described above.

Mori's synthetic approach to the polymerization of thiophenes is very attractive because of its increased atomic efficiency compared to the GRIM methods. 2,5-dibromo-3-hexylthiophene and 2-bromo-3-hexyl-5-iodothiophene have molar masses of 326 and 373 g/mol respectively. The molar mass for the repeat unit of P3HT is 166 g/mol. In other words, 160 or 208 grams of starting material is being wasted for every mole of monomer that is converted to polymer. If these materials are going to be attractive to industry, all waste must be limited. By using Mori's method, the starting molar mass of the monomer is reduced to 247 g/mol resulting in only 81 grams of starting material wasted for every mole of monomer converted to polymer. This approach reduces waste from monomer by half making it more appealing on an industrial scale. In addition, 2-bromo-3-hexylthiophene is a very stable compound, and the Grignard is added only after the TMP extracts a proton leading to exclusive exchange at the 5-position. It could be viewed as if the stability advantage of McCullough's GRIM monomer is combined with the regioregularity advantage of Yokozawa's GRIM polymerization in a single synthetic approach.

Parameters of P3HT That Must be Considered

As is the case with many polymeric materials, there are parameters of P3HT that must be considered and controlled in order to optimize

these materials for device applications. Of the most importance for P3HT and block copolymers incorporating P3HT are molecular weight and regioregularity. These parameters influence charge transport, crystallization behavior, and domain size within the materials. The role each of these parameters play in this behavior is detailed below.

Effect of Molecular Weight on Properties of P3HT

The molecular weight of P3HT plays key roles in the behavior and performance of the material in applications involving homopolymer or block copolymer systems. The influence molecular weight of P3HT has on device performance, surface morphology, and charge transport has been extensively studied [38-54]. However, despite the effort put forth, there is not complete agreement with the findings. Trends certainly exist in the data across the different studies, but the points at which those trends break down varies. One possible source for this discrepancy could be that the molecular weight of P3HT is not being accurately characterized. An entire chapter of this dissertation will be devoted to proper molecular weight characterization of P3HT samples because it is our belief that such a development would positively impact researchers understanding of how to optimize these materials for device applications.

P3HT homopolymers find application in polymer blend systems for bulk heterojunction solar cells. Many times these blends contain P3HT, a p-type semiconductor, with an n-type semiconducting material such as phenyl-C61-butyric methyl ester (PCBM) and form the active layer of bulk heterojunction (BHJ) photovoltaic cells. This active layer phase separates, and the most desired morphology is one that is bicontinuous with domains in the nano-sized range. A domain size of 10 nm is optimum for charge separation with minimization of recombination [42, 51]. The molecular weight of P3HT can have effect on the performance of these devices in more than one way. As is to be expected, the molecular weight of P3HT has an impact on the morphology of the active layer. One way in which this happens is a result of solubility [55]. The solubility of P3HT decreases as molecular weight increases. This phenomenon has been observed in every solvent that this researcher has used for this polymer. The change in solubility as molecular weight changes can affect the BHJ morphology [45]. In addition, molecular weight affects crystallization behavior which can greatly influence morphology [46]. At higher molecular weights, the crystallization behavior of P3HT increases as a result of increased π→π interactions such that it can strongly dictate the final morphology of the material or active layer. This can lead to loss of bicontinuous morphology as higher molecular weight P3HT

tends to form nanofibers[54]. Such a loss of control over morphology can adversely affect device performance [28, 39, 40, 43, 45, 51, 52].

It should not be inferred, however that the answer to increasing device performance lies in using low molecular weight P3HT. Indeed there are tradeoffs when using high, medium, or low molecular weight P3HT for BHJ solar cells. Higher molecular weight P3HT can lead to problems as discussed above, but low molecular weight P3HT can have detrimental effects on ordering in these systems [47]. Turner has pointed out that larger domains of P3HT with low disorder are advantageous for device performance [49]. This fact would seem to favor higher molecular weight P3HT. Lower molecular weight P3HT also exhibits worse charge transport than its higher molecular weight counterparts. It is thought that this is a result of the fact that intrachain transport is typically much faster than interchain charge hopping. Therefore, it is better for the charge to have a long chain on which to travel and be required to hop fewer times in order to reach the electrode [43]. However, low molecular weight P3HT leads to higher rates of diffusion of phenyl-C61-butyric acid methyl ester (PCBM) during annealing [45] which allows for better formation of donor and acceptor domains. Figure 1.4 depicts the structure of PCBM. It is apparent that there is no single, concise answer to this dilemma.

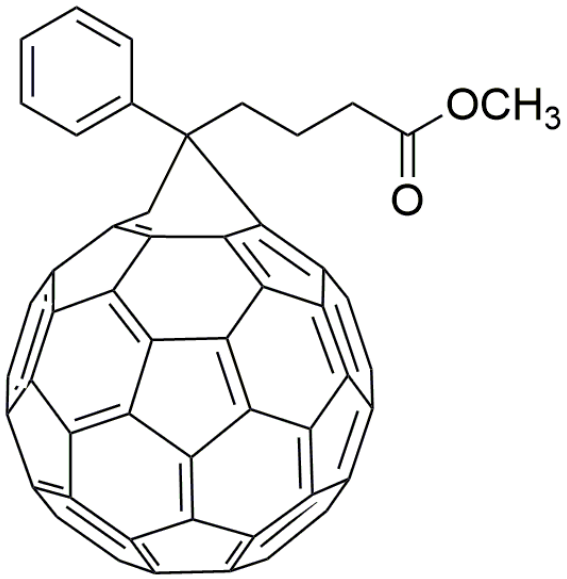

Figure 1.4: Structure of PCBM

Many of the same concerns about optimum molecular weight of P3HT in device applications exist in block copolymer systems as well. For BHJ solar cells P3HT is typically coupled with some fullerene-decorated copolymer to make up the active layer. This approach does not affect molecular weight influence on charge transport, but it can alter morphological effects due to the tethering together of the two components. With the fullerene covalently attached to the P3HT, diffusion of the acceptor material during annealing is no longer a concern. However, higher molecular weight P3HT can still lead to loss of morphological control by the increase in crystallization behavior. In two separate studies, Iovu et al. [56] and Dai et al. [54] looked at block copolymer systems involving P3HT and polystyrene (PS) and poly(2-vinylpiridine) (P2VP) respectively. In each case, the investigators observed nanofiber morphologies at mole percents of P3HT at or above 50%. The P3HT used by Dai was 7 kdal/mol while the P3HT used by Iovu was more than 17 kdal/mol. Iovu observed nanofiber morphology at a 50 mole percent P3HT while Dai did not observe the same morphology until 60 mole percent P3HT. This would seem to indicate that the increased crystallization behavior associated with the higher molecular weight P3HT may be responsible for the morphological differences observed.

The influence that molecular weight of P3HT has on the performance of the material in device applications makes it one of the most important factors to be considered when developing new P3HT-based polymer systems. However, accurate determination of absolute molecular weight remains a challenge. Many researchers still report molecular weight of P3HT relative to PS standards using conventional calibration of SEC despite the documented shortcomings of this approach [57]. This may well be responsible for the inconsistency of reported data. Our approach to remedying this problem will be discussed in detail in the next chapter of this dissertation. The ability to consistently and accurately determine molecular weight of P3HT will provide the ability to better understand the extent of influence molecular weight has on device performance of P3HT in BHJ solar cells.

Effect of Regioregularity on Properties of P3HT

Like molecular weight, effects of regioregularity of P3HT on its optoelectronic properties have received a lot of attention from researchers seeking to optimize its use in organic photovoltaic applications [56, 58-72]. Figure 1 shows the possible linkages that can occur as thiophene monomers are added to the propagating chain. It is clear to see that

such differences in linkages can influence the way these chain pack. The net effects that stem from the different packing scenarios have strong impacts on how these materials behave in BHJ active layers with PCBM. While other polymer blends have been looked at, P3HT:PCBM is by far the most extensively studied and believed to have the greatest opportunity for advancing the field of study.

P3HT, in its pristine form, shows increases in crystallinity, conjugation length, and charge transport as regioregularity is increased [58, 69, 71]. These observations are to be expected as regiodefects can certainly interrupt and hinder chains from coming close enough to each other for strong π→π interactions to occur. It is the π→π stacking that leads to P3HT's high level of crystallinity, and it is this extended conjugation along the polymer backbones that gives P3HT its high mobility. Knowing the increases that would accompany higher degrees of regioregularity drove researchers to develop synthetic methods that would generate P3HT with the highest possible regioregularity [21, 36, 53, 56]. As different properties were studied in regard to regioregularity,

it was observed that specific capacitance and stability of P3HT over repeated charge-discharge cycles were positively affected by increasing regioregularity [67]. Poelking [71] observed a dramatic decrease in charge carrier mobility when regioregularity was reduced from 100% to

90%. In a different study, Aiyar [61] showed that a change in regioregularity as small as 4% had striking influence on both electronic and morphological properties. In addition, Chen [58] showed the strong effects regioregularity has on conjugation length of P3HT. All of this data would seem to indicate that the desired form of P3HT for electronic applications would be completely regioregular. When these polymers are taken from a pristine state and introduced into polymer blends for application, however, issues with very high regioregularity are observed.

It was previously discussed that molecular weight of P3HT plays a large role in its self-assembly behavior in polymer blends and block copolymer systems. Likewise, regioregularity has influence on this behavior and must therefore be considered when optimizing P3HT for BHJ solar cells. In addition to its decreased electronic properties, P3HT with low regioregularity can be detrimental to morphology. As Tsoi [73] has pointed out, using P3HT with low regioregularity in such polymer blends results in a more disordered blend that does not exhibit enough phase separation and therefore a bicontinuity of the phases is not present. Lack of a bicontinuous phases results in the inability for proper charge transport and greatly reduces device performance. On the other end of the spectrum, Li [74] and Thompson [75] have shown that there exists problems when the regioregularity of P3HT is very high. What they have observed is that very high regioregular P3HT causes large

crystalline domains of P3HT to form. These domains are so large that they exceed the exciton diffusion length and result in exciton relaxation and recombination losses. This has great negative effects on the performance of these materials in devices. There must exist a level of regioregularity at which the problems associated with low and high regioregularity are minimized simultaneously. Woo [68] and Sivula [59] have proposed that a regioregularity between 86-93% provides that balance. In addition, they suggest a polydispersity between 2 and 3 would disrupt crystallinity in the P3HT enough to allow for regioregularities of such high levels.

These morphological effects of regioregularity, though they have great impacts on device performance, are less about the polymer blend and more about the microstructure of the polymer chain. Adachi [69] has shown that regioregularity of side chains on P3HT govern the morphology even at the single chain level. This indicates that the regioregularity of P3HT, like molecular weight, determines the optimum ratio between the components in P3HT:PCBM blends. Urien [72] showed that for very high regioregular P3HT, a P3HT:PCBM weight ratio of 1:0.8 achieved the best performance. However, when low regioregular P3HT was used, the ratio for best performance changed to 1:3. This vast change indicates just how important regioregularity of P3HT is for device applications.

As is the case for determining the optimal molecular weight of P3HT needed for applications, finding the most favorable degree of regioregularity requires optimization of different aspects that are seemingly contradictory at times. The electronic properties of P3HT improve as regioregularity is increased. For reasons previously discussed, this is an observation that is consistent with expectations for these materials as the conjugation length and charge mobility depend on regioregular chains to form an extended network on which to transport the charges. If this were the only consideration, P3HT would be taking over the organic electronic markets today. However, when placed in a blend with PCBM, the higher regioregularity can cause problems. Just as higher molecular weight P3HT can dominate morphology in these blends, high regioregularity can do the same thing leading to domains that greatly exceed the 10 nm domains that lead to the highest efficiencies. Woo and Sivula's approaches of using higher polydisperse P3HT to offset the increased crystallization behavior associated with higher regioregularity may be the key finding proper balance in these systems. The goal of researchers moving forward in this area must be to find the aspects of these systems which can be altered in order to allow electronic properties to be maximized without the morphological drawbacks hindering devices. Efficiency levels in BHJ solar cells will require no less to achieve competitiveness with the existing silicon-based

inorganic solar cells. However, with so many moving parts, such a balance will not be an easy one to achieve.

Introduction to the Research Contained within this Dissertation

Over the course of the next few chapters of this dissertation, using the fundamental understandings and following the lead of some of the examples discussed above, the doctoral research that has been conducted over the past five years will be presented. There are three distinct portions of this conjugated polymer project which tie together to form a cohesive and logical path toward better understanding and improving these conducting polymers for optoelectronic applications. We began by studying the dilute solution properties of P3HT homopolymers in an attempt to develop a clear method for accurate determination of absolute molecular weight. As discussed previously, the molecular weight of P3HT plays a large role in the properties of the polymer as well as blends and copolymers of which it may be a part. We also synthesized highly functionalized P3HT and used the functionality to add other polymers and form miktoarm stars. The morphology of these miktoarm

stars were studied and will be presented as well. Finally, we turned our attention to other conjugated polymers such as polyfuran and polyfluorene. We successfully synthesized these polymers with a high degree of functionality which will open the door for block copolymers to be synthesized from these conjugated polymers as well.

CHAPTER 2

DILUTE SOLUTION PROPERTIES STUDY OF POLY(3-HEXYLTHIOPHENE)

Abstract: P3HT has shown to be a difficult polymer for proper molecular weight characterization. Conventional calibration of size-exclusion chromatography (SEC) has been shown to overestimate the molecular weight of this polymer, presumably due to its extended chain conformation. The NMR signals used to calculate the degree of polymerization (DP) are sometimes difficult to baseline resolve resulting in inaccurate integration. In this portion of this work, we endeavored to study the solution properties of P3HT in an effort to apply a universal calibration of SEC to this polymer so that accurate molecular weight measurements might be made in a timely and straightforward manner. In order to do this, we measured the refractive index increment in two different solvents, determined the Mark-Houwink constants for P3HT in THF, and performed triple-detection SEC. We compared the results given by SEC using light scattering to those given by universal calibration and determined that universal calibration fails to provide accurate molecular weight characterization of P3HT.

Introduction

An understanding of how a polymer behaves in solution is of great importance when seeking to develop materials that must be processed for device applications. One of the appealing aspects of P3HT is that it can be processed in common solvents such as THF and chloroform. However, in order to produce materials suitable for their intended use, we must have knowledge of the polymer and its behavior during that processing. The study of dilute solution properties of polymers provides quantitative insight regarding the size, shape, and structure of the polymer chain. Additionally, polymer-polymer and polymer-solvent interactions can be explored during such studies. An understanding of these relationships enables proper selection of the most favorable solvent for a given process with directed properties. Since the time that conjugated polymers, specifically P3HT, began to gain widespread attention from the research community, studies have been performed to attempt to understand the different properties of polythiophenes and other conjugated polymers in an effort to enhance the favorable electronic properties of these materials [55, 76-87]. In this study, we endeavored to produce a detailed description of P3HT from a structural standpoint as well as speak to its behavior in THF. Our intent was to

gain a fundamental understanding of this polymer in solution and to also employ universal calibration of SEC for P3HT to develop a method for the straightforward and accurate determination of absolute molecular weight for these materials. Inaccurate assignments of molecular weights to P3HT samples have led to inconsistent reports of properties when molecular weights are said to be similar. A direct method for accurate molecular weight determination of P3HT would allow for comparisons of measured properties to be normalized.

The Mark-Houwink parameters were determined for P3HT in THF from viscosity data collected via triple detection SEC, and we measured the refractive index increment as well as multi-angle light scattering for a series of P3HT samples with a range of molecular weights. The series of polymers were synthesized using two distinct procedures to compare the materials that result from each method. The two methods used were GRIM as developed by McCullough [21] and dehydrobrominative polycondensation as developed by Mori [36]. To our knowledge, this is the first study that has attempted to compare materials synthesized using these two synthetic approaches. Some attention was also given to P3HT in chloroform due to the regularity with which chloroform is used as a solvent for this polymer.

Aspects of P3HT Studied Herein

Introduction to Mark-Houwink Parameters for P3HT

The Mark-Houwink equation listed below (Equation 1) defines the relationship between intrinsic viscosity and molecular weight of a polymer sample. It states that the intrinsic viscosity of a polymer solution is equal to some parameter *K* times molecular weight raised to some power *a*. *K* is simply a coefficient that scales molecular weight with intrinsic viscosity. The *a* term, however, provides insight into the rigidity of the polymer in solution as well as theta conditions for the polymer/solvent system. This relationship is specific to individual polymer/solvent systems, and can be a powerful tool in the proper determination of either molecular weight of intrinsic viscosity when only one of the two parameters can be adequately measured.

$$[\eta] = KM^a \qquad \textbf{Equation 2.1}$$

$$K_1 M_1^{1+a_1} = K_2 M_2^{1+a_2} \qquad \textbf{Equation 2.2}$$

Also, when these parameters are known, the molecular weights of two different polymers in the same solvent can be related using Equation 2.

Application of the Mark-Houwink relationship is advantageous for systems involving P3HT because of the shortcomings of conventional SEC analysis to properly assign an accurate molecular weight due to the extended chain conformation that results from the polymer's semi-rigid backbone. However, viscosity measurements do not suffer from this issue and can be accurately measured for P3HT.

Mark-Houwink parameters for P3HT have been previously reported by Holdcroft [88] as well as Heffner and Pearson [89]. Both of these reports came out around the same time in the early 1990s, but there was not complete agreement in their findings. Holdcroft reported values for K and a of 2.28E-03 cm^3/g and 0.96, respectively. Heffner and Pearson, on the other hand reported values for K and a of 1.2E-03 cm^3/g and 0.58, respectively. The differences in the a term between these two studies is significant as this parameter can be indicative of both theta solvent conditions as well as rigidity of the polymer chain. A value of a equal to 0.5 indicates theta solvent conditions. Also, the a parameter for most flexible polymers is between 0.5 and 0.8. A value of a equal to or greater than 0.8 is consistent for semi-flexible polymers, and a value of a equal to 2 indicates a completely rigid rod [90].

It can be seen, then, that the implications of the values reported by Holdcroft and Heffner are very different. According to Heffner and

Pearson, P3HT behaves as a flexible polymer in THF, Holdcroft's findings indicate that P3HT is only semi-flexible in THF which is more consistent with the prevailing thought that conjugation along the backbone limits flexibility. The nature of the chain has far-reaching implications beyond just dilute solution properties and so proper characterization is essential. It is for this reason that we endeavored to find these parameters for P3HT in THF. It is our belief that our study will be an improvement on the previous work discussed above because our synthetic procedures and instrumentation for characterizing samples have been greatly improved over the more than 20 years since this work was originally performed.

Introduction to Refractive Index Increment (dn/dc) for P3HT

In order to obtain quality light scattering data the dn/dc value must be known for the polymer/solvent system. Dn/dc simply identifies the change in refractive index as a function of concentration. A typical dn/dc plot versus molecular weight shows a slight dependence of dn/dc on molecular weight at the low molecular weight end. At some point, the slope flattens out and dn/dc remains essentially constant going to higher and higher molecular weights. Many times this flattening out occurs at such low molecular weights that dn/dc may be essentially considered a

constant for most samples. In the case of P3HT, dn/dc values have been reported with a good amount of consistency between studies [77, 88, 89]. Nonetheless, the dn/dc of every sample was measured as a part of this solution properties study to ensure the highest degree of confidence in the light scattering data that is reported. Accurate measurement of dn/dc is essential as Mw determined by light scattering depends on $(dn/dc)^2$. Therefore, any error in dn/dc values results in a significant error in molar mass determination.

Introduction to Universal Calibration of Size-Exclusion Chromatography (SEC)

SEC has proven to be a very powerful tool for polymer chemists in the determination of the molecular weights and polydispersities of polymeric materials. In the case of flexible polymers, conventional calibration using narrow polystyrene (PS) standards provides accurate characterization of molecular weight and polydispersity of a sample in a concise manner. Conventional calibration is based on a relationship between elution volume and molecular weight. It is accurate because flexible polymers tend to coil up in very similar manners causing samples of two different flexible polymers to display hydrodynamic volumes that

are quite similar to each other. Conventional calibration of SEC becomes less accurate, however, as the polymer sample becomes less and less like the polymer used to generate the calibration curve. For example, a polymer that is less flexible than PS may not coil as much. Even if the two polymers are the same molecular weight, the more rigid polymer will yield a higher molecular weight value when analyzed relative to PS via conventional calibration due to the increased hydrodynamic volume.

P3HT, with its semi-flexible, conjugated backbone, is different enough from PS to render conventional calibration of SEC flawed at best. As McCullough originally pointed out, conventional calibration of SEC overestimates the molecular weight of P3HT samples by a factor of 1.6-2.0 [57]. This observation comes from comparing molecular weights and molecular weight distributions as reported by SEC to the same parameters determined using MALDI-TOF and NMR spectroscopies. With such a large discrepancy associated with using conventional calibration for P3HT, a more accurate method for determining molecular weight and molecular weight distribution of this material is desirable.

P3HT is not the first polymeric material for which conventional calibration has failed to accurately determine molecular weight and polydispersity. When this occurs, universal calibration can be used to properly determine molecular weight and molecular weight distribution.

Universal calibration, developed by in the 1960s by Benoit et al., and shown in Figure 2.1, has been shown to be an accurate method for determination of these molecular weight parameters for many different types of linear polymers as well as branched architectures [91].

Rather than assuming that elution volume is directly related to the molecular weight of a polymer sample, universal calibration considers that elution volume is equal to the product of molecular weight and intrinsic viscosity. In other words, elution volume is equal to the product of intrinsic viscosity and molecular weight. In order to use this approach Mark-Houwink parameters must be known for both the standards and the analyte. When these parameters are known, rearrangement and substitution of the Mark-Houwink equation provides a direct method to calculate the molecular weight of a polymer sample as shown in Equations 3-5 where A is the analyte and S is the standard.

$$[\eta]M_A = [\eta]M_S \qquad \textbf{Equation 2.3}$$

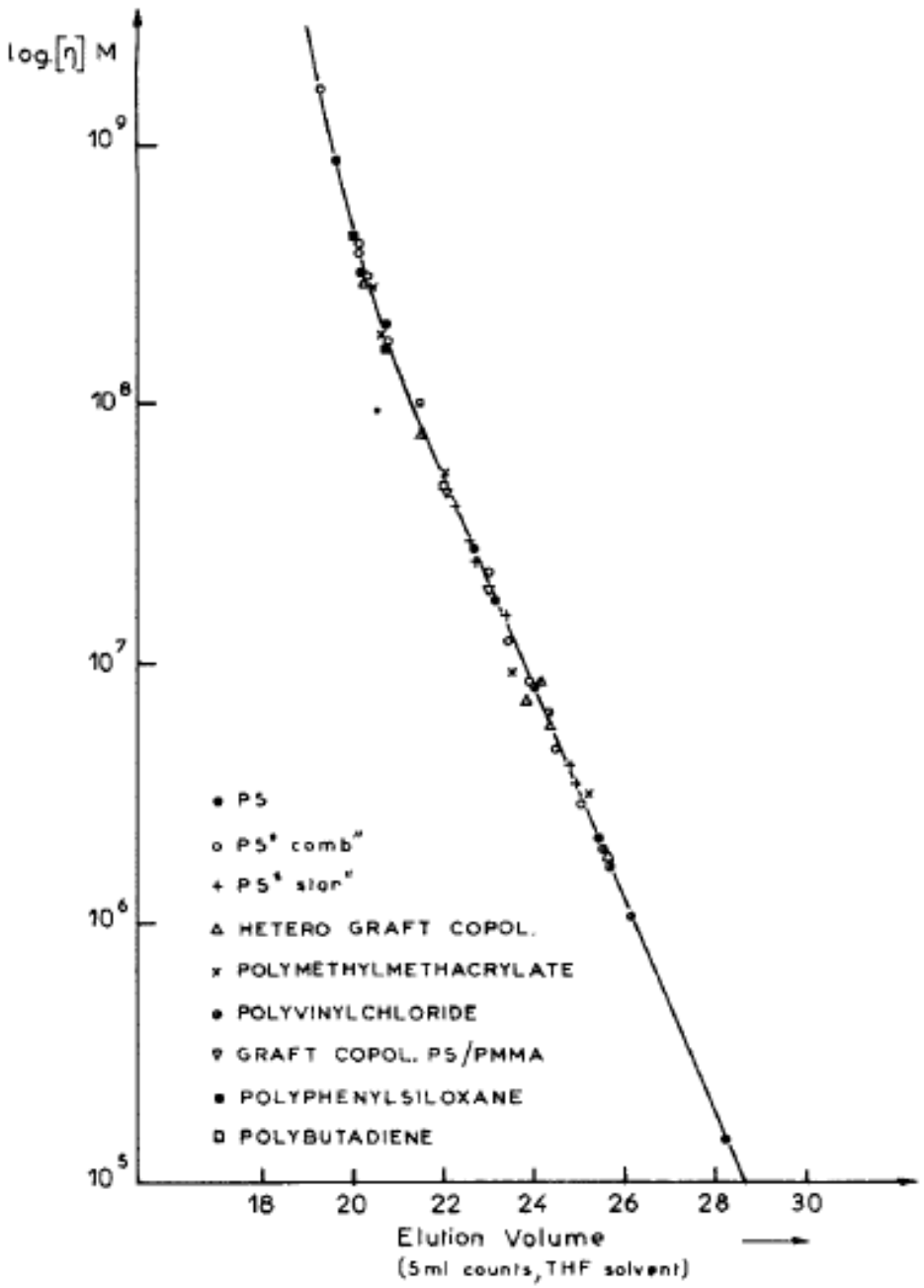

Figure 2.1: The original universal calibration plot that details how different polymers with different compositions all fall on the same universal calibration curve

$$[\eta] = KM^{a}$$ **Equation 2.1**

$$K_A M_A^{a_A+1} = K_S M_A^{a_S+1}$$ **Equation 2.4**

$$M_A = \left(\frac{K_S M_S^{a_S+1}}{K_A} \right)^{\frac{1}{a_A+1}}$$ **Equation 2.5**

Today, software such as Astra performs these calculations automatically, but the equations above show the direct correlation that makes universal calibration an excellent alternative method when conventional calibration fails to provide accurate molecular weight information.

Synthetic Procedures

General Procedure for Polymerization of 2,5-dibromo-3-hexylthiophene via GRIM (JR-1-211)

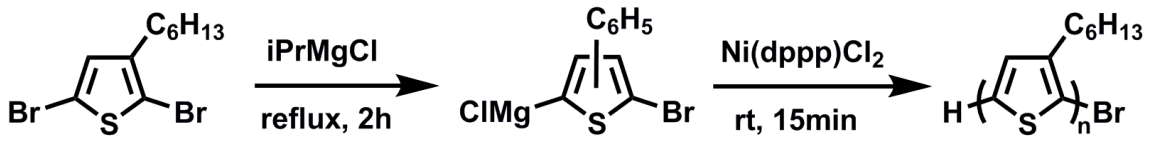

Scheme 2.1: Reaction schematic for the synthesis of P3HT via McCullough's version of GRIM

The apparatus consisted of a 250 mL 3-neck round bottom flask equipped with a magnetic stir bar. It was dried in a 124ºC oven overnight and cooled under a nitrogen purge. One side neck was equipped with a ribbed inlet adapter that was connected to a nitrogen flow. The other side neck was capped with a rubber septum, and the middle neck was equipped with a condenser. The ground glass joint at the top of the condenser was equipped with a ribbed inlet adapter that was connected to a bubbler filled with mineral oil. A very slow purge of nitrogen was passed through the apparatus throughout the reaction to

protect the headspace from any impurities that may interfere with the Grignard exchange reaction.T

To the apparatus was added 50 mL of dry THF which had been collected from an Innovative Technology, Inc. PureSolv PS-MD-5 system in dry glassware and used immediately. The apparatus was placed in an oil bath set to 80°C. While heating, 3.5 g (10.7 mmol) of 2,5-dibromo-3-hexylthiophene was added via syringe, and 8.1 mL (10.5 mmol) of a 1.3 M solution of isopropylmagnesium chloride·lithium chloride solution in THF was injected. It was important to ensure the ratio of monomer to Grignard was less than 1:1 to limit monomers that may have had two exchange reactions occur. Such an occurrence would lead to a polymer chain propagating in two directions simultaneously which would adversely affect the polydispersity of the sample and hinder control of end groups. Once the reaction solution was heated, it was stirred and refluxed for 1 hour. After refluxing, the solution was removed from the oil bath, cooled to room temperature and 23.7 mg (0.04 mmol) of $Ni(dppp)Cl_2$ was added. The solution was stirred at room temperature for 15 minutes before being quenched with 5 mL of 5M hydrochloric acid and stirred 10 minutes.

The resulting polymer was precipitated by pouring into 400 mL of stirring methanol. Methanol and polymer where poured through a

cellulose Soxhlet thimble, and the thimble was placed in a Soxhlet extractor apparatus. The polymer was extracted (in order) with methanol, hexanes, and chloroform. With each solvent, extraction was continued until solvent around the thimble was colorless. Characterization data reported here is from the chloroform fraction. The chloroform was removed via a rotary evaporator to produce a dark purple layer of polymer on the walls of the flask. The polymer was redissolved in benzene and freeze-dried to remove any residual solvent that may have been trapped prior to analysis.

General Procedure for Polymerization of 2-bromo-3-hexylthiophene via Mori's Method (JR-1-253)

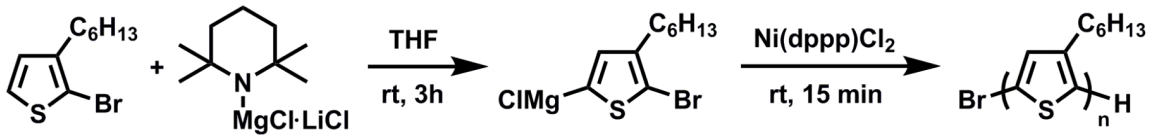

Scheme 2.2: Reaction schematic for the synthesis of P3HT via Mori's method

The apparatus consisted of a 250 mL round bottom flask equipped with a magnetic stir. It was dried in a 124°C oven overnight and was cooled under a nitrogen purge. The neck was capped with a rubber septum, and a nitrogen inlet and bubbler were used via needles through

the septum. A slow purge of nitrogen was passed through the apparatus during the addition of reagents. After reagents were injected, the nitrogen line and bubbler were replaced by a nitrogen-filled balloon. The balloon served to keep positive pressure inside the flask and protect the headspace from impurities during the dehydrobrominative exchange reaction.

To the flask was added 3.0 g (12.2 mmol) of 2-bromo-3-hexylthiophene and 12.1 mL (12.1 mmol) of a 1.0 M solution of TMPMgCl·LiCl solution in THF. The solution was stirred at room temperature for 3 hours. 50 mL of THF which had been collected from an Innovative Technologies, Inc. PureSolv system in dry glassware and used immediately was injected. 109.3 mg (0.2 mmol) of Ni(dppp)Cl_2 was added. The solution was stirred at room temperature for 15 minutes before being quenched with 5 mL of 5M hydrochloric acid and stirred 10 minutes.

The resulting polymer was precipitated by pouring into 400 mL stirring methanol. Methanol and polymer where poured through a cellulose Soxhlet thimble, and the thimble was placed in a Soxhlet extractor apparatus. The polymer was extracted (in order) with methanol, hexanes, and chloroform. Characterization data reported is from the chloroform fraction. With each solvent, extraction was

continued until solvent around the thimble was colorless. The chloroform was removed via a rotary evaporator to produce a dark purple layer of polymer. The polymer was redissolved in benzene and freeze-dried to remove any residual solvent that may have been trapped prior to analysis.

Characterization Techniques

Nuclear Magnetic Resonance Spectroscopy (NMR)

Nuclear magnetic resonance spectroscopy (NMR) was performed on a Varian 500 MHz spectrometer. Deuterated chloroform was used as the solvent, and samples were prepared at a concentration of 10 mg/mL. Each sample was analyzed at 25°C. 128 scans were collected with a 45° pulse angle and 5 second relaxation time.

Matrix-Assisted Laser Desorption/Ionization – Time-of-Flight Mass Spectroscopy (MALDI-TOF/MS)

MALDI-TOF/MS was performed using a Bruker Daltonics Autoflex II mass spectrometer equipped with a N2 laser (λ=337 nm) with 25 Hz frequency and accelerating voltage of 20 kV. The matrix was trans-2-[3-(4-tert-butylphenyl)-2-methyl-2-propenylidene]malononitrile (DCTB, >99%, Fluka). Solutions of the matrix and samples in THF were made at concentrations of 20 mg/mL and 10mg/mL respectively. The ratio of matrix to sample used for collection of spectra was 5:1, and spectra were collected in reflectron mode employing an external calibration using polystyrene standards.

Refractometry

Refractometry measurements were performed on a Wyatt Optilab REX instrument (λ=658 nm) using a Harvard Apparatus PHD 2000 Infustion syringe pump. For this study, dn/dc for each sample was determined in both THF and in chloroform. All solutions were completely dissolved and filtered using a PTFE syringe filter with 0.2 μm pore size prior to analysis, and the measurements were conducted at 25°C.

Size-Exclusion Chromatography (SEC)

HPLC-grade THF that had been passed through a 1 μm filter was purchased and used as received as the SEC eluent at a temperature of 35ºC and a flow rate of 1 mL/min. The instrument was a Waters Alliance 2695 Separations Module equipped with three Polymer Labs PLgel 5 μm mixed-C columns. Triple detection was used via a refractive index detector (Waters 2414 RI, λ=880 nm), a viscometer (Wyatt Viscostar 126), and a light scattering detector (Precision Detector Instruments 2020 LS detectors at 15º and 90º). All samples were filtered using a PTFE syringe filter with 0.2 μm pore size and analyzed at a concentration of 1 mg/mL.

Results

Determination of Regioregularity via NMR

NMR is a powerful tool to probe the structural connectivity of polymeric materials. Concerning P3HT, NMR enables the researcher to quantify the regioregularity of the polymer chain. As previously discussed, regioregularity plays a large role in the performance of P3HT

in device applications. Figures 2.2 and 2.3 show the NMR spectrum of sample Sample G and a magnification of the aryl region. The proton labeled "b" on the thiophene ring shifts according to the connectivity to their neighboring thiophene repeat units. The large multiplet around 6.98 ppm results from head-tail coupled repeat units while the smaller features around 6.80 – 6.85 ppm indicate the presence of head-head and tail-tail coupled repeat units on the polymer chain. Integrating these peaks provides a quantitative picture of the degree of regioregularity for each polymer sample. Table 2.1 lists the degree of regioregularity for each sample as determined by NMR.

End-Group Analysis via MALDI-TOF

Control of the end-groups of P3HT is of great importance for the synthesis of block copolymers. In fact, an entire chapter of this dissertation is dedicated to the work that was done synthesizing conjugated polymers with high degrees of end-group control. Looking at Schemes 2.1 and 2.2, it can be seen that for both traditional GRIM and Mori's method, a chain that initiates and propagates in a single direction before being quenched with acid will have the end-groups, Br/H. Early termination due to improper conversion of the thiophene monomer to the

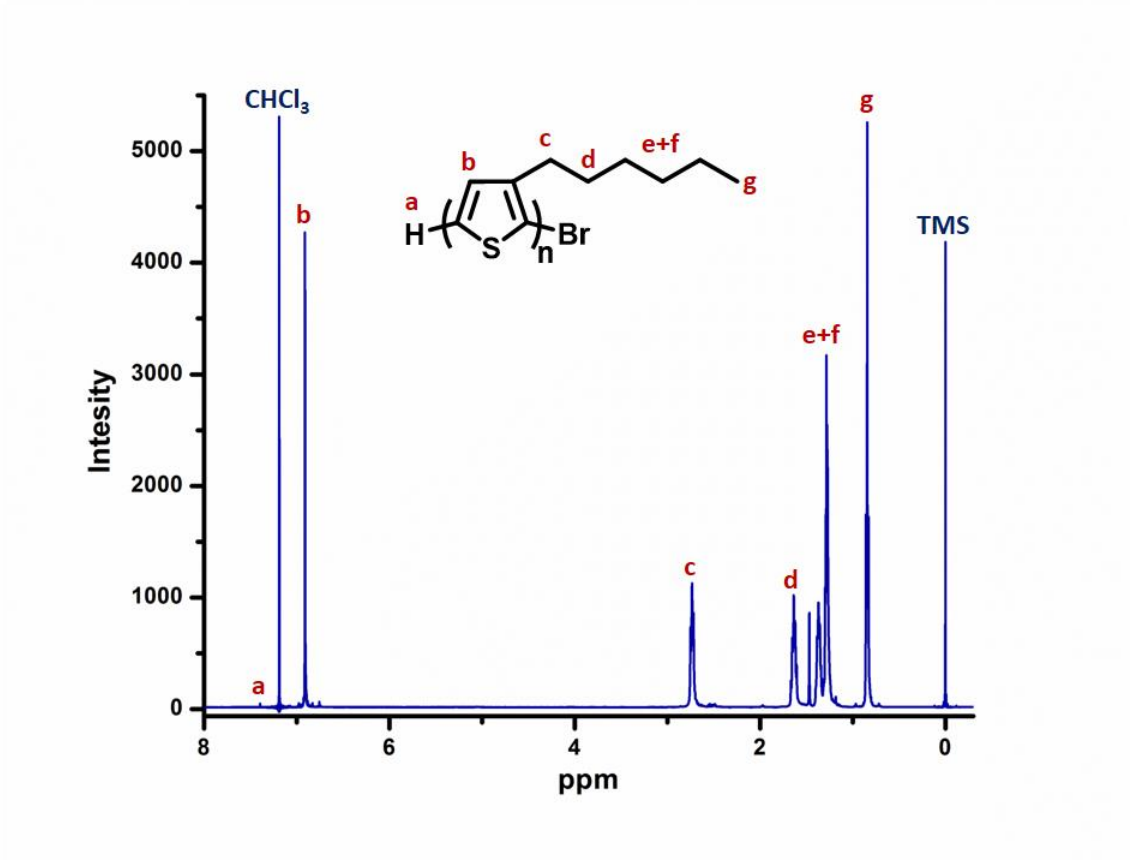

Figure 2.2: Full NMR spectrum of P3HT homopolymer, Sample G

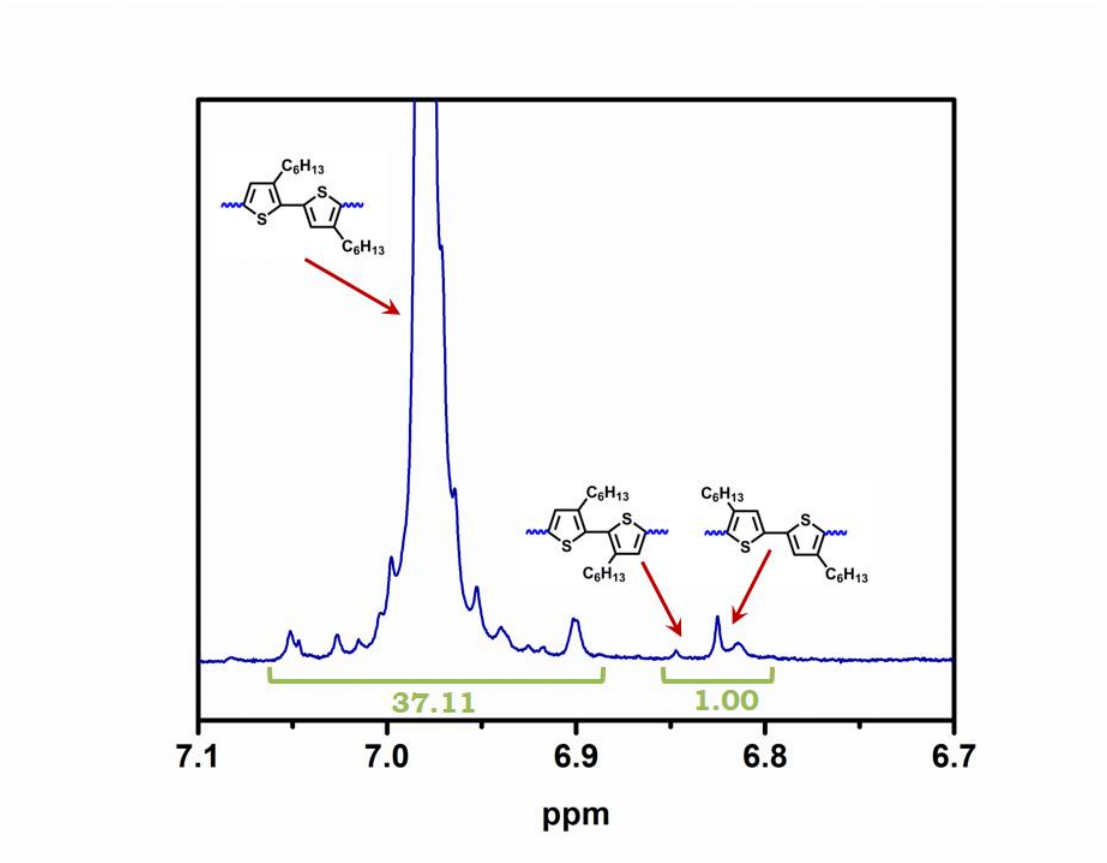

Figure 2.3: NMR spectrum of Sample G zoomed in on the aryl region of the spectrum.

Table 2.1: Collection of the structural characterization data collected in this dilute solution properties study. Regioregularity was calculated using NMR data as described in the text. End-groups were determined using MALDI-TOF data.

Sample	Regioregularity (%)	End-Groups Br/H	H/H	Br/Br
A	96	75.1	11.8	13.1
B	96	71.8	12.6	15.5
C	97	44.5	20.3	35.2
D	96	89.9	5.1	5.0
E	97	49.9	30.4	19.7
F	97	39.1	37.9	23.0
G	97	42.5	38.2	19.4
H	95	56.1	7.9	36.0
I	97	53.2	32.2	14.6
J	96	19.9	72.9	7.2
K	97			
L	97			

active form or bilateral propagation can lessen the control over the end-groups. However, there have been reports of P3HT being synthesized with 100% Br/H end-groups [92].

In order to properly identify the end-groups, MALDI-TOF was employed. Using the instrument and conditions described above, most samples were analyzed. Limitations of MALDI-TOF include the inability to analyze larger polymers. When polymers become too large the laser power of the MALDI-TOF must be turned up in order to ionize. However, large polymers will either be unable to ionize and fly or will be destroyed by the increased intensity of the laser. In the case of P3HT, MALDI-TOF can analyze samples up to about 16 kg/mol. Using monoisotopic masses for each element, the number of repeat units and end-groups can be identified. Figure 2.4 shows the MALDI-TOF spectrum for Sample G with each feature labeled. Table 2.1 lists the end-group analysis for each polymer that could be analyzed using MALDI-TOF.

Determination of Mark-Houwink parameters

Using the instrument described above and Astra software, viscosity datum was collected from SEC runs of each sample in THF at 35°C. Plotting log [η] versus log molecular weight leads to a linear fit line that

can be used to find the K and a parameters for this polymer/solvent system as shown in Figure 2.5. The molecular weight used for this plot was the weight-average molecular weight found using light scattering because light scattering analysis was able to assign an absolute molecular weight to each sample.

Once the data was plotted as shown above, the Mark-Houwink parameters were determined as follows: K is the inverse log of the intercept of the linear regression line. In this case, the linear fit line has an intercept of -2.80 so K is equal to $\log^{-1}$ (-2.80) or 1.57E-03 cm^3/g. The parameter, a, is equal to the slope of the linear regression line, 1.04. In the case of the P3HT samples being investigated and plotted here, a is equal to 1.04.

Our findings for the Mark-Houwink parameters for P3HT in THF are in good agreement with Holdcroft [88] who reported K and a values of 2.28E-03 cm^3/g and 0.96, respectively. Our findings support Holdcroft's assertion that P3HT is a semi-flexible chain. In contrast, the Mark-Houwink parameters calculated here are different than those reported by Heffner and Pearson [89]. Pearson reported K and a values of 1.2E-03 cm^3/g and 0.58, respectively. Data from this study is plotted beside the data from Holdcroft and from Heffner and Pearson in Figure 2.6.

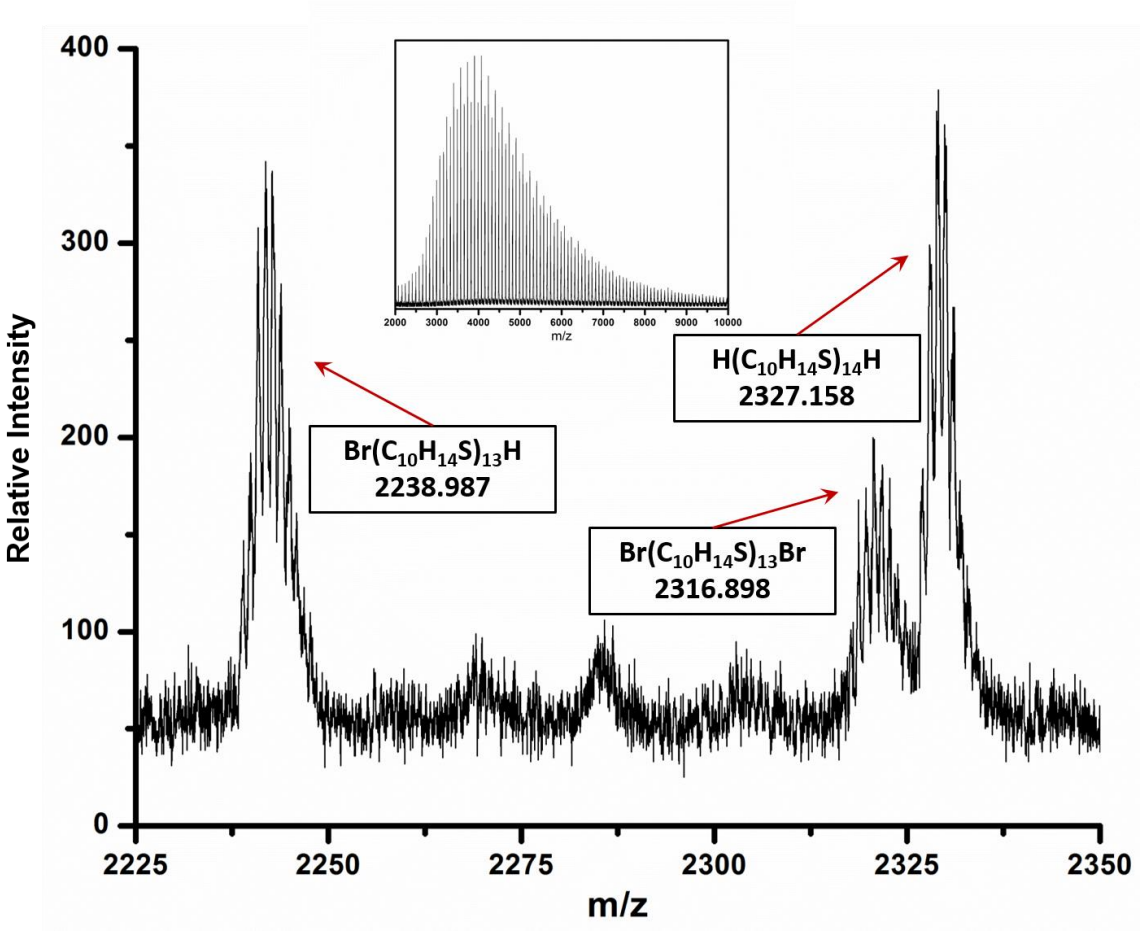

Figure 2.4: MALDI-TOF spectrum of Sample G. The values listed for each peak are the monoisotopic mass for P3HT with the listed end-groups and number of repeat units

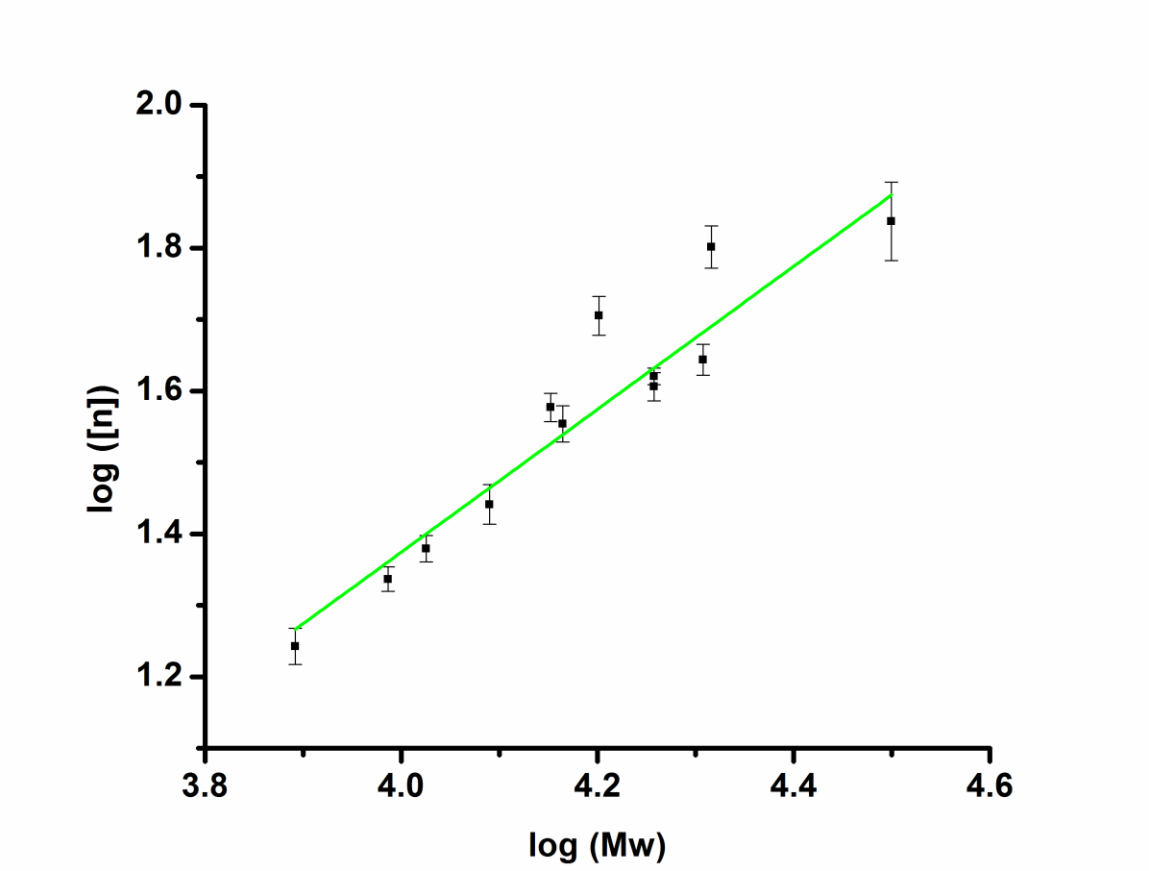

Figure 2.5: Log-log plot of intrinsic viscosity and weight-average molecular weight used to find the Mark-Houwink parameters for P3HT in THF.

[1]Mw was determined by SEC analysis using a light scattering detector

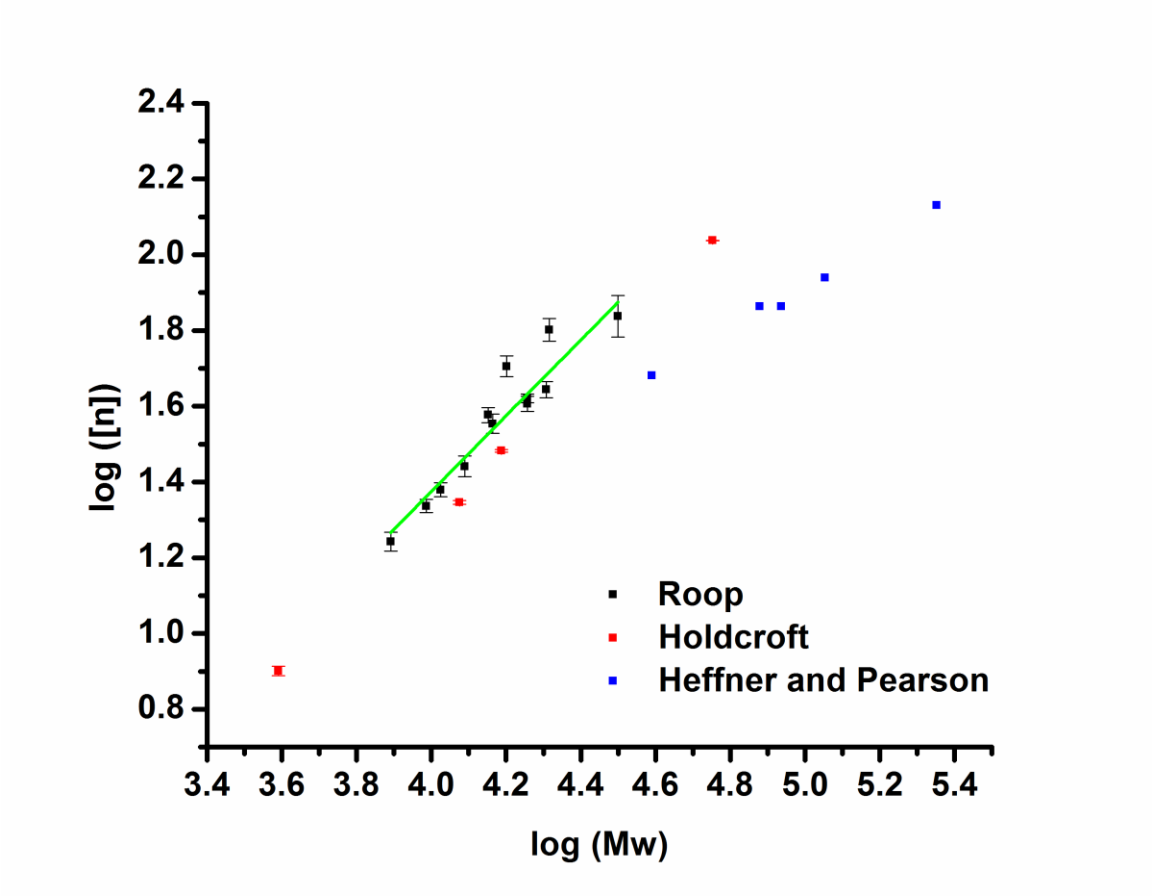

Figure 2.6: Log-log plot of intrinsic viscosity and molecular weight data from all three solution properties studies discussed in the text.

Although the values reported by Pearson differ from those reported here and also by Holdcroft, this discrepancy may be explained by examining the sample sets. In the case of our study the molecular weights of the P3HT samples was between 7800 and 31600 g/mol as determined by light scattering. Holdcroft did not report molecular weight values according to light scattering, but the Mn values for his sample set ranged from 4500 to 47500 g/mol relative to PS standards. Conversely, Pearson studied much higher molecular weight P3HT samples. By light scattering, his samples ranged in molecular weight from 41000 to 223000 g/mol. This large difference in molecular weights being studied may contribute to the differences in values reported. At very long chain lengths, such as the ones studied by Pearson, it is possible that P3HT begins to behave more like a random coil. This is supported by the agreement Pearson observed between molecular weights relative to PS standards and those determined via light scattering. In order for conventional calibration of SEC relative to PS to provide accurate molecular weight characterization, the polymer sample must be flexible.

Measuring the Differential Index of Refraction (dn/dc)

One main goal of this study was to find an accurate and straightforward method for the determination of the absolute molecular

weight of P3HT. Light scattering provides absolute molecular weight information, however, it requires the dn/dc of the system to be known. Pearson reported dn/dc values for P3HT in THF and chloroform as 0.307 and 0.269 mL/g, respectively [89]. In a study published in 2011, Peng displayed that dn/dc changed slightly with molecular weight up to about 10000 g/mol [77]. The molecular weights for the samples prepared for this study fell across that threshold with molecular weights ranging from 7800 g/mol to 31600 g/mol. The dn/dc of every sample was measured in both THF and chloroform for comparison and to ensure the highest confidence in light scattering characterization. We determined dn/dc of P3HT in THF to be 0.316 mL/g. This value represents the average of dn/dc values for every sample in this study. As seen in Figures 2.6 and 2.7, no molecular weight dependence was observed for dn/dc in either solvent. Therefore, the average of the 12 values was taken to be correct. In like manner, we determined dn/dc of P3HT in chloroform to be 0.257 mL/g. Both of these values are in agreement with Pearson's measurements. While these values are higher than Peng reported, it is possible that the molecular weight dependence at low molecular weights observed in that study contributed to this difference. These measurements were made in both THF and chloroform since these are the two most commonly used solvents for these polymers.

For each set of measurements a stock solution of 15 mL was prepared at a concentration of 3 mg/mL or 2 mg/mL in chloroform or THF, respectively. The reason for the difference in starting concentrations is because P3HT has lower solubility in THF, especially at molecular weights at or above 20 kDal/mol. Aliquots were taken of the stock solution, placed in separate vials, and diluted to make a total of 5 concentrations per sample. All concentrations were determined by mass to ensure the highest confidence in the measurements. An example of how these solutions were prepared can be found in Table 2.2.

Measurements were made using the Wyatt Optilab Rex instrument described above, and data was collected using Astra software. A syringe pump ensured consistent flow rate of 0.2 mL/min through the sample chamber. Once a steady baseline was established, the solutions were passed through the instrument in order from least concentrated to most concentrated. Steady readings over a 5-10 minute time period were achieved prior to switching to the next concentration. At the end of each experiment, pure solvent was passed through the instrument to return the readings to baseline. The software calculated the dn/dc from the data collected, and a sample of that data along with results can be seen in Figure 2.7. All data collected during this portion of the study can be found in Table 2.3. Figures 2.7 and 2.8 shows dn/dc plotted versus molecular weight in each solvent.

Table 2.2: Example of the sample preparation for refractometry measurements.

Sample Preparation for dn/dc measurement of Sample G in THF			
5	0.0337 g P3HT 13.3941 g THF	13.4278 g total 15.063 mL THF[1]	0.00251 g P3HT/g solution 2.237 mg/mL
4	3.5629 g stock sol'n 0.7812 g THF	0.0089 g P3HT[2] 4.875 mL THF[1]	1.826 mg/mL
3	2.5181 g stock sol'n 1.7454 g THF	0.0063 g P3HT[2] 4.788 mL THF[1]	1.316 mg/mL
2	1.7291 g stock sol'n 2.7692 g THF	0.0043 g P3HT[2] 5.054 mL THF[1]	0.851 mg/mL
1	1.0309 g stock sol'n 3.6840 g THF	0.0026 g P3HT[2] 5.299 mL THF[1]	0.491 mg/mL

[1] Calculated by dividing g THF by density of THF (0.8892 g/cm^3)
[2] Calculated by multiplying (g stock sol'n) by (0.00251 g P3HT/g solution)

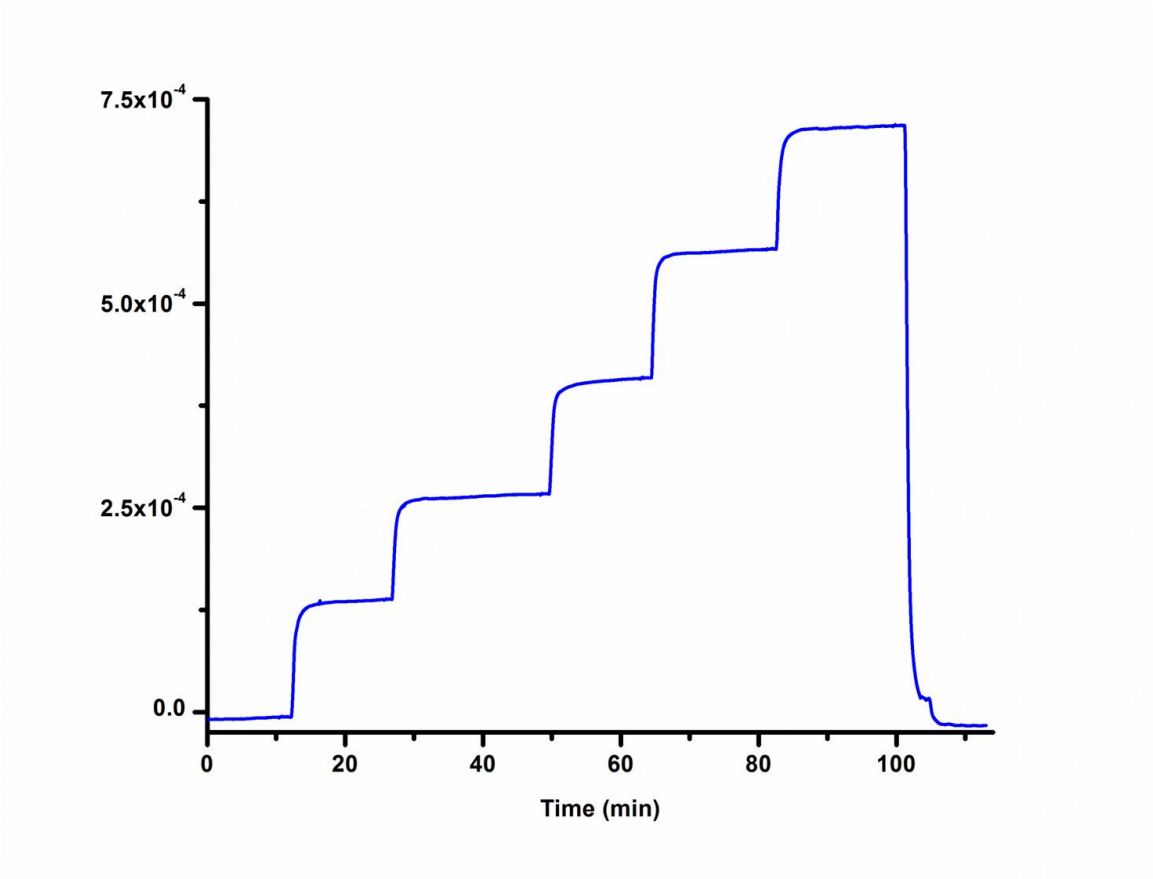

Figure 2.7: Actual data collected during refractomoetry measurements for sample Sample G.

Table 2.3: dn/dc values for all samples in this study.

Sample	M_w [1]	dn/dc (THF)[2]	dn/dc (CHCl3) [2]
A	7800	0.293	0.255
B	9700	0.302	0.273
C	10600	0.295	0.253
D	12300	0.308	0.253
E	14200	0.333	0.256
F	14600	0.320	0.272
G	15900	0.370	0.262
H	18100	0.321	0.283
I	18100	0.311	0.262
J	20300	0.315	0.260
K	20700	0.369	0.270
L	31600	0.341	0.266

[1] **Weight-average molecular weight as determined using light scattering (g/mol) in THF**
[2] **cm^3/g**

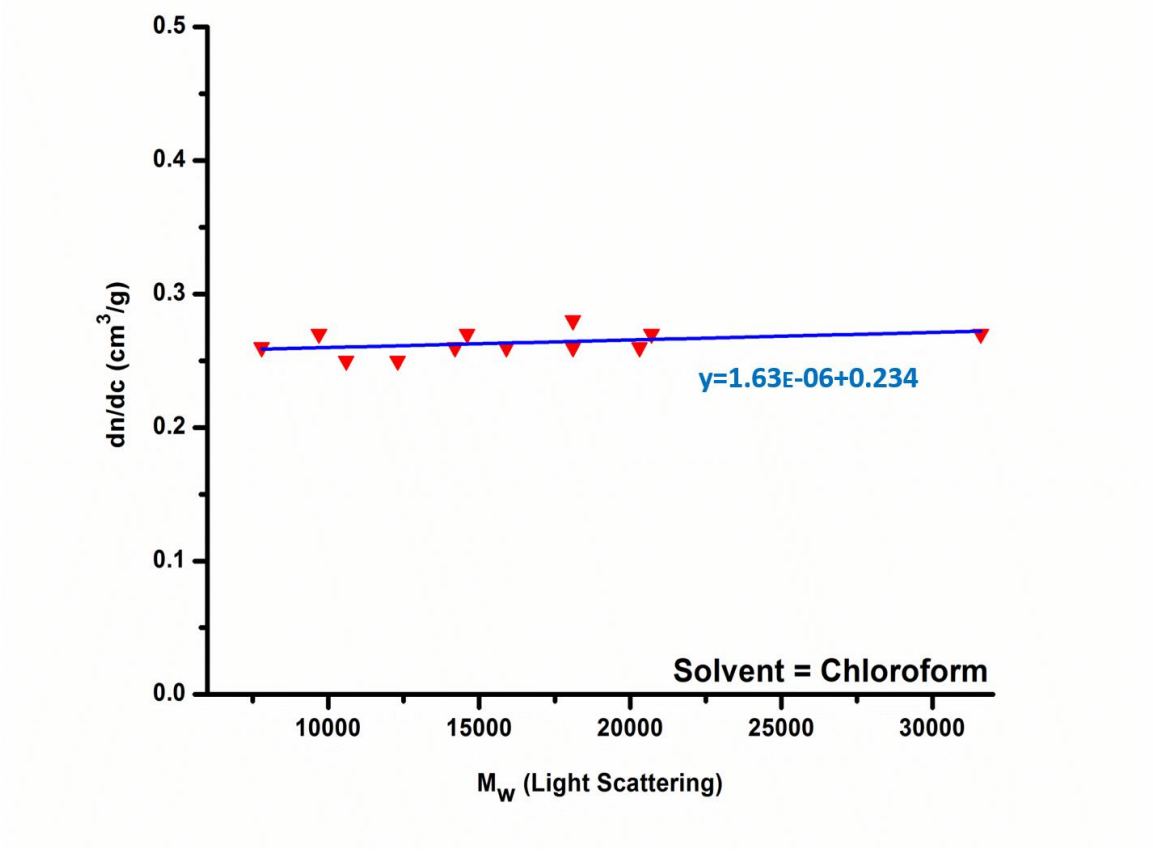

Figure 2.8: Plot of measured dn/dc in chloroform versus the Mw as determined by light scattering detector on SEC.

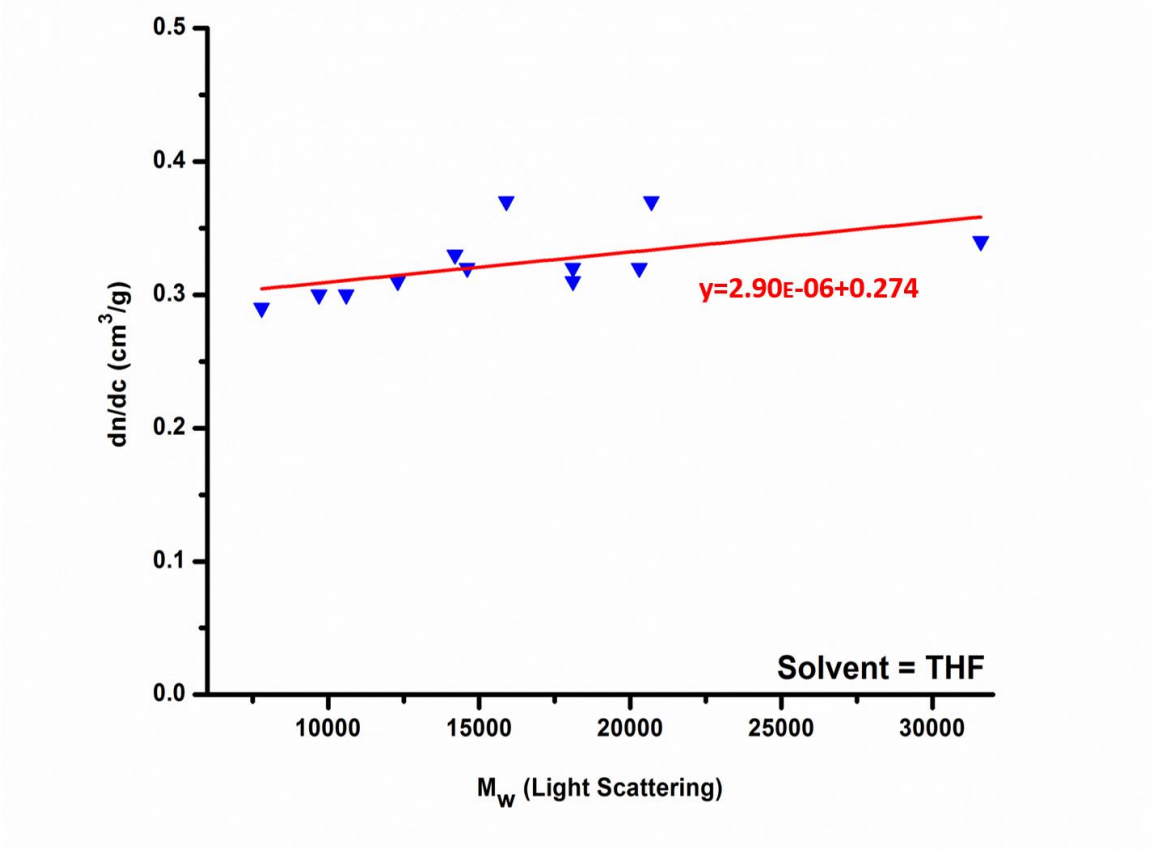

Figure 2.9: Plot of measured dn/dc in THF versus Mw as determined by light scattering detecor on SEC.

Applying Universal Calibration to Determine Molecular Weight

Using SEC with triple detection, a universal calibration curve was generated using narrow PS standards. This calibration was used to assess each sample in this study, and the results were compared with molecular weight data collected using light scattering. The molecular weight characterization data for all three methods (conventional calibration, light scattering, and universal calibration) can be seen in Table 2.4.

In every sample, conventional calibration gave a molecular weight value that was considerably higher than the other two methods. This is consistent with McCullough's findings and reinforces the need for a different way to accurately assign molecular weights to P3HT samples. Shifting focus and comparing light scattering to universal calibration also revealed trends in the data. Universal calibration consistently gave molecular weight values that were at or slightly below those given by light scattering. While the values derived using these two methods are not drastically different, many of them fall well outside the acceptable variance in SEC measurements of 5%. It can be concluded, therefore, that these two methods are not giving the same answer for the majority of the P3HT samples in this study. Plotting the molecular weight values

Table 2.4: Summary of the molecular weights determined for each sample using the three different methods.

Sample	Conventional Calibration			Light Scattering			Universal Calibration			Diff
	M_w[1]	M_n[1]	PDI[2]	M_w[1]	M_n[1]	PDI[2]	M_w[1]	M_n[1]	PDI[2]	(%)[3]
A	11000	9400	1.17	7800	7100	1.10	7600	6500	1.17	2.6
B	14800	13300	1.11	9700	9000	1.08	10300	8700	1.18	6.0
C	15800	13800	1.14	10600	9800	1.08	10600	9100	1.16	0.0
D	18000	13900	1.29	12300	10200	1.21	10900	8600	1.27	12.1
E	24800	18200	1.36	14200	11400	1.25	12700	10000	1.27	10.4
F	24200	19300	1.25	14600	12500	1.17	12200	8700	1.40	17.9
G	30800	21400	1.44	15900	12300	1.29	13500	9800	1.38	16.3
H	30100	23500	1.28	18100	15600	1.16	15400	11600	1.33	16.1
I	29300	26300	1.11	18100	17200	1.05	16000	13300	1.20	12.3
J	33600	23100	1.45	20300	15600	1.30	16600	11900	1.39	20.1
K	40600	31200	1.30	20700	17300	1.20	18100	11600	1.56	13.4
L	55800	41000	1.36	31600	26300	1.20	25500	19400	1.31	21.4

[1] g/mol [2] Calculated using PDI = M_w/M_n
[3] Percent difference between light scattering and universal calibration [((Mw (LS))-(Mw(UniCal)))/Average Mw]*100

derived from each method against each other for each sample yields the plot in Figure 2.10.

Conclusions

This study of the dilute solution properties of P3HT homopolymers provided a detailed picture of several aspects that may affect material and electronic properties of the materials in device applications. The synthetic procedures employed were well-established methods from literature that produced consistent polymers. Although the two different polymerization methods generated the active thiophene monomer in a slightly different manner, the polymers produced by the two synthetic methods were very similar from a structural standpoint.

As discussed in the Introduction chapter of this dissertation, the ratio of monomer to catalyst is responsible for targeting degree of polymerization for P3HT. However, when the same monomer to catalyst ratio was used with each of the polymerization methods, Mori's method consistently produced polymers with higher molecular weights. For example, Samples G and K had monomer to catalyst ratios of 303 and 300, respectively. Traditional GRIM polymerization used to polymerize Sample G yielded a polymer with Mw=15.9 kDal/mol

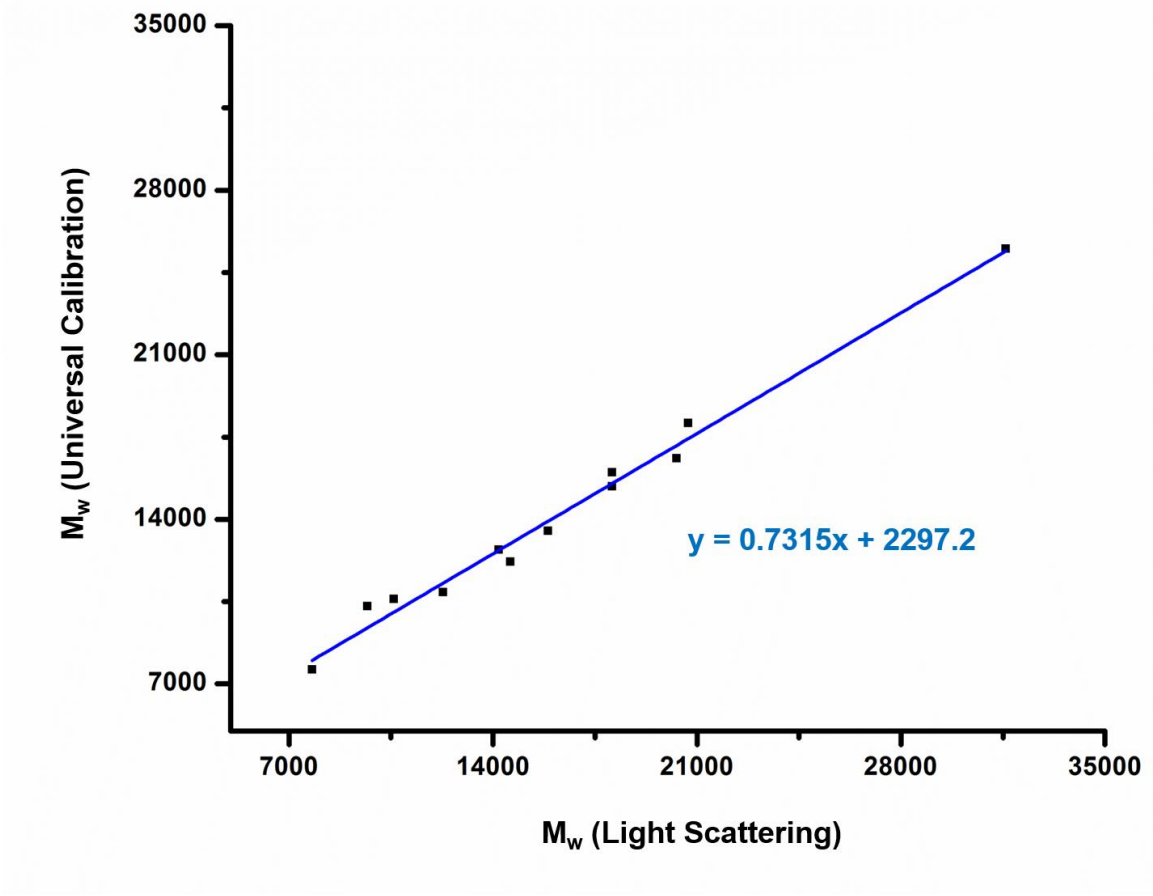

Figure 2.10: Plot of molecular weight as determined by universal calibration versus molecular weights as determined using light scattering.

according to light scattering. However, Mori's method used for Sample K produced a polymer with Mw=20.7 kDal/mol. This trend was consistent across the sample set and may have been a result of the more favorable isomeric mixture produced by Mori's method. As discussed previously, when using Mori's method the Grignard can only add to the thiophene ring in the after TMPMgCl·LiCl has extracted the proton. This leads to nearly exclusive Grignard addition at the desired 5-position. This improved ratio may have resulted in more active monomer being present in the reaction solution which would lead to more repeat units being added to the propagating chain end during the polymerization.

The structural characteristics of the polymer chains displayed more consistency between the two synthetic methods. Concerning regioregularity, In nearly every sample, the degree of regioregularity was at or above 95%. This indicates that the lone regio-defect in these polymer chains was a result of the tail-tail coupling at initiation. It is difficult to speak to trends concerning the end-group analysis performed using MALDI-TOF because of our inability to analyze all samples. Nonetheless, there is not a clear trend in the data that indicates either synthetic method is superior to the other in this regard.

Comparing the values determined for the Mark-Houwink parameters for P3HT in THF to the earlier work by Holdcroft and Heffner

shows that our results are more consistent with the findings of Holdcroft. The K value we found is not closely consistent with either of the earlier studies as it falls between the two previous values given for K. However, the a value we report here is only slightly different than Holdcroft's findings but significantly different than Heffner and Pearson. Our determined value for a of 0.93 indicates that P3HT is a semi-flexible polymer in better than theta conditions in THF at 35°C. This finding is in agreement with Holdcroft's published work and consistent with the conventionally held belief that P3HT is semi-rigid due to the conjugation along the backbone.

Looking at the plots of dn/dc versus molecular weight in Figure 2.6, there does not appear to be any molecular weight dependence of dn/dc for P3HT within the molecular weight range being studied. There was some variance in the dn/dc values that were measured in both THF and chloroform, but those variations do not appear to follow any molecular weight trend. Most likely, those inconsistencies were a result of the uncertainties associated with the measurements of concentrations. It is also possible that improper or inconsistent baseline measurements may have contributed to variations in these measurements. While great care was taken to ensure exact concentrations were used and steady baseline readings were observed prior to and following sample solutions

being measured, these are the two areas most likely responsible for variations in dn/dc values.

For the purposes of characterizing the molecular weights of the polymer samples by light scattering in THF, a dn/dc value of 0.317 mL/g. This value represents the average of all dn/dc measurements made in THF for this series of samples. It is in agreement with Pearson's reported value for dn/dc of P3HT in THF [89], but is higher than Peng reports [77]. Peng studied lower molecular weight P3HT, Mw from 5000 to 11900 g/mol by light scattering, while Pearson's samples were of much higher molecular weights, Mw from 41000 to 223000 g/mol by light scattering. Peng demonstrated that dn/dc had a dependence on molecular weight up to a molecular weight of about 10000 g/mol. Only one sample in the study being reported here had a molecular weight below that threshold so taking the average of the measurements was acceptable.

Even considering that Peng studied low molecular weight samples, the dn/dc values are still lower than Pearson found and lower than reported here. Two of the samples from Peng's study were at or above the reported threshold for molecular weight dependence of dn/dc in THF. Taking those to two samples to be on the plateau would result in dn/dc of P3HT in THF to be about 0.28 mL/g. It is likely that the solvent used

and the manner in which the solvent was handled played a significant role in this discrepancy.

To this point, the dn/dc of Sample H was remeasured using different solvent and handling. Sample H has a Mw of 18100 g/mol according to light scattering. In the reported values above, THF was used straight from the bottle with no purification or drying techniques employed. Consistency across the diluted solutions was achieved by taking all the solvent from the same bottle and using that solvent for baseline measurements. However, when the dn/dc measurement of Sample H was revisited, the THF used was taken from a PureSolv solvent purification system into a round-bottom flask that had been dried in the oven and cooled under a nitrogen purge. The THF was stored under nitrogen in the flask and collection of THF for use in the measurements was achieved with a syringe through the rubber septum. The solutions were prepared as described above and heated to 40°C to ensure the polymer was completely dissolved. Again, the solutions were filtered using a 0.2 μm syringe filter just prior to the measurement. What we observed was a decrease in dn/dc of Sample H in THF from the original value of 0.32 mL/g to 0.26 mL/g. The first measurement is consistent with Pearson, but the second measurement is more consistent with Peng. The dn/dc value used for our light scattering analysis, however remained 0.32 mL/g because the THF used in the original measurements was

more consistent with the SEC setup used for light scattering measurements. The THF for the SEC is a bottle with the tubes running through holes in the lid. It is not protected from moisture. Nonetheless, the short experiment described above demonstrates how sensitive dn/dc can be to water in the solvent.

The SEC results also provided useful information concerning proper characterization of P3HT. When molecular weight as determined by light scattering was plotted versus molecular weight as determined by universal calibration, as seen in Figure 2.8, it confirmed the earlier assertion that the data from light scattering was not in agreement with the data from universal calibration. We know that light scattering gives an absolute molecular weight value as long as dn/dc and concentration are known. The proper work was done in this study to ensure that these values are known with a high degree of certainty. Therefore, the molecular weight characterization using light scattering was considered to be correct for these samples. Had universal calibration been valid for this sample set, the slope of the line in Figure 8 would have been 1. The slope of the line in Figure 8, however, is 0.73 indicating that universal calibration fails to determine the absolute molecular weight of P3HT within the size range studied here.

Through a systematic and thorough approach, we were able to extensively characterize a series of P3HT homopolymers. It was observed that the dehydrobrominative exchange reaction led to more controlled polymers than traditional GRIM. The Mark-Houwink parameters and dn/dc values determined here will serve to make accurate determination of molecular weights and polydispersities easier moving forward. In addition, we ultimately concluded that universal calibration of SEC is not an applicable method for molecular weight characterization of P3HT homopolymers.

CHAPTER 3

Synthesis and Characterization of Highly Functionalized Conjugated Polymers

Abstract: The ability to functionalize the end-groups of polymers is an important aspect for the synthesis of block copolymers. Because few block copolymers are able to be synthesized through sequential addition of monomers, the need for the chain end to allow for further growth or grafting is vital to the synthesis of block copolymers and the introduction of branching to many systems. In the case of conjugated polymers as discussed here, the need for incorporation of different polymers for device applications has been discussed. In this chapter, we detail our approach using Suzuki polymerization techniques that led to the synthesis highly functionalized P3HT and poly(9,9-dihexylfluorene) (PFO). The approach includes the synthesis of boronic acid pinacol ester monomers that can be polymerized through palladium-catalyzed coupling reactions. We were able to obtain P3HT and PFO with uniform end-groups which allowed for synthesis of miktoarm star block copolymers to be performed in the next chapter.

Introduction

The control of end-groups of P3HT and other conjugated polymers is of great importance if well-defined block copolymer systems with tailored properties are to be synthesized. The ability to impart functionality onto a polymer through end-group control enables the conjugated polymer to be used as a macroinitiator from which to grow a different polymer, to be grafted onto another polymer, or to be a convalently attached to a more complex molecular architecture such as miktoarm stars. Great advances have been made in the area of end-group control through the development and modifications of GRIM as well as other polymerization techniques used for the synthesis of conjugated polymers such as Suzuki-Miyaura and Stille cross-coupling reactions.

Tkachov et al. has shown that the nickel catalyst in GRIM randomly walks along the chain during polymerization which can lead to bilateral propagation [92]. In the case of a simple GRIM of P3HT quenched with water, bilateral propagation results in both ends of the chain being terminated with a proton instead of the Br/H end groups that would result from unilateral propagation. This phenomenon is considered to be a minor occurrence in GRIM, but nonetheless, it affects

end group control. An enormous amount of effort has gone into development of functionalized end groups on P3HT [53-57, 92-139]. These functionalities are typically achieved either by controlled polymerization techniques, quenching with a functional quenching reagent, or post-polymerization modification of end groups. While no method can guarantee 100% control over every polymer chain, the most recent methods lead to very good control over the end groups of P3HT. Such ability to direct end groups is important not only for characterization of the polymer [139] but is also essential for development of block copolymers, grafted copolymers, and other incorporations of P3HT with different polymers and surfaces. It is these copolymer systems that are thought to be the pathway to the next advances in this field.

Block copolymer systems incorporating P3HT have been studied in depth by many researchers due to the expected advantages over blends of P3HT with acceptor materials such as PCBM in optoelectronic applications [98, 101, 117, 122, 123, 127, 131, 132, 140]. The covalent bonding of two or more components together may limit the size of nanostructure formation which could enable optimization of BHJ solar cells. Control of end group composition is of particular interest in the synthesis of these materials as the imparted functionality enables the P3HT chains to be attached to another chain or serve as ex-situ

macroinitiators for the polymerization of the next block. In an early example, Tu synthesized a donor-acceptor-donor triblock copolymer of P3HT and cyanophenylenevinylene (CN-PPV) [131]. A controlled GRIM polymerization produced P3HT with Br/H end groups which were attached to a dibromo-CN-PPV acceptor core via a Ni-catalyzed coupling reaction to form the triblock copolymer. This resulting material was well-defined and exhibited high structural order. The synthesis of each block individually prior to assembling the block copolymer allows for excellent molecular weight control.

Imparting functionalities that enable "click" chemistry to be used in the synthesis of block copolymers involving P3HT is an approach that more than one researcher has investigated [98, 117, 127, 132, 140]. Developed by Sharpless in 2001, "click" chemistry has been shown to be a very effective coupling reaction for joining together both small molecules and polymers. In the case of P3HT, adding alkyne functional groups to the end(s) of P3HT chains allows for the addition of these chains to azide functionalities. Park used to "click" chemistry coupled with anion polymerization to synthesize a AB_2 miktoarm star block copolymer of PMMA and P3HT. Park first synthesized PMMA using anionic techniques and attached one living chain to 1,3,5-tris(bromomethyl)benzene. Reaction of the core molecule with sodium azide converted the remaining two bromines to azides. P3HT was

synthesized via GRIM and quenched with ethynylmagnesium bromide to produce monoethynyl-capped P3HT. "Click" chemistry was carried out using a copper catalyst to attach two P3HT arms onto the core. They observed a red-shift in the UV-vis spectrum of the miktoarm star compared to the linear analogue. They also observed an increase in the fibril width indicating that the two P3HT arms were stacking along the nanofibril axis. This was a clear indicator of how strong the π→π interaction between the two P3HT arms really is.

Synthesis of block copolymers is not the only reason the control of end groups on P3HT is important. End groups on P3HT have been shown to influence morphology [100], affect crystallinity [118], and impact the dispersion of carbon nanotubes in solutions and thin films [95]. Kim et al. has reported that changes in morphology of P3HT/PCBM blends with changing end groups on P3HT is a result of the surface energy differences imparted by the different end groups [107]. They looked at P3HT chains with the following end groups: -Br, --OH, $-CH_3$, and $-CF_3$. It was observed that a correlation between surface energies of P3HT and morphologies of the blends exists. Of particular note, P3HT with perfluoro end group ($-CF_3$) had a surface energy that nearly matched that of PCBM. When these components were blended at a 1:1 weight ratio, a fully blended morphology was observed. Upon thermal annealing, the P3HT- CF_3 blend had much smaller aggregates of PCBM

than the other end groups with different surface energies. It was concluded that the -CF_3 end group, and its subsequent surface energy, suppressed PCBM aggregate growth to a level that was advantageous for device performance. This was a significant discovery that can be used for optimization of P3HT-based materials of varied molecular architectures.

In addition to the synthesis of block copolymers and control of morphological and crystallization behavior of P3HT, end group control is important for attachment of the polymer to surfaces and nanoparticles [94, 96, 111, 121]. These types of hybrid materials are another route by which advances in organic electronic applications may come. Boon et al. functionalized P3HT with a carboxystyryl end group which allowed the conjugated polymer to be bound to the surface of TiO_2 nanoparticles [96]. This resulting hybrid material exhibited increased electron transfer efficiency, presumably due to the chelation of the -COOH end group to the TiO_2 surface. Krüger et al. used a different synthetic route to add carboxylic acid functionality to P3HT in order to bind it to TiO2, but they also reported marked improvements in electronic properties of the hybrid material over either component individually [111]. Proper control of the end groups of P3HT is imperative to these materials being viable options for device applications.

Introduction to Suzuki Polymerization

One synthetic pathway that has proven effective in the synthesis of conjugated polymers is the Suzuki-Miyaura cross-coupling reaction. Developed in 1979 [141, 142] and widely used for different applications, Suzuki cross-coupling can be applied to polymers to produce regioregular polymer chains with controlled end groups [136, 137, 143-149]. Suzuki polymerization allows for the coupling of an aryl halide with an aryl boronic acid in the presence of palladium catalyst. In the case of the P3HT synthesized in this work, the monomer used was 2-(5-bromo-4-hexylthiophen-2-yl)-4,4,5,5-tetramethyl-1,3,2-dioxaborolane. The nature of the monomer, having distinct functional groups at the desired locations, serves to ensure the highest level of regioregularity in the resulting polymer. Through a catalyst-transfer mechanism, polymerization begins when cross-coupling occurs between the dioxaborolane group of one monomer and the bromine on another monomer. In the case of ex situ initiation as described below, the initial catalyzed cross-coupling reaction occurs between the bromine of 4-bromo benzophenone and the dioxaborolane functional group of a monomer unit. After the initial cross-coupling, the catalyst moves from the newly formed bond to the growing chain end and adds another

monomer to continue propagation. The polymers produced by this method are well-defined with relatively narrow polydispersities and controlled end groups. One drawback to this method is that P3HT with molecular weights greater than about 10 kDal/mol have not been able to be synthesized to date. The need for polymerization techniques for conjugated polymers which provide this type of control over regioregularity, molecular weight, and end groups are essential for furthering the progress in this field and will be discussed in detail below.

Yokozawa et al. has explored Suzuki for synthesis of P3HT as well as polyfluorenes and polyphenylenes [136, 137]. In one case, they showed the ability of Suzuki polymerization to synthesize P3HT and polyfluorene individually. Each type of polymer had controlled molecular weights and controlled end group compositions [136]. In the same study, they showed the catalyst-transfer nature of Suzuki polymerization by polymerizing fluorene. After the fluorene monomers had been consumed, thiophene monomers with boronic pinacol ester functionality were added to the reaction solution. The end groups of the resulting block copolymer were still able to be controlled, and the polydispersity was relatively low (PDI of 1.50 for the block copolymer, PDI was 1.37 for polyfluorene prepolymer).

Suzuki polymerization offers a controlled route to synthesis of conjugated polymers. The ability to control molecular weight and maintain desired end groups make it an attractive method for the goals of this research. It enables the production of functionalized conjugated polymers without the need for post-polymerization modification of the end groups. In later chapters, use of Suzuki polymerization methods will be detailed in the synthesis of well-defined, highly-functionalized conjugated polymers. One of these polymers, P3HT with benzophenone functionality, will be further reacted to form miktoarm block copolymers to demonstrate the effectiveness of this approach.

Synthetic Procedures

Preparation of 2-(5-bromo-4-hexylthiophen-2-yl)-4,4,5,5-tetramethyl-1,3,2-dioxaborolane

3-hexylthiophene was reacted with N-bromosuccinimide (NBS) in THF for 2 hours at room temperature. The product was extracted with diethyl ether, washed with potassium hydroxide and water, and dried over magnesium sulfate overnight. The next day the solution was filtered to remove the drying agent and the solvent was removed via rotary

evaporation to yield a pale yellow oil. 2-bromo-3-hexylthiophene was isolated from the product mixture by distillation under reduced pressure. Purity of the molecule was revealed by GC-MS to be 100%.

2-bromo-3-hexylthiophene was reacted with lithium diisopropylamide (LDA) in THF at -41°C for 1 hour. To the chilled reaction solution was added 2-isopropoxy-4,4,5,5-tetramethyl-1,3,2-dioxaborolane and the solution was warmed to room temperature and allowed to react for 4 hours. The reaction was quenched with water, and the product was extracted with DCM. Solvent was removed via rotary evaporation and the desired product was isolated by silica gel chromatography. GC-MS indicated the borolated thiophene monomer to be present at a purity of >97%. The <3% impurity was believed to be thiophene monomer in which borolation occurred at the 4-position instead of the 5-position. There were no adverse effects observed on polymerzations using this monomer due to the slight impurity.

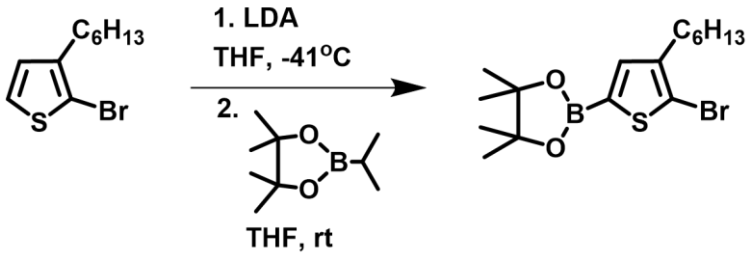

Scheme 3.1: Preparation of borolated 3-hexylthiophene monomer for Suzuki polymerization

Preparation of 2-(7-Bromo-9,9-dioctyl-9H-fluoren-2-yl)-4,4,5,5-tetramethyl-1,3,2-dioxaborolane

The fluorene monomer was prepared in the same fashion as the thiophene monomer described above. The same reactants, ratios, and temperatures were effective at yielding a boronic acid-functionalized monomer for Suzuki polymerization. The reaction schematic can be seen below in Scheme 3.2.

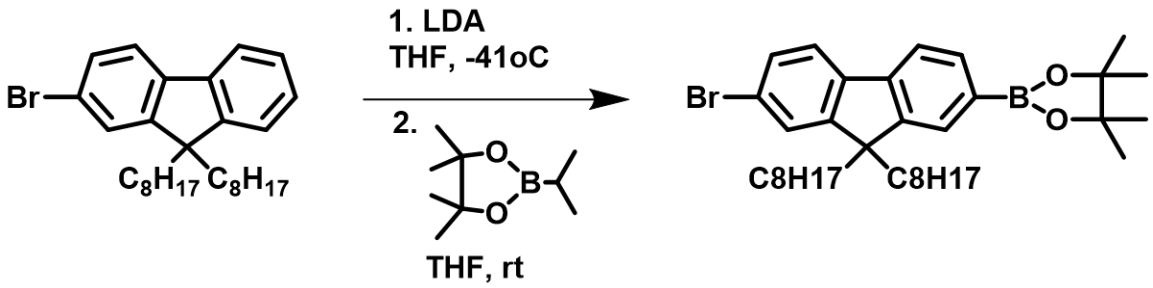

Scheme 3.2: Preparation of borolated fluorene monomer for Suzuki polymerization

Polymerization of P3HT or PFO from 4-bromobenzophenone

The synthesis of functionalized P3HT from the ex-situ initiator, 4-bromobenzophenone, was accomplished by preparing the initiator and monomer solutions separately and then combining for the polymerization. Formation of the initiating species required insertion of

the palladium catalyst into the aryl bromide bond on the benzophenone molecule. Insertion was facilitated using tri-tert-butyl phosphine. Due to the extreme volatility of the phosphine, the formation of the initiator required use of a glove box with argon atmosphere. The monomer was mixed with base to and the resulting solution was placed in an ice bath to prepare the reaction solution for the initiator. The solutions were combined and the polymerization was carried out for 10-15 minutes. Pheylboronic acid was used to end-cap the polymer chains in order to remove any residual bromines on the chain ends that could interfere with post-polymerization reactions. A sample reaction for this process is described below.

The apparati for this polymerization were two round bottom flasks equipped with Teflon coated stir bars. Both flasks were dried in a 124°C oven overnight and cooled under a nitrogen purge. Each flask was equipped with a rubber septum that allowed the solutions to be syringed in or out of the flasks while protecting the reactants from the air. The monomer solution flask had a nitrogen-filled balloon to further protect the atmosphere from the air.

The initiator solution was prepared in a glove box under an argon atmosphere by combining 0.4767 g (1.82 mmol) of 4-bromobenzophenone, 9 mL (2.22 mmol) of a tri-tert-butylphosphine,

(P^tBu_3) solution and 0.0492 g (0.052 mmol) of tris(dibenzylideneacetone)dipalladium (0) (Pd_2dba_3) in 36 mL THF. The ratio of initiator to phosphine to catalyst was 1:1.2:0.03 respectively. The solution was stirred at room temperature in the glove box for 1 hour to allow complete insertion of the catalyst into the aryl bromine bond of the initiator. Meanwhile, 3.0787 g (8.25 mmol) of the borolated thiophene monomer was combined in 150 mL THF with 12.4 mL (82.7 mmol) of an aqueous solution of potassium phosphate. The ratio of monomer to phosphate as 1:10. The reaction flask was placed in an ice bath and stirred at 0°C.

The initiator solution was taken into a syringe inside the glove box. The syringe was taken from the glove box and solution was immediately injected into the chilled monomer solution through the septum. The reaction flask remained in the ice bath at 0°C as the polymerization was allowed to proceed for 15 minutes. To the reaction solution was added 6.6855 g (54.8 mmol) phenylboronic acid. The flask was removed from the ice bath and warmed to room temperature. The solution was stirred at room temperature overnight. A reaction schematic for this procedure can be seen in Scheme 3.

The following day, the polymer was extracted with dichloromethane, (DCM). The solution was concentrated via rotary

evaporation, and the catalyst was removed by passing the solution through a small silica gel column. THF was the initial eluent used for the column. However, polymer remained at the top of the column after THF had been passed through. Chloroform was used to wash the rest of the polymer from the column. The two solvent fractions were characterized separately. In each case, solvent was removed by rotary evaporation and the sample was freeze-dried using benzene prior to characterization.

Polymerization of PFO from 4-bromobenzphenone was carried out just as described for P3HT above.

Polymerization of P3HT from 4-bromobenzyl alcohol

The polymerization of P3HT from 4-bromobenzyl alcohol was carried out in the same fashion as described above for the polymerization of P3HT from 4-bromobenzophenone. The molar ratios of reactants were the same. Additionally, the procedure for polymerization and work-up where identical. A reaction schematic for this procedure can be seen in Scheme 3.3.

Characterization Techniques

Gas Chromatography/Mass Spectroscopy (GC-MS)

GC-MS was performed on an Agilent 7890A gas chromatograph equipped with an Agilent 5975C inert XL EI/CI MSD. Samples were introduced to the system with an Agilent 7683 Series autosampler and Agilent 7683B Series injector. The carrier gas was argon.

Nuclear Magnetic Resonance Spectroscopy (NMR)

Nuclear magnetic resonance spectroscopy (NMR) was performed on a Varian 500 MHz spectrometer. Deuterated chloroform was used as the solvent, and samples were prepared at a concentration of 10 mg/mL. Each sample was analyzed at 25°C. 128 scans were collected with a 45° pulse angle and 5 second relaxation time.

Size-Exclusion Chromatography (SEC)

Size exclusion chromatography (SEC) was performed using an Agilent 1260 HPLC pump system, equipped with four PhenoGel columns (all columns 10 μm particles; 7.8 mm x 300 mm column dimensions; 2 x

10E05 Å, 1 x 10E04 Å, 1 x 10E03Å; in series) in THF eluent at a flow rate of 1.0 ml/min and temperature of 35°C. The system was equipped with an Agilent 1260 UV detector operating at 254 nm, a Wyatt Dawn Heleos-II 18-angle light scattering detector, and a Wyatt Optilab T-rEX differential refractometer. Astra software was used to calculate molecular weights from light scattering.

Matrix-Assisted Laser Desorption/Ionization – Time-of-Flight Mass Spectroscopy (MALDI-TOF/MS)

MALDI-TOF/MS was performed using a Bruker Daltonics Autoflex II mass spectrometer equipped with a N2 laser (λ=337 nm) with 25 Hz frequency and accelerating voltage of 20 kV. The matrix was trans-2-[3-(4-tert-butylphenyl)-2-methyl-2-propenylidene]malononitrile (DCTB, >99%, Fluka). Solutions of the matrix and samples in THF were made at concentrations of 20 mg/mL and 10mg/mL respectively. The ratio of matrix to sample used for collection of spectra was 5:1, and spectra were collected in reflectron mode employing an external calibration using polystyrene standards.

Results

In this work, functionalized P3HT was achieved using two different initiating molecules, 4-bromobenzyl alcohol and 4-bromobenzophenone. In each case, propagation began after insertion of the palladium catalyst into the aryl bromine bond of the initiator. Termination of the polymerization with phenylboronic acid was important as it removed the bromine from the growing chain end which prevented interfering side-reactions in subsequent reactions with the P3HT samples. The next chapter of this dissertation will detail the addition and growth of other arms on the benzophenone-functionalized P3HT to form miktoarm star block copolymers.

The investigation into using this polymerization method for synthesis of functionalized P3HT began using 4-bromobenzyl alcohol as the initiator. The approximate ratio of reactants were ascertained through a collaboration with Dr. Qiao-Sheng Hu's research group at City University of New York, College of Staten Island. Their interest in these reactions was to study the mechanism and kinetics of the palladium-catalyzed cross-coupling. After spending time working with Dr. Hongai Zhang of their group both at their labs in New York as well as at the Center for Nanophase Materials Science (CNMS) at Oak Ridge National Laboratory, we were able to scale-up and slightly alter the polymerization

reaction to produce enough polymer for in-depth characterization as well as further reactions toward block copolymer systems.

In the case of polymerization of P3HT from 4-bromobenzyl alcohol, early reactions failed to produce polymer while we modified the synthetic procedure from that of the CUNY group. Although they performed most of the reaction in a glove box, preparing both solutions in the glove box and bringing them out only for the polymerization, we desired to utilize the glove only as much as necessary. With that goal in mind, we attempted to combine the monomer solution in the fume hood rather than the glove box. We knew the ratio of THF to water that was required to properly facilitate Suzuki polymerization, but adding solid K_3PO_4 to the flask allowed contamination of the headspace in the reaction flask despite careful attempts to prevent this. Contamination caused failed polymerization attempts. This issue was overcome by making an aqueous solution of K_3PO_4 at a concentration such that the proper amount of water and K_3PO_4 would be added together. By having a solution rather than a solid, all reactants could be added via syringe through the rubber septum, thereby protecting the nitrogen headspace from any air that might foul the reaction. This modification to the procedure was successful and P3HT was produced from every subsequent reaction.

Functionalized P3HT synthesized using this Suzuki polymerization method had molecular weights between 5000 and 8000 g/mol Inability of Suzuki polymerization to produce conjugated polymers with molecular weights above 10000 g/mol remains a limitation of the method. Using the ratio of monomer to initiator described in the sample procedure detailed above, functionalized P3HT with molecular weight around 6000 g/mol was obtained. Lower molecular weight P3HT was also produced during these polymerizations, but these lower molecular weight polymer chains contained a mixture of end-groups.

As described above, two solvent fractions were obtained from the silica gel column used to remove the catalyst from the concentrated polymer solution. The higher molecular weight fraction collected using chloroform as the eluent consistently showed a very high degree of functionality according to MALDI-TOF. A labeled MALDI-TOF spectrum of the chloroform fraction of JR-2-105 can be seen in Figure 3.1. A small amount of non-functionalized P3HT is observed in the spectrum, but the desired 4-bromobenzyl alcohol-functionalized P3HT constituted more than 90% of the sample. The MALDI-TOF spectrum of the THF fraction of the same sample was more of a mixture of end-groups. The sample was of very low molecular weight and as a result, the spectrum was cut-off because the MALDI-TOF instrument suppresses signals below m/z=1000 in order to eliminate matrix signals that would

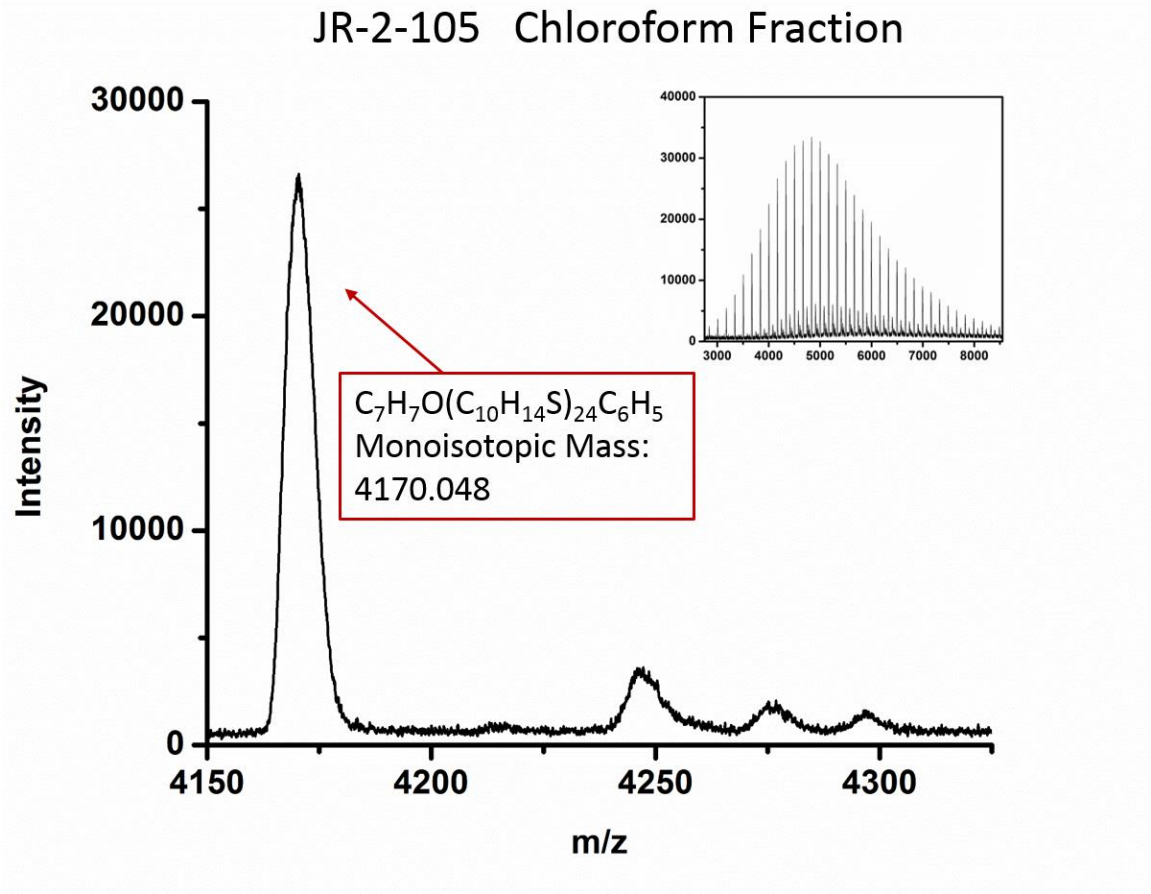

Figure 3.1: MALDI-TOF spectrum of the chloroform fraction of JR-2-105.

overpower the sample signals. It was still evident, however, that the desired functionalized P3HT is only a part of the mixture of end-groups present. The rest of the mixture includes P3HT with phenyl rings on each end as well as P3HT chains with a phenyl ring on one end and a proton on the other.

The results were very similar for P3HT initiated from 4-bromobenzophenone. The THF fraction collected during the column chromatography contained a mixture of end-groups. These end-groups were the same observed in the THF fractions of the benzyl alcohol-functionalized P3HT samples. However, 100% functionalized P3HT was observed in the chloroform fraction of JR-2-062. The MALDI-TOF spectrum and SEC trace for this sample can be seen in Figures 3.2 and 3.3. The MALDI-TOF spectrum of the THF fraction showed a mixture of end-groups just as described for JR-2-105 above.

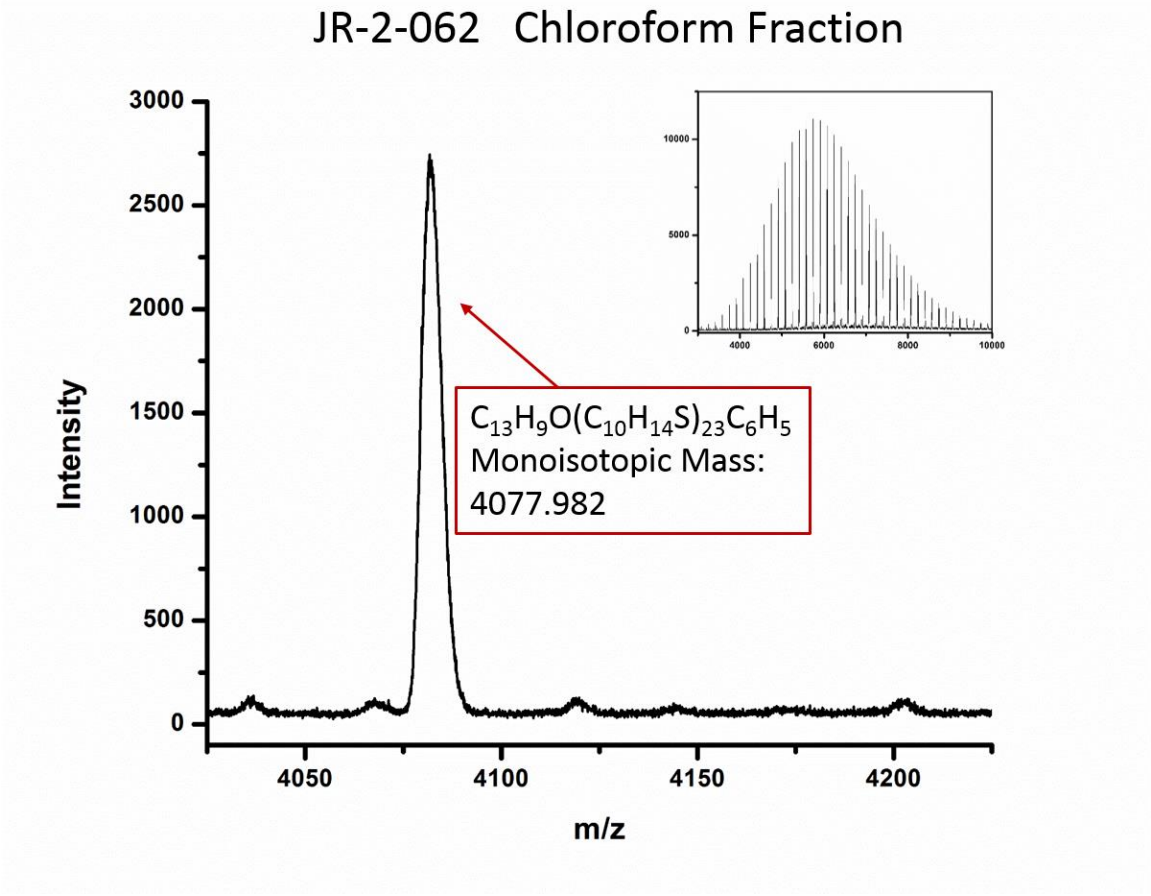

Figure 3.2: MALDI-TOF spectrum of the chloroform fraction of JR-2-062

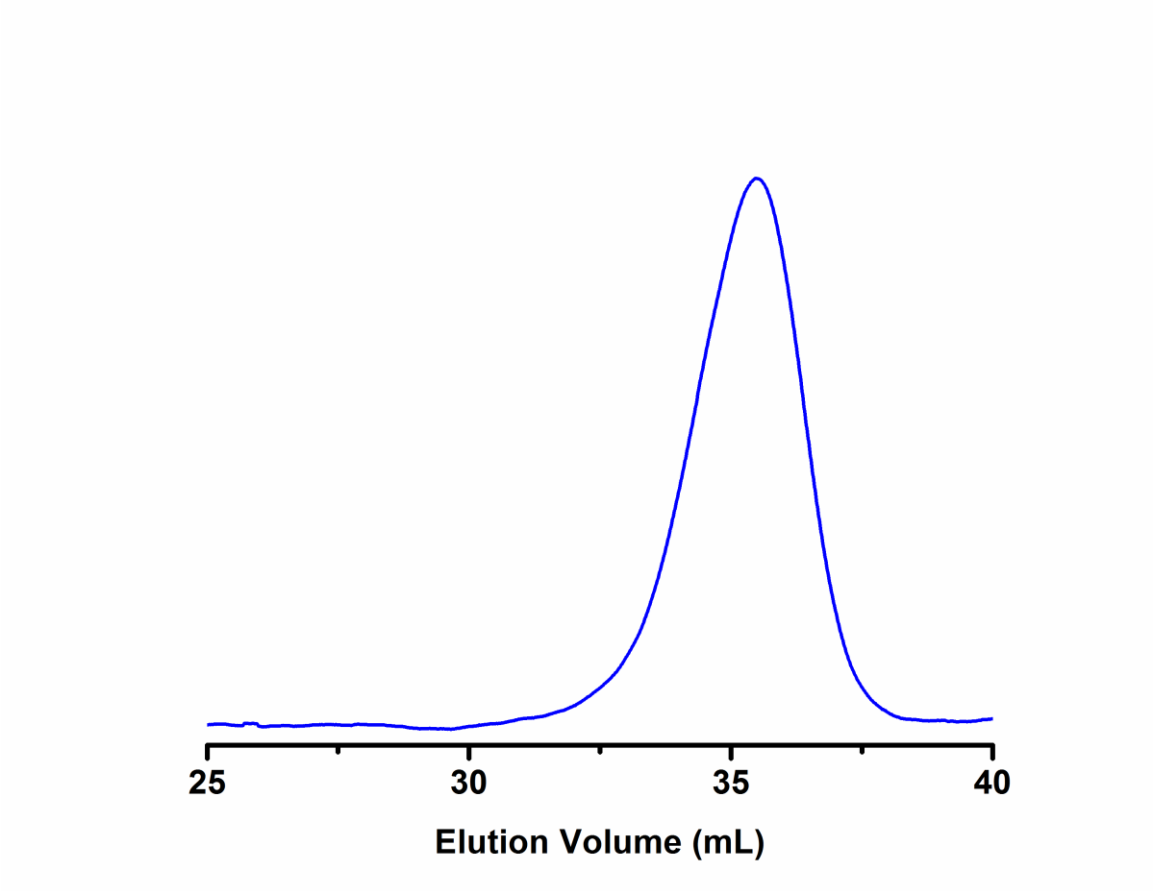

Figure 3.3: SEC trace for the chloroform fraction of JR-2-062

CHAPTER 4

SYNTHESIS AND MORPHOLOGICAL STUDY OF MIKTOARM STAR BLOCK COPOLYMER INCORPORATING P3HT, PI AND PEO

Abstract: The ability to synthesize miktoarm star block copolymers incorporating P3HT and other conjugated polymers may lead to improved materials for device applications. It has been shown by theoreticians and experimentalists that increases in the branching of block copolymer molecular architecture can lead to different morphologies than those observed at the same volume fraction in linear diblock copolymers [150-156]. The synthetic procedures described in this chapter possess the versatility to be expanded beyond the scope discussed here to even more conjugated and non-conjugated polymers. We detail here the synthetic procedure by which these materials were produced. We also show NMR and GPC data that confirm their structure.

Introduction

Block copolymers have long been used as a way to tailor the properties of copolymer systems in such a way that maintains morphological control over the material so as to influence the final properties of the material. For decades, seemingly countless combinations of coil-coil block copolymers have been studied to investigate the effects of such things as volume fraction of each component and the Flory-Huggins interaction parameter, x. The interaction parameter describes how strongly the two different polymers will segregate from each other. As a result of this preference, interactions between two (or more) components of the copolymer system lead to phase separation and a variety of morphologies. Based on the interaction parameter and volume fractions of each component, Matsen and Bates were able to construct the well-known phase diagram shown in Figure 1 which depicts the expected morphology of coil-coil block copolymer systems [157]. An understanding of how to manipulate this phase separation behavior using volume fractions has led to a great number of common, valuable materials. This approach has worked well for coil-coil copolymer systems where x and volume fraction are the driving forces behind phase separation.

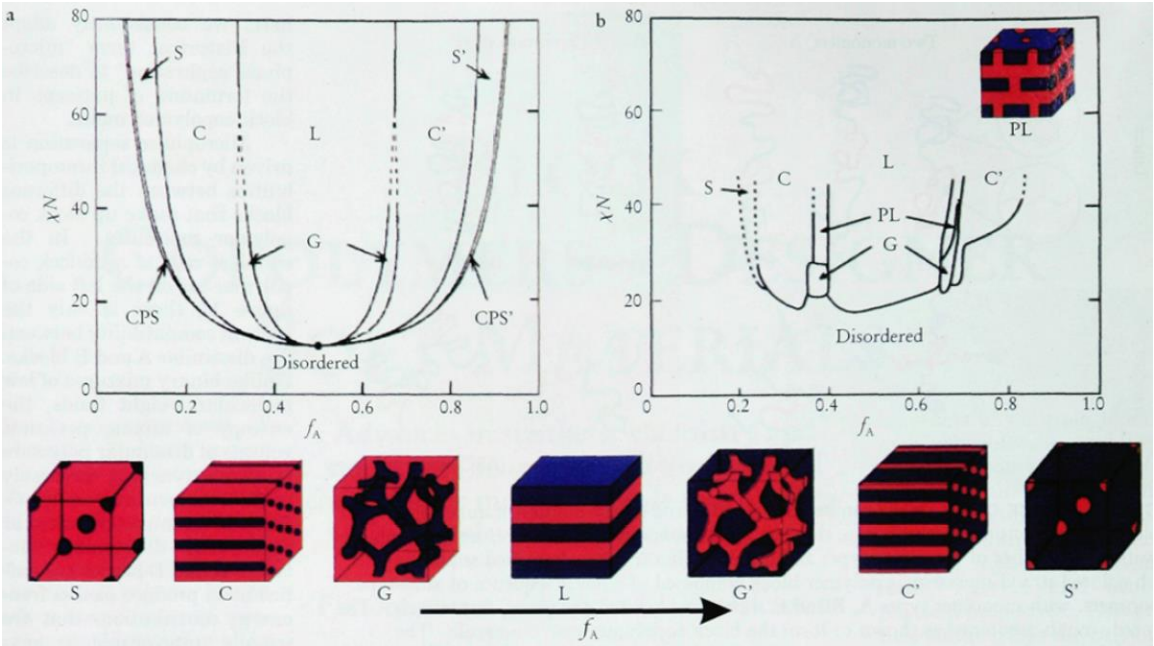

Figure 4.1: Phase diagrams for coil-coil diblock copolymers. The phase diagram on the left represents Bates and Matsen's theoretical work [157]. The phase diagram on the right is a result of experimental work, and the cubes along the bottom provide 3-D representations of the possible morphologies. Refs [157-159]

When a rod-like polymer, such as P3HT, is introduced to copolymer systems the dynamics of self-assembly behavior are impacted. No longer can only x and volume fraction be considered when predicting the morphology of the material. In the case of P3HT, the π-stacking that results from the conjugation of the backbone plays a large role in how block copolymer systems self-assemble. However, even in systems where the rod-like component is not conjugated and does not exhibit such π→π interactions, the stiffness of the rod changes the phase diagram of such systems by impacting the effective hydrodynamic volume of the stiffer chain. This causes shifts in morphology as a function of volume fraction to be toward more flat interfaces. These shifts limit the number of different morphologies available across the range of usable volume fractions, thereby, limiting the applicability of these block copolymer systems. Rod-coil block copolymer systems remain under-studied when compared with coil-coil bock copolymers, but there are fundamental truths that allow researchers to understand and manipulate these systems.

One method for addressing these adverse morphological effects is through the use of miktoarm star block copolymer architectures. Miktoarm stars are block copolymers consisting of three or more arms which are all joined to a common core molecule. There are different approaches to the synthesis of miktoarm stars. In some cases, the

polymer arms are grown successively from the core. Other times, the polymer arms are first synthesized before being attached to the core molecule. Our approach in this work was a combination of the two methods. As described in the previous chapter, Suzuki polymerization enabled the functionalization of P3HT through ex-situ initiation of the polymerization. The functionalities imparted were chosen to facilitate the formation of block copolymers, and benzophenone, in particular, was used to allow the addition of living anionic polymer chains to form miktoarm stars. The reasoning for our approach can be traced back to theoretical work performed in the mid-1990s. In 1994, Scott Milner published a work in which he examined the effects of chain architecture and asymmetric elastic properties of copolymers on their self-assembly behavior in the strong-segregation region. From this work he generated a phase diagram, Figure 4.2, for these systems that displayed some very observations. The x-axis of Figure 4.2 is the volume fraction of component B, φB, while the y-axis is different than the Flory-Huggins phase diagram in Figure 4.2. Milner incorporated both the number of arms of each component and the elastic parameters of each component into a single parameter, ε. If the two components are the same, and the volume fraction remains constant, Milner's phase diagram allows the prediction of morphology as a function of branching.

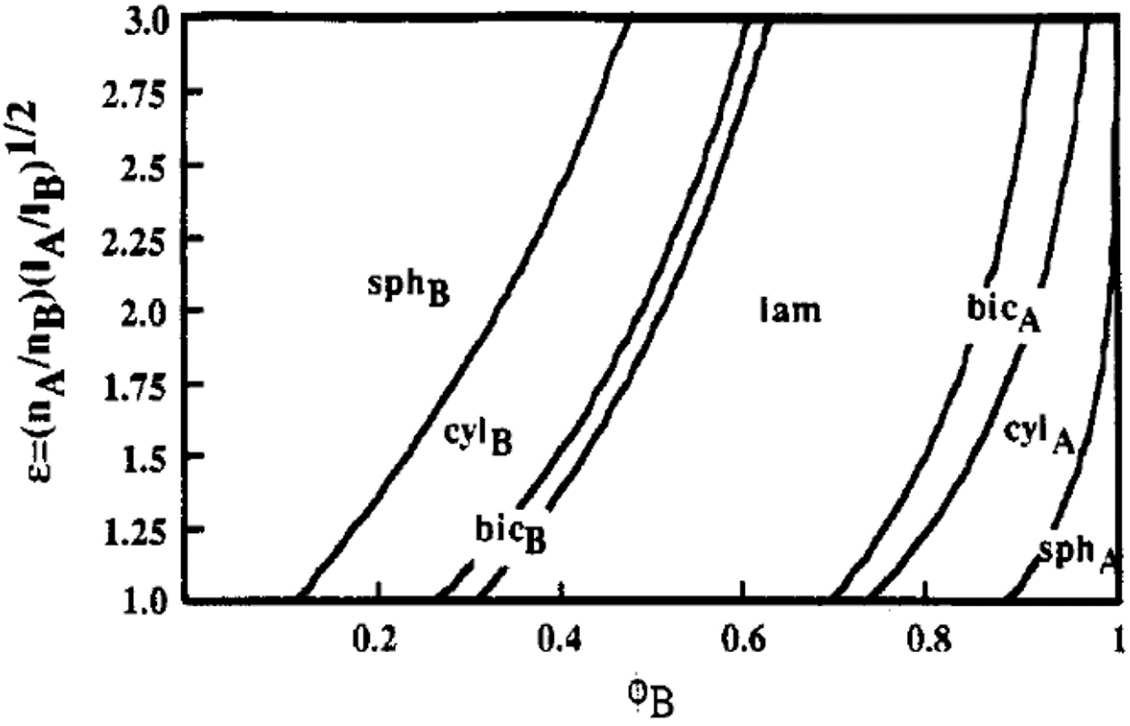

Figure 4.2: Milner's phase diagram for the strong-segregation region for a block copolymer containing polymers of much different elasticities

Milner predicted with his calculations, which have been confirmed by experimentalists, that increased branching in these copolymer systems leads to increased curvature at the interface. For example, looking at a linear block copolymer with φB equal to 0.5, the expected morphology would be lamellar. This prediction is consistent with Flory-Huggins as equal parts of the two components would separate to produce layers of each component. However, as branching is increased by having two arms of component A, the morphology changes to cylinders of B. When branching is increased further to three arms of A, Milner predicts a morphology of spheres of B. He explained these predictions in terms of chain stretching. If volume fractions are held constant, but component A now has two arms instead of one, those new arms of A are only half as long as the arm of B. As a result, the arms of A would have to stretch further to achieve the same lamellar morphology observed in the linear diblock system. Instead of increased stretching, component A would take on a more curved posture. The same concept can be extended to higher numbers of arms. As the number of arms are increased while holding volume fractions constant, curvature at the interface is more favorable.

Previously in this dissertation, the effects of molecular weight of P3HT on polymer blends have been extensively discussed. The effects of increases in molecular weight can be extended to understand the effects

of increasing the volume fraction of P3HT in linear diblock copolymer systems. Just as P3HT at relatively high molecular weights can essentially hijack morphological control of the system due to its crystallinity behavior, P3HT present in relatively high volume fractions can do the same. At higher volume fractions, there just is not enough of the copolymer present to adequately disrupt the π-stacking of P3HT. Defects in regioregularity can also disturb π-stacking, but this interference comes at the cost of reducing charge transport properties. In order to maximize the electronic properties of P3HT and still be able to incorporate enough of this polymer to make efficient materials for optoelectronic applications, another approach is needed. Based on the fundamental findings of Milner, our assertion is that incorporating P3HT into miktoarm star block copolymer systems will provide opportunity to fulfill both of these preferences. The increase in branching will encourage curvature of the interface with will help to overcome trapping of morphology due to the crystallization behavior of P3HT. By reducing this demerit of these systems, more P3HT will be able to be incorporated into materials without losing morphological control. In addition, miktoarm star block copolymers have been shown to be an effective vehicle to impart long-range order across block copolymeric materials.

Synthetic Procedures

Functionalized P3HT and PFO were synthesized and purified as described in the previous chapter. For the first attempt at a miktoarm star block copolymer described below, JR-2-096 was used as the starting material. This P3HT sample had a Mn=4.9 kdal/mol, Mw=5.0 kdal/mol, and PDI-1.02 according to MALDI-TOF. MALDI-TOF spectrum and SEC chromatogram can be seen in Figures 4.3 and 4.4, respectively. High-vacuum techniques were required for the addition of living $PI^{-}Li^{+}$ to the star core. Subsequently, ethylene oxide was grown anionically from the star core to complete the ABC miktoarm star. A specialized blown-glass reactor was constructed by Dr. Kunlun Hong of the CNMS at ORNL to carry out the anionic addition and growth of the PI and PEO arms on the star core. Illustrated in Figure 4.5, the reactor consisted of a flask with two side arms and a ground glass fitting for connection to the vacuum line. A constriction was on the neck of the ground glass fitting to allow the reactor to be cut from the vacuum line.

On one side arm of the reactor, an ampuole of living PI-Li+ was attached. On the other side arm, an ampuole of P4 base and an ampuole of ethylene oxide were attached. The walls of the reactor were silylated with chlorotrimethyl silane prior to addition of reagents.

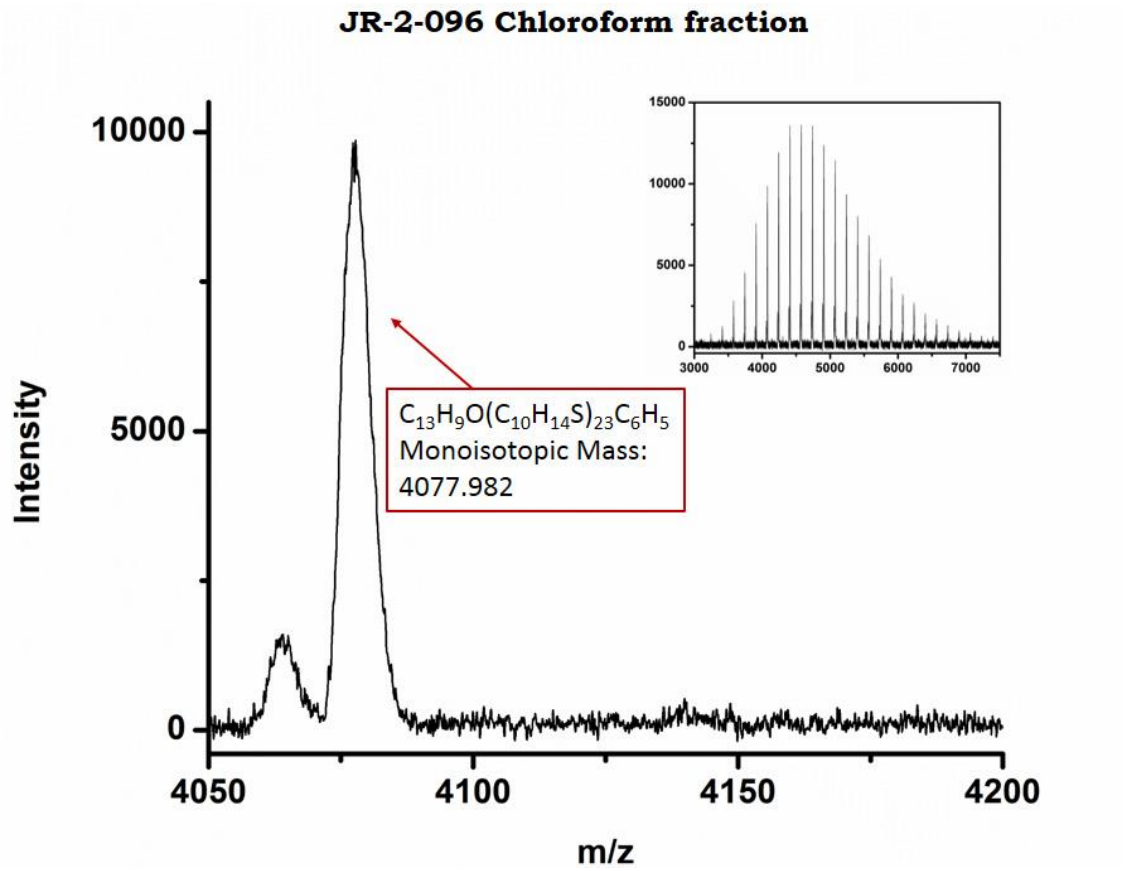

Figure 4.3: MALDI-TOF spectrum of the starting material (JR-2-096) for the synthesis of miktoarm star block copolymer.

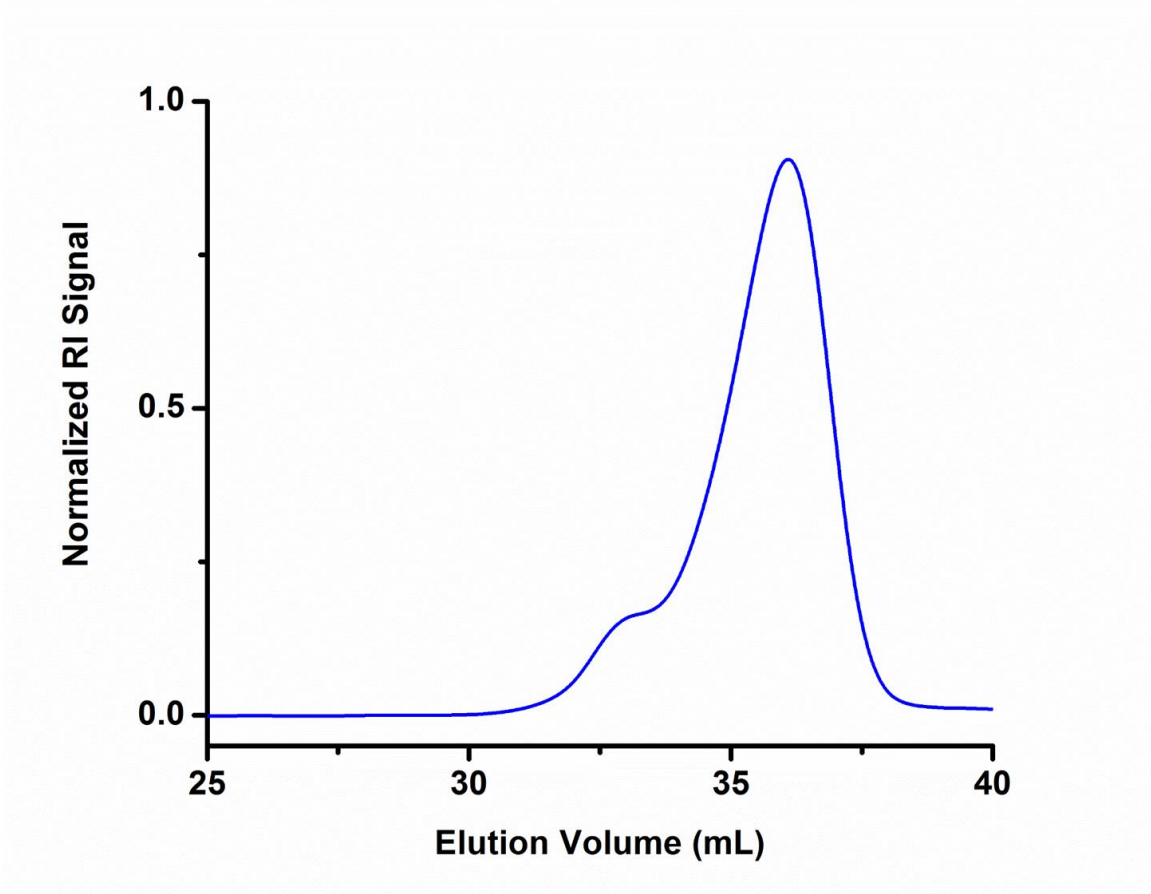

Figure 4.4: SEC trace of the starting material (JR-2-096) for the synthesis of miktoarm star block copolymer.

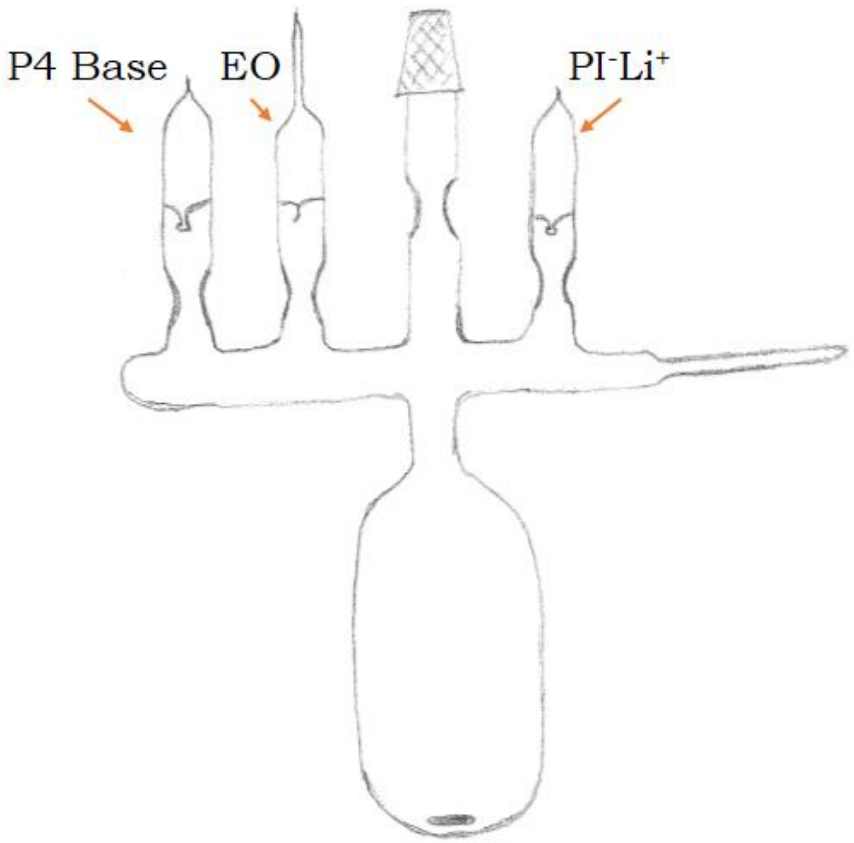

Figure 4.5: Illustration of reactor used in reaction to synthesize P3HT-PI-PEO miktoarm star block copolymer

100 mg of P3HT was placed in the reactor, and a small amount of benzene (2-3 mL) was used to ensure quantitative transfer of the polymer. The benzene was frozen using liquid nitrogen and the reactor was placed on the vacuum line. The benzene was removed under dynamic vacuum and the polymer remained under dynamic vacuum overnight. The following day 15 mL of THF was distilled from over sodium metal into the reactor. The reactor was placed under static vacuum. The solution was slightly heated with a heat gun in order to get the polymer to go completely into solution. Once dissolved, the polymer remained in solution even when the solution returned to room temperature. The constriction on the neck of the reactor was washed with pure solvent using a towel dipped in liquid nitrogen to ensure no polymer residue was present, and the reactor was cut from the vacuum line at the constriction using a torch.

The breakseal on the ampoule containing living PI-Li+ solution in benzene was ruptured to allow reaction of the living polymer with the carbonyl on the benzophenone end-group of P3HT. Reaction continued for 30 hours. The solution was then heated to 40°C and the breakseal on the ampuole containing the P4 base was ruptured. The solution was stirred for 10 minutes at which time the breakseal on the ampuole containing ethylene oxide was ruptured. The solution stirred at 40°C for

18 hours to form the miktoarm star block copolymer. A schematic of this procedure can be seen in Scheme 4.1.

Characterization Techniques

Nuclear Magnetic Resonance Spectroscopy (NMR)

Nuclear magnetic resonance spectroscopy (NMR) was performed on a Varian 500 MHz spectrometer. Deuterated chloroform was used as the solvent, and samples were prepared at a concentration of 10 mg/mL. Each sample was analyzed at 25°C. 128 scans were collected with a 45° pulse angle and 5 second relaxation time.

Size-Exclusion Chromatography (SEC)

Size exclusion chromatography (SEC) was performed using an Agilent 1260 HPLC pump system, equipped with four PhenoGel columns (all columns 10 μm particles; 7.8 mm x 300 mm column dimensions; 2 x 10E05 Å, 1 x 10E04 Å, 1 x 10E03Å; in series) in THF eluent at a flow rate

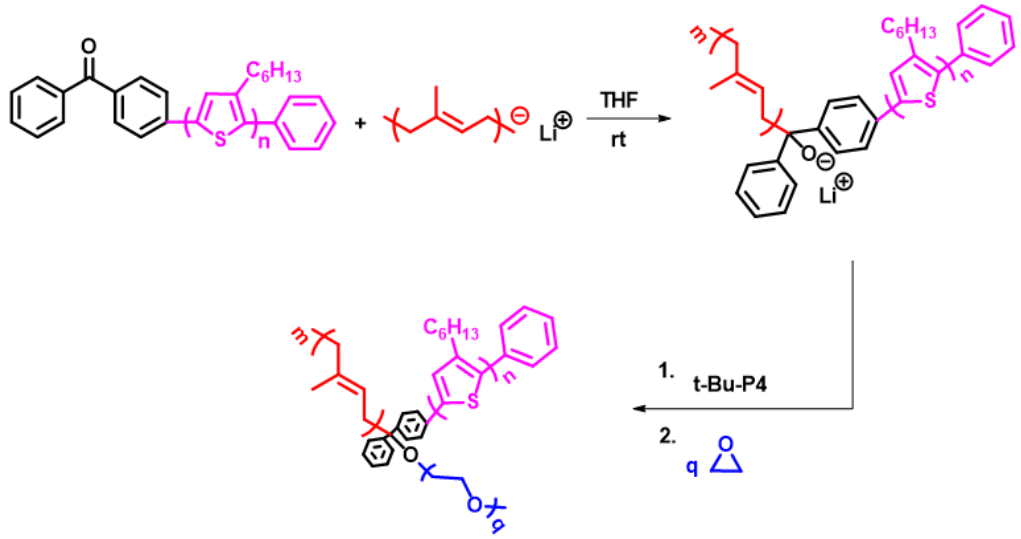

Scheme 4.1: Reaction schematic of synthesis of P3HT-PI-PEO miktoarm star.

of 1.0 ml/min and temperature of 35°C. The system was equipped with an Agilent 1260 UV detector operating at 254 nm, a Wyatt Dawn Heleos-II 18-angle light scattering detector, and a Wyatt Optilab T-rEX differential refractometer. Astra software was used to calculate molecular weights from light scattering.

Results

The synthesis of an ABC-type miktoarm star consisting of P3HT, PI, and PEO was monitored by SEC after each step. An aliquot of the reaction solution was taken prior to addition of ethylene oxide to examine the extent to which the P3HT-PI diblock copolymer had been formed. We observed complete formation of the diblock copolymer. After addition of ethylene oxide monomer and reaction, however, there was no discernable change in the SEC trace indicating limited to no growth of PEO from the oxyanion generated when living PI added to the carbonyl of the benzophenone. These SEC traces can be seen in Figure 4.6.

With SEC giving no indication of a third arm being present, the sample was analyzed using NMR spectroscopy. The results indicate The presence of PEO, albeit a small amount. Figures 4.7-4.9 show overlaid NMR spectra from each step of the synthesis. Figure 4.7 shows the full

spectra, Figure 4.8 is zoomed in on the region where the $-CH_2O$ signal of PEO is expected. Figure 4.9 is zoomed in even further to show the triplet associated with PEO. These results indicate a mixture of diblock and miktoarm star copolymers with the diblock being the major product present. The growth of PEO is a slow process, and it is possible that extended reaction time for that step in the procedure would increase the amount of PEO on the star core.

Conclusion

In conclusion, we have shown the ability to anionically add living PI to the functionalized P3HT synthesized in the previous chapter. The mixture of diblock copolymer and a small amount of miktoarm star block copolymer in the final material indicates that reaction conditions need to be modified to produce the miktoarm star in greater yield. Nonetheless, our work in the synthesis of highly functionalized conjugated polymers described in Chapter 3 of this dissertation shows that different conjugated polymers could be incorporated in miktoarm star block copolymers using this approach. Additionally, our use of anionic polymerization techniques to add the second arm and grow the third arm opens the possibility for a wide variety of different polymers to be

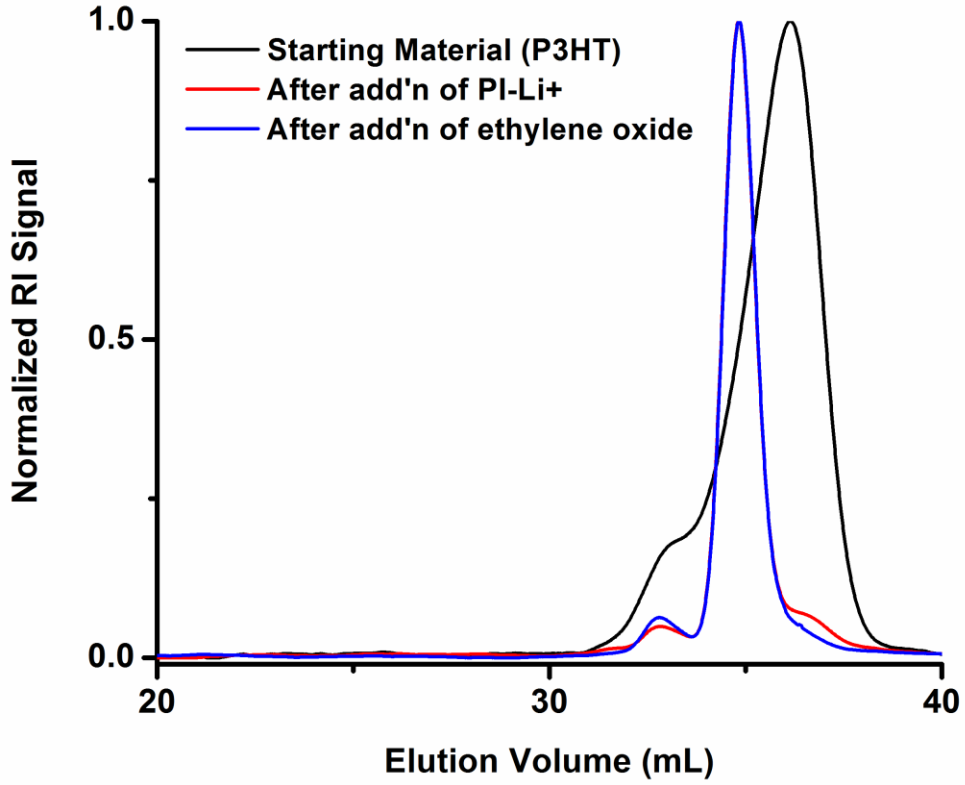

Figure 4.6: SEC traces from each step of the miktarm star block copolymer synthetic process

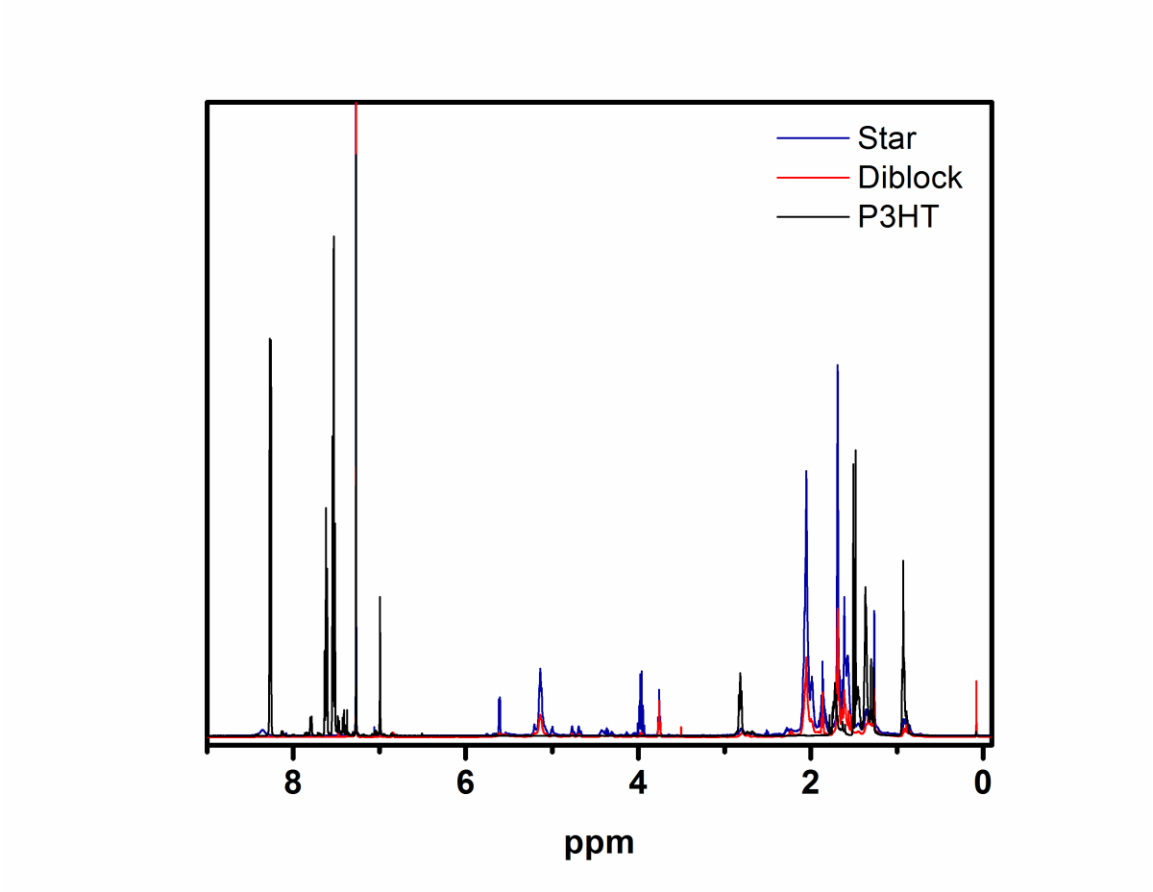

Figure 4.7: Full NMR spectra of the miktoarm star block copolymer after each step.

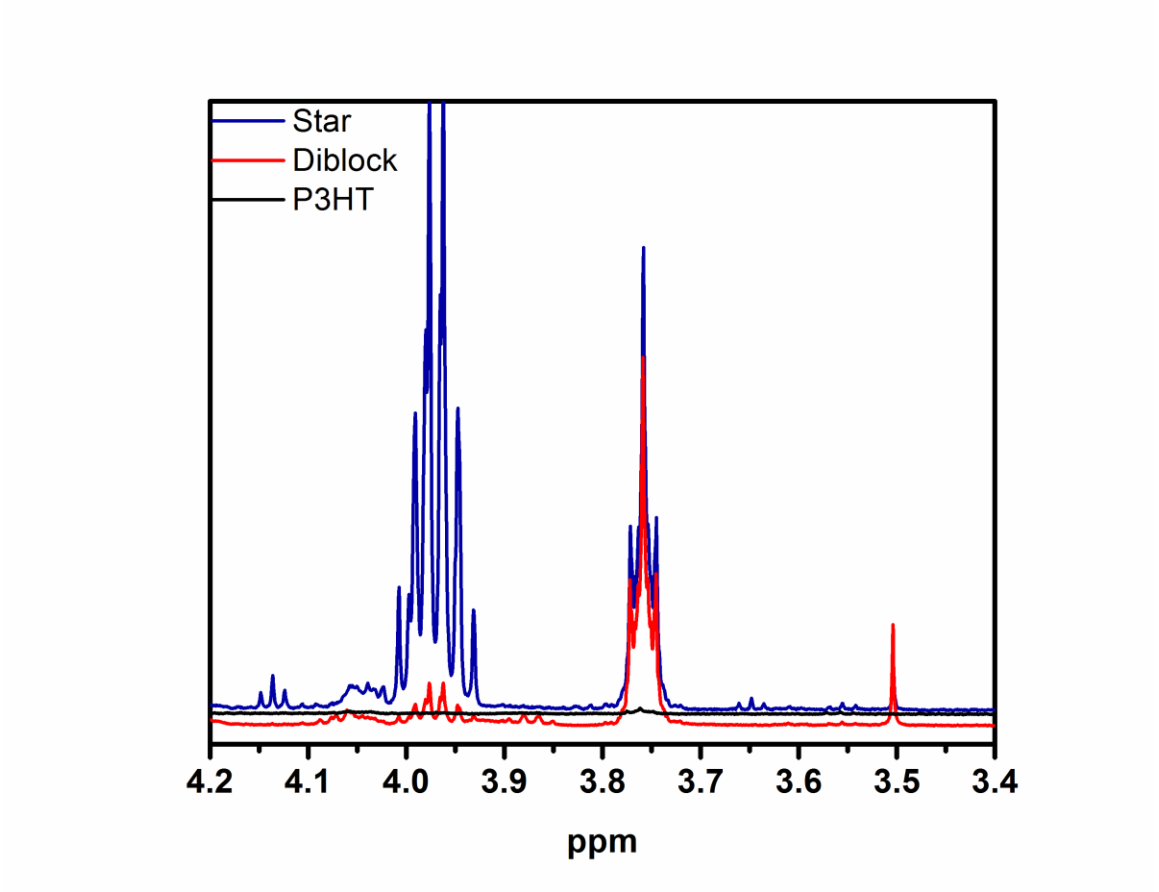

Figure 4.8: An expanded view of the region of the NMR spectrum where the -CH2O- signal of PEO should be seen.

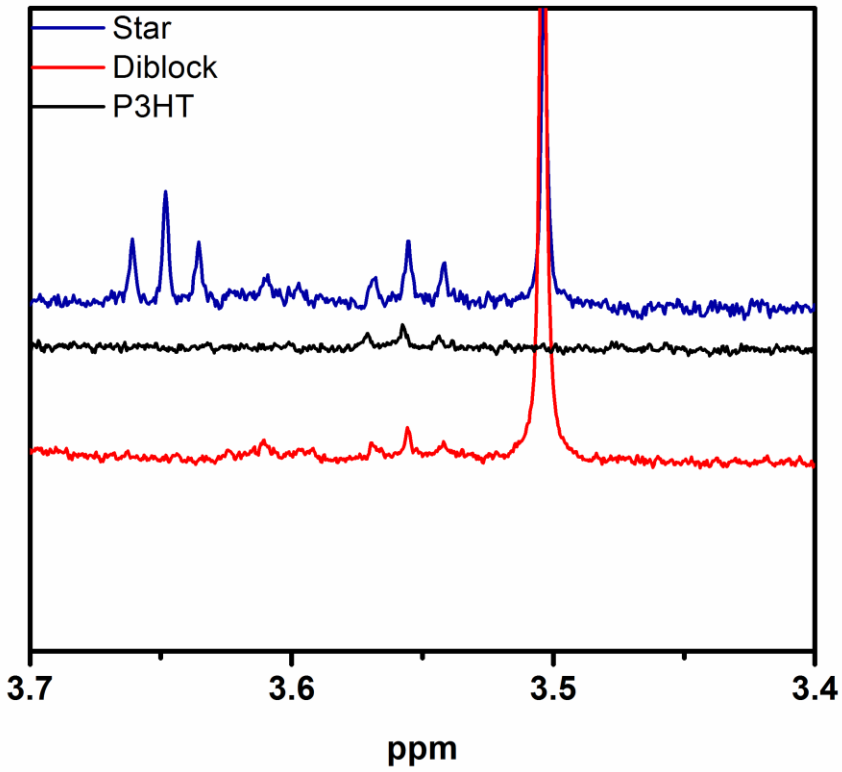

Figure 4.9: A closer zoom of the ^{1}H NMR spectrum focusing on the PEO triplet at 3.65 ppm

included in future systems synthesized in this manner. More discussion of these possible next steps can be found in the “Future Works” section of the following chapter.

CHAPTER 5

CONCLUDING REMARKS AND FUTURE WORKS

Abstract: Throughout this dissertation, the motivation has been to understand conjugated polymers on a fundamental level so that block copolymer systems may be designed to maximize efficiency of these materials for device application. We began by studying the dilute solution behavior of P3HT in an effort to develop a concise and accurate way to find the true molecular weight of these polymers. Our findings excluded the use of a universal calibration for P3HT, thought to be due to its extended chain conformation. The synthetic portion of this work began by developing an approach by which conjugated polymers with high degrees of functionality could be synthesized. Using a modified Suzuki polymerization method, we were able to synthesize P3HT and PFO with desired functionalities. Further proving the utility of functionalized conjugated polymers, we used one of our samples to produce a miktoarm star block copolymer in a manner not previously reported. Our work here has served to further the field of conjugated polymers for organo-electronic applications. Concluding remarks on this project as well as the future direction that should be taken are discussed in this chapter.

Concluding Remarks

In the field of conjugated polymers, there is an ever-advancing march toward improving the efficiency of these materials for optoelectronic device applications. Often times, these improvements are sought by incorporation of different copolymers or polymers in blends that enhance the electronic properties of conjugated polymers which have garnered the intense attention of researchers for nearly two decades. However, to some degree, a lack of fundamental understanding of how to properly characterize these polymers has proven to be a hindrance to these attempts. This problem is no more evident than in molecular weight characterization. Before the turn of the century, McCullough et al. reported the shortcoming of conventional calibration of SEC to properly determine the true molecular weight of P3HT due to the extended chain confirmation of the stiffer P3HT which causes it to possess a larger hydrodynamic volume than its PS analogue. This in turn makes SEC render a value for molecular weight that is higher than reality. Due to its ease of use, however, SEC analysis relative to PS standards remains the most common method for determining the molecular weight of P3HT.

We sought to address this issue through a systematic dilute solution properties study of P3HT homopolymer. We synthesized P3HT samples that spanned molecular weights from around 3.0 kdal/mol to more than 30 kdal/mol. We began by taking refractometry measurements of each sample to determine the refractive index increment (dn/dc) of the polymers in two of the most commonly used solvents for these materials, THF and chloroform. Our data indicated no molecular weight dependence of dn/dc of P3HT in either solvent across the molecular weight range studied. The dn/dc values we obtained were 0.26 mL/g in chloroform and 0.32 mL/g in THF. These values represent the average across the series of samples and are in agreement with dn/dc values reported in literature.

In order to determine the regioregularity of each sample, NMR was employed. The controlled polymerization methods that were used to synthesize these polymers consistently yield polymer chains with a high degree of regioregularity. The regioregularity of each sample except for one was determined to be equal to or greater than 95%. Sample JR-2-083 had a regioregularity of only 91% but this sample only had a DP around 11. The initiating dimer that is formed when P3HT begin propagation is tail-tail coupled which means there is always at least a single region-defect. It is this initial region-defect in the very short chain that is reflected in the lower regioregularity, not a flawed synthesis.

MALDI-TOF MS was used to examine the end-groups of the polymer chains. Limitations of MALDI-TOF to analyze larger P3HT samples prevented every sample from being analyzed in this manner, but the results that were obtained indicate that there was a mixture of different end groups on these polymer chains. The inclusion of H/H and Br/Br end-groups to such a degree as observed indicates improper Grignard exchange reaction occurred prior to polymerization. This was most likely due to a concentration of the Grignard reagent that was lower than expected. The notable exception to this conclusion is again JR-2-083 which had 100% H/Br end-groups suggesting that this polymerization occurred with completely converted monomer. JR-2-075 and JR-2-083 were synthesized later than the rest to examine the dilute solution behavior of oligimeric and very low molecular weight polymers. The Grignard reagent used for these syntheses was freshly opened, and the two samples were synthesized within a couple of days of each other. Better care should have been taken with the earlier samples to monitor monomer conversion prior to addition of the nickel catalyst. This could have been achieved by analyzing the monomer solution with GC/MS.

With the structural characterization complete, and using the dn/dc values obtained from the refractometry measurements, we next embarked on applying universal calibration of SEC to P3HT. Using an SEC instrument equipped with triple detection (viscometer, light

scattering detector, and refractive index detector) we collected data for each sample. We analyzed the data using several different methods. As a starting reference point, we analyzed the RI data using conventional calibration relative to narrow PS standards. Our knowledge of the dn/dc values for these samples allowed us to determine the absolute molecular weight of each sample using the light scattering data, and the values of Mw found using light scattering were plotted versus the intrinsic viscosity values obtained during these runs on a log-log plot to determine the Mark-Houwink parameters for this polymer/solvent system. In this way, the viscometry measurements allowed the application of a universal calibration curve to the data in order to assign a molecular weight.

Comparison of these three methods confirmed that conventional calibration of SEC relative to PS overestimates the molecular weight of P3HT. This was not surprising, but this direct comparison with light scattering analysis served to show how flawed the values given using this method truly are. When the light scattering molecular weights were compared with the same values determined using universal calibration, they did not match up. The weight-average molecular weights obtained from these two methods were plotted against each other, and the slope of the linear fit line on this plot had a slope of 0.73. This result showed conclusively that universal calibration of SEC is not applicable to P3HT as agreement between the data would have produced a plot with a linear

fit line with a slope of 1. It was therefore concluded that the two best methods for determining the true molecular weight of P3HT samples are to use light scattering or intrinsic viscosity. Light scattering analysis using SEC can be simplified across this molecular weight range now that it has been determined that dn/dc is not molecular weight dependent. Additionally, using the Mark-Houwink parameters, intrinsic viscosity of a sample can be converted to molecular weight.

Concerning the first synthetic portion of the research contained in this dissertation, we were able to synthesize conjugated polymers with consistently high degrees of functionality. This was an important fact as it provides a synthetic route to block copolymer systems that will allow researchers to explore materials not previously possible. While we are not the first to report the synthesis of miktoarm star block copolymers incorporating P3HT, the synthetic method we have developed has been shown to be quite versatile. The modified Suzuki polymerization as described in this work has proven to be an effective avenue to the synthesis of both polythiophenes and polyfluorenes with high degrees of functionality. This is an essential property of these conjugated polymers in order to produce block copolymers with different molecular architectures. Miktoarm star block copolymers were the goal of this project from the outset, and this method for the production of highly functionalized P3HT provided the means to reach that goal.

The final portion of this dissertation work was the synthesis of miktoarm star block copolymers from the functionalized P3HT discussed above. To achieve this, anionic polymerization was employed. The carbonyl on the benzophenone end-group of P3HT gave opportunity for attack by living polyisoprene. This coupled the polyisoprene to the P3HT to form a diblock copolymer. Additionally, the anionic coupling of the living chain to the carbonyl generated an anion at the junction point after attachment. This anion was used, along with P4 base, to initiate polymerization of ethylene oxide and grow the third arm of the miktoarm star.

We have succeeded in providing fundamental insight into proper molecular weight characterization of P3HT homopolymer, developed a method by which conjugated polymers may be synthesized with high degrees of functionality, and we have demonstrated that functionalized P3HT synthesized in this manner can be further reacted to generate miktoarm star. It was vital that the P3HT have controlled end-groups in order to allow for the addition of a PI arm and the subsequent growth of a PEO arm on the miktoarm star core.

Future Work

The versatile nature of the developed methodology leads to the conclusion that other conjugated polymers could be synthesized in like manner. Furans and phenylenes each possess similar properties and structures to thiophenes and fluorenes, and these two types of monomers would be excellent candidates for polymerization by the modified Suzuki method detailed here. While not as heavily studied as polythiophenes and polyfluorenes, polyfurans and polyphenylenes may well be able to contribute positive attributes if incorporated into block copolymer systems, and the methodology prescribed herein is capable of imparting functionality on these polymers that could lead to those types of molecular structures.

Furthermore, the efficiency of the ex-situ initiation by this method is not limited to the 4-bromobenzyl alcohol and 4-bromobenzophenone used in this work. These two initiators served as model compounds to illustrate the ability of Suzuki polymerization to grow conjugated polymers. Beyond simple proof-of-concept reactions, the benzophenone-functionalized P3HT enable the synthesis of an ABC-type miktoarm star. The aryl bromine bond appears to be the key to successful initiation from these molecules. With only that requirement, the number of possible ex-situ initiators for the growth of conjugated polymers is very great.

Impartation of different functionalities could lead to a wide variety of materials not previously possible.

The next steps in this research are to explore other monomers to ifu gkydcvudib ve9k;9j o0i4ml,o ;kvbj5jv32123456kverify that the Suzuki polymerization method is truly versatile enough to generate polymers beyond the two studied here. Ability to polymerize these other monomers could lead to different miktoarm stars according to the procedure developed here. In addition, fully-conjugated block copolymers by sequential monomer addition would serve to illustrate the living nature of this polymerization. All in all, this new approach to the synthesis of conjugated polymers presents a great opportunity to synthesize an extensive series of different block copolymers and molecular architectures that could lead to the next advance in the field of conjugated polymers for orano-electronic applications.

LIST OF REFERENCES

1. Chiang, C.K., et al., *Synthesis of highly conducting films of derivatives of polyacetylene, (CH)x.* Journal of the American Chemical Society, 1978. **100**(3): p. 1013-1015.

2. Chiang, C.K., et al., *Electrical Conductivity in Doped Polyacetylene.* Physical Review Letters, 1977. **39**(17): p. 1098-1101.

3. Shirakawa, H., et al., *Synthesis of electrically conducting organic polymers: halogen derivatives of polyacetylene, (CH).* Journal of the Chemical Society, Chemical Communications, 1977(16): p. 578-580.

4. Pron, A. and M. Leclerc, *Imide/amide based π-conjugated polymers for organic electronics.* Progress in Polymer Science, 2013. **38**(12): p. 1815-1831.

5. Rasmussen, S.C. and S.J. Evenson, *Dithieno[3,2-b:2',3'-d]pyrrole-based materials: Synthesis and application to organic electronics.* Progress in Polymer Science, 2013. **38**(12): p. 1773-1804.

6. Scharber, M.C. and N.S. Sariciftci, *Efficiency of bulk-heterojunction organic solar cells.* Progress in Polymer Science, 2013. **38**(12): p. 1929-1940.

7. Zhao, Y., Y. Guo, and Y. Liu, *25th Anniversary Article: Recent Advances in n-Type and Ambipolar Organic Field-Effect Transistors.* Advanced Materials, 2013. **25**(38): p. 5372-5391.

8. Abdulrazzaq, O.A., et al., *Organic Solar Cells: A Review of Materials, Limitations, and Possibilities for Improvement.* Particulate Science and Technology, 2013. **31**(5): p. 427-442.

9. Barford, W., *Excitons in Conjugated Polymers: A Tale of Two Particles.* The Journal of Physical Chemistry A, 2013. **117**(13): p. 2665-2671.

10. Carr, J.A. and S. Chaudhary, *The identification, characterization and mitigation of defect states in organic photovoltaic devices: a review and outlook.* Energy & Environmental Science, 2013. **6**(12): p. 3414-3438.

11. Gao, F., S. Ren, and J. Wang, *The renaissance of hybrid solar cells: progresses, challenges, and perspectives.* Energy & Environmental Science, 2013. **6**(7): p. 2020-2040.

12. Yassar, A., et al., *Rod–coil and all-conjugated block copolymers for photovoltaic applications.* Progress in Polymer Science, 2013. **38**(5): p. 791-844.

13. Coughlin, J.E., et al., *Design and Synthesis of Molecular Donors for Solution-Processed High-Efficiency Organic Solar Cells.* Accounts of Chemical Research, 2013. **47**(1): p. 257-270.

14. Guo, X., M. Baumgarten, and K. Müllen, *Designing π-conjugated polymers for organic electronics.* Progress in Polymer Science, 2013. **38**(12): p. 1832-1908.

15. Song, Z. and H. Zhou, *Towards sustainable and versatile energy storage devices: an overview of organic electrode materials.* Energy & Environmental Science, 2013. **6**(8): p. 2280-2301.

16. You, J., et al., *Recent trends in polymer tandem solar cells research.* Progress in Polymer Science, 2013. **38**(12): p. 1909-1928.

17. Mercier, L.G. and M. Leclerc, *Direct (Hetero)Arylation: A New Tool for Polymer Chemists.* Accounts of Chemical Research, 2013. **46**(7): p. 1597-1605.

18. Myers, J.D. and J. Xue, *Organic Semiconductors and their Applications in Photovoltaic Devices.* Polymer Reviews, 2012. **52**(1): p. 1-37.

19. Xie, L.-H., et al., *Fluorene-based macromolecular nanostructures and nanomaterials for organic (opto)electronics.* Philosophical Transactions of the Royal Society A: Mathematical, Physical and Engineering Sciences, 2013. **371**(2000).

20. Bryan, Z.J. and A.J. McNeil, *Conjugated Polymer Synthesis via Catalyst-Transfer Polycondensation (CTP): Mechanism, Scope, and Applications.* Macromolecules, 2013. **46**(21): p. 8395-8405.

21. Loewe, R.S., S.M. Khersonsky, and R.D. McCullough, *A Simple Method to Prepare Head-to-Tail Coupled, Regioregular Poly(3-alkylthiophenes) Using Grignard Metathesis.* Advanced Materials, 1999. **11**(3): p. 250-253.

22. Sheina, E.E., et al., *Chain Growth Mechanism for Regioregular Nickel-Initiated Cross-Coupling Polymerizations.* Macromolecules, 2004. **37**(10): p. 3526-3528.

23. Miyakoshi, R., A. Yokoyama, and T. Yokozawa, *Synthesis of Poly(3-hexylthiophene) with a Narrower Polydispersity.* Macromolecular Rapid Communications, 2004. **25**(19): p. 1663-1666.

24. Fechtenkotter, A.F., R. H.; MacKenzie, J. D.; Moons, E.; Mullen, K.; Schmidt-Mende, L., *Self-organized discotic liquid crystals for high-efficiency organic photovoltaics.* Science, 2001. **293**: p. 1119-1122.

25. Granstrom, M.P., K.; Arias, A. C.; Lux, A.; Anderson, M. R.; Friend, R. H., *Laminated fabrication of polymeric photovoltaic devices.* Nature, 1998. **395**: p. 257-260.

26. Coakley, K.M. and M.D. McGehee, *Conjugated Polymer Photovoltaic Cells.* Chemistry of Materials, 2004. **16**(23): p. 4533-4542.

27. Sandberg, H.G.O., et al., *Ultrathin Regioregular Poly(3-hexyl thiophene) Field-Effect Transistors.* Langmuir, 2002. **18**(26): p. 10176-10182.

28. Yang, H., et al., *Effect of Mesoscale Crystalline Structure on the Field-Effect Mobility of Regioregular Poly(3-hexyl thiophene) in Thin-Film Transistors.* Advanced Functional Materials, 2005. **15**(4): p. 671-676.

29. Sirringhaus, H., et al., *Microstructure–mobility correlation in self-organised, conjugated polymer field-effect transistors.* Synthetic Metals, 2000. **111–112**(0): p. 129-132.

30. Liu, J., et al., *Oriented Poly(3-hexylthiophene) Nanofibril with the π−π Stacking Growth Direction by Solvent Directional Evaporation.* Langmuir, 2011. **27**(7): p. 4212-4219.

31. Bernardi, M., M. Giulianini, and J.C. Grossman, *Self-Assembly and Its Impact on Interfacial Charge Transfer in Carbon Nanotube/P3HT Solar Cells.* ACS Nano, 2010. **4**(11): p. 6599-6606.

32. Yokoyama, A., R. Miyakoshi, and T. Yokozawa, *Chain-Growth Polymerization for Poly(3-hexylthiophene) with a Defined Molecular Weight and a Low Polydispersity.* Macromolecules, 2004. **37**(4): p. 1169-1171.

33. Iovu, M.C., et al., *Experimental Evidence for the Quasi-"Living" Nature of the Grignard Metathesis Method for the Synthesis of Regioregular Poly(3-alkylthiophenes).* Macromolecules, 2005. **38**(21): p. 8649-8656.

34. Wu, Z.-Q., et al., *One pot synthesis of a poly(3-hexylthiophene)-b-poly(quinoxaline-2,3-diyl) rod-rod diblock copolymer and its tunable light emission properties.* Polymer Chemistry, 2013. **4**(17): p. 4588-4595.

35. Wu, Z.-Q., et al., *Synthesis of conjugated diblock copolymers: two mechanistically distinct, sequential living polymerizations using a single catalyst.* Polymer Chemistry, 2012. **3**(4): p. 874-881.

36. Tamba, S., et al., *Nickel-catalyzed Dehydrobrominative Polycondensation for the Practical Preparation of Regioregular Poly(3-substituted thiophene)s.* Chemistry Letters, 2011. **40**(4): p. 398-399.

37. Tamba, S., et al., *Synthesis of High-molecular-weight Head-to-tail-type Poly(3-substituted-thiophene)s by Cross-coupling Polycondensation with [CpNiCl(NHC)] as a Catalyst.* Chemistry Letters, 2013. **42**(3): p. 281-283.

38. Ballantyne, A.M., et al., *The Effect of Poly(3-hexylthiophene) Molecular Weight on Charge Transport and the Performance of Polymer:Fullerene Solar Cells.* Advanced Functional Materials, 2008. **18**(16): p. 2373-2380.

39. Brinkmann, M. and P. Rannou, *Effect of Molecular Weight on the Structure and Morphology of Oriented Thin Films of Regioregular Poly(3-hexylthiophene) Grown by Directional Epitaxial Solidification.* Advanced Functional Materials, 2007. **17**(1): p. 101-108.

40. Brinkmann, M. and P. Rannou, *Molecular Weight Dependence of Chain Packing and Semicrystalline Structure in Oriented Films of Regioregular Poly(3-hexylthiophene) Revealed by High-Resolution Transmission Electron Microscopy*. Macromolecules, 2009. **42**(4): p. 1125-1130.

41. Dante, M., J. Peet, and T.-Q. Nguyen, *Nanoscale Charge Transport and Internal Structure of Bulk Heterojunction Conjugated Polymer/Fullerene Solar Cells by Scanning Probe Microscopy*. The Journal of Physical Chemistry C, 2008. **112**(18): p. 7241-7249.

42. Halls, J.J.M., et al., *Efficient photodiodes from interpenetrating polymer networks.* Nature, 1995. **376**(6540): p. 498-500.

43. Kline, R.J., et al., *Controlling the Field-Effect Mobility of Regioregular Polythiophene by Changing the Molecular Weight.* Advanced Materials, 2003. **15**(18): p. 1519-1522.

44. Kline, R.J., et al., *Dependence of Regioregular Poly(3-hexylthiophene) Film Morphology and Field-Effect Mobility on Molecular Weight.* Macromolecules, 2005. **38**(8): p. 3312-3319.

45. Ma, W., et al., *Effect of the Molecular Weight of Poly(3-hexylthiophene) on the Morphology and Performance of Polymer Bulk Heterojunction Solar Cells.* Macromolecular Rapid Communications, 2007. **28**(17): p. 1776-1780.

46. Nicolet, C., et al., *Optimization of the Bulk Heterojunction Composition for Enhanced Photovoltaic Properties: Correlation between the Molecular Weight of the Semiconducting Polymer and Device Performance.* The Journal of Physical Chemistry B, 2011. **115**(44): p. 12717-12727.

47. Schilinsky, P., et al., *Influence of the Molecular Weight of Poly(3-hexylthiophene) on the Performance of Bulk Heterojunction Solar Cells.* Chemistry of Materials, 2005. **17**(8): p. 2175-2180.

48. Sirringhaus, H. and P.J. Brown, *Two-dimensional charge transport in self-organized, high-mobility conjugated polymers.* Nature, 1999. **401**(6754): p. 685.

49. Turner, S.T., et al., *Quantitative Analysis of Bulk Heterojunction Films Using Linear Absorption Spectroscopy and Solar Cell Performance.* Advanced Functional Materials, 2011. **21**(24): p. 4640-4652.

50. Virkar, A.A., et al., *Organic Semiconductor Growth and Morphology Considerations for Organic Thin-Film Transistors.* Advanced Materials, 2010. **22**(34): p. 3857-3875.

51. Yang, X., et al., *Nanoscale Morphology of High-Performance Polymer Solar Cells.* Nano Letters, 2005. **5**(4): p. 579-583.

52. Zen, A., et al., *Effect of Molecular Weight and Annealing of Poly(3-hexylthiophene)s on the Performance of Organic Field-Effect Transistors.* Advanced Functional Materials, 2004. **14**(8): p. 757-764.

53. Iovu, M.C.J.-e., M.; Sheina, E. E.; Cooper, J. R.; McCullough, R. D., *Regioregular poly(3-alkylthiophene) conducting block copolymers.* Polymer, 2005. **46**(19): p. 8582-8586.

54. Dai, C.-A., et al., *Facile Synthesis of Well-Defined Block Copolymers Containing Regioregular Poly(3-hexyl thiophene) via Anionic Macroinitiation Method and Their Self-Assembly Behavior*. Journal of the American Chemical Society, 2007. **129**(36): p. 11036-11038.

55. Yang, H., et al., *Insights into poly(3-hexylthiophene)-b-poly(ethylene oxide) block copolymer: Synthesis and solvent-induced structure formation in thin films.* Journal of Polymer Science Part A: Polymer Chemistry, 2012. **50**(24): p. 5060-5067.

56. Iovu, M.C., et al., *Conducting Block Copolymer Nanowires Containing Regioregular Poly(3-Hexylthiophene) and Polystyrene.* Journal of Macromolecular Science: Pure & Applied Chemistry, 2006. **43**(12): p. 1991-2000.

57. Liu, J., R.S. Loewe, and R.D. McCullough, *Employing MALDI-MS on Poly(alkylthiophenes): Analysis of Molecular Weights, Molecular Weight Distributions, End-Group Structures, and End-Group Modifications.* Macromolecules, 1999. **32**(18): p. 5777-5785.

58. Chen, P.-Y., et al., *Conformation and Fluorescence Property of Poly(3-hexylthiophene) Isolated Chains Studied by Single Molecule Spectroscopy: Effects of Solvent Quality and Regioregularity.* Macromolecules, 2013. **46**(14): p. 5657-5663.

59. Sivula, K., et al., *Enhancing the Thermal Stability of Polythiophene:Fullerene Solar Cells by Decreasing Effective Polymer Regioregularity.* Journal of the American Chemical Society, 2006. **128**(43): p. 13988-13989.

60. Aiyar, A.R., et al., *Ultrasound-Induced Ordering in Poly(3-hexylthiophene): Role of Molecular and Process Parameters on Morphology and Charge Transport.* ACS Applied Materials & Interfaces, 2013. **5**(7): p. 2368-2377.

61. Aiyar, A.R., J.-I. Hong, and E. Reichmanis, *Regioregularity and Intrachain Ordering: Impact on the Nanostructure and Charge Transport in Two-Dimensional Assemblies of Poly(3-hexylthiophene).* Chemistry of Materials, 2012. **24**(15): p. 2845-2853.

62. Andrey, E.R., A.L. Alia, and C.T. Barry, *Influence of β-linkages on the morphology and performance of DArP P3HT–PC 61 BM solar cells.* Nanotechnology, 2014. **25**(1): p. 014005.

63. Ates, M., *A review study of (bio)sensor systems based on conducting polymers.* Materials Science and Engineering: C, 2013. **33**(4): p. 1853-1859.

64. Kim, Y., et al., *A strong regioregularity effect in self-organizing conjugated polymer films and high-efficiency polythiophene:fullerene solar cells.* Nat Mater, 2006. **5**(3): p. 197-203.

65. Singh, C.R., et al., *Correlation of charge transport with structural order in highly ordered melt-crystallized poly(3-hexylthiophene) thin films.* Journal of Polymer Science Part B: Polymer Physics, 2013. **51**(12): p. 943-951.

66. Sirringhaus, H., and Richard H. Friend, *Integrated optoelectronic devices based on conjugated polymers.* Science, 1998. **280**.

67. Sivaraman, P., et al., *Effect of regioregularity on specific capacitance of poly(3-hexylthiophene).* Electrochimica Acta, 2012. **69**(0): p. 134-138.

68. Woo, C.H., et al., *The Influence of Poly(3-hexylthiophene) Regioregularity on Fullerene-Composite Solar Cell Performance.* Journal of the American Chemical Society, 2008. **130**(48): p. 16324-16329.

69. Adachi, T., et al., *Regioregularity and Single Polythiophene Chain Conformation.* The Journal of Physical Chemistry Letters, 2011. **2**(12): p. 1400-1404.

70. Bolinger, J.C., et al., *Conformation and Energy Transfer in Single Conjugated Polymers.* Accounts of Chemical Research, 2012. **45**(11): p. 1992-2001.

71. Poelking, C. and D. Andrienko, *Effect of Polymorphism, Regioregularity and Paracrystallinity on Charge Transport in Poly(3-hexylthiophene) [P3HT] Nanofibers.* Macromolecules, 2013. **46**(22): p. 8941-8956.

72. Urien, M., et al., *Effect of the regioregularity of poly(3-hexylthiophene) on the performances of organic photovoltaic devices.* Polymer International, 2008. **57**(5): p. 764-769.

73. Tsoi, W.C., et al., *Effect of Crystallization on the Electronic Energy Levels and Thin Film Morphology of P3HT:PCBM Blends.* Macromolecules, 2011. **44**(8): p. 2944-2952.

74. Li, G., R. Zhu, and Y. Yang, *Polymer solar cells.* Nat Photon, 2012. **6**(3): p. 153-161.

75. Thompson, B.C.K., P. P.; Burkhard, B.; Avilies, A. E.; Rudenko, A.; Shultz, G. V.; Ng, C. F.; Mangubat, L. B, *Polymer-based solar cells: state-of-the-art principles for the design of active layer components.* Green, 2011. **1**: p. 29-54.

76. Huang, Y.C., H.; Han, C. C., *Temperature induced structure evolution of regioregular poly(3-hexylthiophene) in dilute solution and its influence on thin film morphology.* Macromolecules, 2010. **43**: p. 10031-10037.

77. Peng, Q., et al., *Influence of molecular weight on the spectroscopic properties of a series of well-defined poly(3-hexylthiophene) polymers.* Canadian Journal of Chemistry, 2010. **89**(1): p. 27-33.

78. Gettinger, C.L.H., A. J.; Drake, J. M.; Pine, D. J, *A photoluminescence study of poly(phenylene vinylene) derivatives: The effect of intrinsic persistence length.* Journal of Chemical Physics, 1994. **101**.

79. Gallazzi, M.C., F. Toscano, and E. Montoneri, *Chromic effects and molecular weight in poly(3-alkylthiophenes).* Journal of Materials Science Letters, 1999. **18**(12): p. 971-973.

80. De Wit, M., et al., *Mark-Houwink-Sakurada Constants for the Methoxy Precursor of Poly(2,5-thienylenevinylene).* Macromolecules, 1995. **28**(14): p. 5144-5146.

81. Huang, Y., H. Cheng, and C.C. Han, *Unimer–Aggregate Equilibrium to Large Scale Association of Regioregular Poly(3-hexylthiophene) in THF Solution.* Macromolecules, 2011. **44**(12): p. 5020-5026.

82. Heffner, G.W., D.S. Pearson, and C.L. Gettinger, *Characterization of poly(3-octylthiophene). I: Molecular characterization in dilute solution.* Polymer Engineering & Science, 1995. **35**(10): p. 860-867.

83. Yue, S.B., G. C.; McCullough, R. D, *Intermolecular association and supramolecular organization in dilute solution. 1. Regioregular poly(3-dodecylthiophene).* Macromolecules, 1996. **29**: p. 933-939.

84. Heffner, G.W., W.E. Rochefort, and D.S. Pearson, *Characterization of poly(3-octylthiophene). II: Melt rheological characterization.* Polymer Engineering & Science, 1995. **35**(10): p. 868-875.

85. Shibaev, P.V.S., K.; Bjornholm, T.; Norgaard, K, *Conformation of polythiophene derivatives in solution.* Synthetic Metals, 1998. **97**: p. 97-104.

86. Xu, W.L., L.; Tang, H.; Li, H.; Zhao, X.; Yang, X, *Solvent-induced crystallization of poly(3-dodecylthiophenes): Morphology and kinetics.* Journal of Physical Chemistry B, 2011. **115**: p. 6412-6420.

87. Zhao, L.P., R.; Zhuo, J.; Wong, L.; Tang, J.; Su, Y.; Chua, L., *Role of borderline solvents to induce pronounced etended-chain lamellar order in pi-stackable polymers.* Macromolecules, 2011. **44**: p. 9692-9702.

88. Holdcroft, S., *Determination of molecular weights and Mark–Houwink constants for soluble electronically conducting polymers.* Journal of Polymer Science Part B: Polymer Physics, 1991. **29**(13): p. 1585-1588.

89. Heffner, G.W. and D.S. Pearson, *Molecular characterization of poly(3-hexylthiophene).* Macromolecules, 1991. **24**(23): p. 6295-6299.

90. Hiemenz, P.C.L., T. P., *Polymer Chemistry*. 2 ed. 2007, Boca Raton, FL: CRC Press.

91. Grubisic, Z., P. Rempp, and H. Benoit, *A universal calibration for gel permeation chromatography.* Journal of Polymer Science Part B: Polymer Letters, 1967. **5**(9): p. 753-759.

92. Tkachov, R., et al., *Random Catalyst Walking along Polymerized Poly(3-hexylthiophene) Chains in Kumada Catalyst-Transfer Polycondensation.* Journal of the American Chemical Society, 2010. **132**(22): p. 7803-7810.

93. Antoun, T., et al., *A Simple Route to Rod-Coil Block Copolymers of Oligo- and Polythiophenes with PMMA and Polystyrene.* Macromolecular Chemistry and Physics, 2011. **212**(11): p. 1129-1136.

94. Awada, H., et al., *Versatile functional poly(3-hexylthiophene) for hybrid particles synthesis by the grafting onto technique: Core@shell ZnO nanorods.* Journal of Polymer Science Part A: Polymer Chemistry, 2014. **52**(1): p. 30-38.

95. Boon, F., et al., *Synthesis and Characterization of Nanocomposites Based on Functional Regioregular Poly(3-hexylthiophene) and Multiwall Carbon Nanotubes.* Macromolecular Rapid Communications, 2010. **31**(16): p. 1427-1434.

96. Boon, F., et al., *Synthesis and characterization of carboxystyryl end-functionalized poly(3-hexylthiophene)/TiO2 hybrids in view of photovoltaic applications.* Synthetic Metals, 2012. **162**(17–18): p. 1615-1622.

97. Boudouris, B.W., et al., *Synthesis, Optical Properties, and Microstructure of a Fullerene-Terminated Poly(3-hexylthiophene).* Macromolecules, 2009. **42**(12): p. 4118-4126.

98. Britze, A., et al., *Synthesis of Blockcopolymers P3HT-b-PS Using a Combination of Grignard-Metathesis and Nitroxide-Mediated Radical Polymerization.* Macromolecular Chemistry and Physics, 2011. **212**(7): p. 679-690.

99. Campo, B.J., et al., *Ester-functionalized poly(3-alkylthiophene) copolymers: Synthesis, physicochemical characterization and performance in bulk heterojunction organic solar cells.* Organic Electronics, 2013. **14**(2): p. 523-534.

100. Chen, Y.-H., et al., *Stabilization of poly(3-hexylthiophene)/PCBM morphology by hydroxyl group end-functionalized P3HT and its application to polymer solar cells.* Organic Electronics, 2012. **13**(2): p. 283-289.

101. Fujita, H., et al., *Synthesis and Postfunctionalization of Rod–Coil Diblock and Coil–Rod–Coil Triblock Copolymers Composed of Poly(3-hexylthiophene) and Poly(4-(4'-N,N-dihexylaminophenylethynyl)styrene) Segments.* Macromolecules, 2012. **45**(24): p. 9643-9656.

102. Hiorns, R.C., et al., *Extremely regio-regular poly (3-alkylthiophene)s from simplified chain-growth Grignard metathesis polymerisations and the modification of their chain-ends.* Polymer International, 2006. **55**(6): p. 608-620.

103. Alves, N.M. and J.F. Mano, *Chitosan derivatives obtained by chemical modifications for biomedical and environmental applications.* International Journal of Biological Macromolecules, 2008. **43**(5): p. 401-414.

104. Kang, S., R.J. Ono, and C.W. Bielawski, *Synthesis of poly(3-hexylthiophene)-block-poly(ethylene)-block-poly(3-hexylthiophene) via a combination of ring-opening olefin metathesis polymerization and grignard metathesis polymerization.* Journal of Polymer Science Part A: Polymer Chemistry, 2013. **51**(18): p. 3810-3817.

105. Kim, H.J., et al., *Molecular Design of "Graft" Assembly for Ordered Microphase Separation of P3HT-Based Rod–Coil Copolymers.* Macromolecules, 2013. **46**(21): p. 8472-8478.

106. Kim, H.-J., et al., *Synthesis of multiarmed poly(3-hexyl thiophene) star polymer with microgel core by GRIM and ATRP methods.* Journal of Polymer Science Part A: Polymer Chemistry, 2011. **49**(19): p. 4221-4226.

107. Kim, J.S., et al., *High-Efficiency Organic Solar Cells Based on End-Functional-Group-Modified Poly(3-hexylthiophene).* Advanced Materials, 2010. **22**(12): p. 1355-1360.

108. Kim, Y., et al., *Effect of the End Group of Regioregular Poly(3-hexylthiophene) Polymers on the Performance of Polymer/Fullerene Solar Cells.* The Journal of Physical Chemistry C, 2007. **111**(23): p. 8137-8141.

109. Kochemba, W.M., S.M. Kilbey, and D.L. Pickel, *End-group composition of poly(3-hexylthiophene)s prepared by in situ quenching of the grignard metathesis polymerization: Influence of additives and reaction conditions.* Journal of Polymer Science Part A: Polymer Chemistry, 2012. **50**(14): p. 2762-2769.

110. Kochemba, W.M., et al., *In Situ Formation of Pyridyl-Functionalized Poly(3-hexylthiophene)s via Quenching of the Grignard Metathesis Polymerization: Toward*

Ligands for Semiconductor Quantum Dots. Chemistry of Materials, 2012. **24**(22): p. 4459-4467.

111. Krüger, R.A., et al., *End-Group Functionalization of Poly(3-hexylthiophene) as an Efficient Route to Photosensitize Nanocrystalline TiO2 Films for Photovoltaic Applications.* ACS Applied Materials & Interfaces, 2011. **3**(6): p. 2031-2041.

112. Lee, J.U., et al., *Synthesis and photophysical property of well-defined donor-acceptor diblock copolymer based on regioregular poly(3-hexylthiophene) and fullerene.* Journal of Materials Chemistry, 2009. **19**(10): p. 1483-1489.

113. Lee, Y.-H., et al., *Self-assembly and phase transformations of [small pi]-conjugated block copolymers that bend and twist: from rigid-rod nanowires to highly curvaceous gyroids.* Soft Matter, 2011. **7**(21): p. 10429-10442.

114. Lim, H., et al., *Facile syntheses, morphologies, and optical absorptions of P3HT coil-rod-coil triblock copolymers.* Journal of Polymer Science Part A: Polymer Chemistry, 2010. **48**(15): p. 3311-3322.

115. Lohwasser, R.H., J. Bandara, and M. Thelakkat, *Tailor-made synthesis of poly(3-hexylthiophene) with carboxylic end groups and its application as a polymer sensitizer in solid-state dye-sensitized solar cells.* Journal of Materials Chemistry, 2009. **19**(24): p. 4126-4130.

116. Lohwasser, R.H. and M. Thelakkat, *Toward Perfect Control of End Groups and Polydispersity in Poly(3-hexylthiophene) via Catalyst Transfer Polymerization.* Macromolecules, 2011. **44**(9): p. 3388-3397.

117. Lohwasser, R.H. and M. Thelakkat, *Synthesis of Amphiphilic Rod–Coil P3HT-b-P4VP Carrying a Long Conjugated Block Using NMRP and Click Chemistry*. Macromolecules, 2012. **45**(7): p. 3070-3077.

118. Lohwasser, R.H. and M. Thelakkat, *Synthesis and Characterization of Monocarboxylated Poly(3-hexylthiophene)s via Quantitative End-Group Functionalization.* Macromolecules, 2010. **43**(18): p. 7611-7616.

119. Mao, Z., et al., *Synthesis of Perfluoroalkyl End-Functionalized Poly(3-hexylthiophene) and the Effect of Fluorinated End Groups on Solar Cell Performance*. Macromolecules, 2012. **46**(1): p. 103-112.

120. Miyakoshi, R., A. Yokoyama, and T. Yokozawa, *Catalyst-Transfer Polycondensation. Mechanism of Ni-Catalyzed Chain-Growth Polymerization Leading to Well-Defined Poly(3-hexylthiophene).* Journal of the American Chemical Society, 2005. **127**(49): p. 17542-17547.

121. Monnaie, F., et al., *Synthesis of End-Group Functionalized P3HT: General Protocol for P3HT/Nanoparticle Hybrids.* Macromolecules, 2013. **46**(21): p. 8500-8508.

122. Moon, H.C., et al., *Facile Synthetic Route for Well-Defined Poly(3-hexylthiophene)-block-poly(methyl methacrylate) Copolymer by Anionic Coupling Reaction.* Macromolecules, 2011. **44**(7): p. 1894-1899.

123. Moon, H.C., et al., *Facile Synthesis of Well-Defined Coil−Rod−Coil Block Copolymer Composed of Regioregular Poly(3-hexylthiophene) via Anionic Coupling Reaction.* Macromolecules, 2010. **43**(4): p. 1747-1752.

124. Mougnier, S.-J., et al., *Design of Well-Defined Monofunctionalized Poly(3-hexylthiophene)s: Toward the Synthesis of Semiconducting Graft Copolymers.* Macromolecular Rapid Communications, 2012. **33**(8): p. 703-709.

125. Mougnier, S.-J., et al., *Facile and versatile synthesis of rod-coil poly(3-hexylthiophene)-based block copolymers by nitroxide-mediated radical polymerization.* Journal of Polymer Science Part A: Polymer Chemistry, 2012. **50**(12): p. 2463-2470.

126. Ouhib, F.D., S.; Lazzaroni, R.; De Winter, J.; Gerbaux, P.; Jerome, C.; Detrembleur, C., *Thermally induced coupling of poly(thiophene)-based block copolymers prepared by Grignard metathesis polymerization: a straightforward route toward highly regioregular multiblock conjugated copolymers.* Macromolecules, 2012. **45**(17): p. 6796-6806.

127. Park, J., H.C. Moon, and J.K. Kim, *Facile synthesis for well-defined A2B miktoarm star copolymer of poly(3-hexylthiophene) and poly(methyl methacrylate) by the combination of anionic polymerization and click reaction.* Journal of Polymer Science Part A: Polymer Chemistry, 2013. **51**(10): p. 2225-2232.

128. Rashid, M.D.H.-O., et al., *Synthesis and self-assembly of diblock copolymers composed of poly(3-hexylthiophene) and poly(fluorooctyl methacrylate) segments.* Journal of Polymer Science Part A: Polymer Chemistry, 2011. **49**(21): p. 4680-4686.

129. Rudenko, A.E., et al., *Optimization of direct arylation polymerization conditions for the synthesis of poly(3-hexylthiophene).* Journal of Polymer Science Part A: Polymer Chemistry, 2013. **51**(12): p. 2660-2668.

130. Smith, K.A., et al., *Synthesis and Crystallinity of Conjugated Block Copolymers Prepared by Click Chemistry.* Macromolecules, 2013. **46**(7): p. 2636-2645.

131. Tu, G., et al., *Conjugated Triblock Copolymers Containing Both Electron-Donor and Electron-Acceptor Blocks.* Macromolecules, 2006. **39**(13): p. 4327-4331.

132. Urien, M., et al., *Poly(3-hexylthiophene) Based Block Copolymers Prepared by "Click" Chemistry.* Macromolecules, 2008. **41**(19): p. 7033-7040.

133. Wang, J., et al., *Synthesis and Characterization of All-Conjugated Graft Copolymers Comprised of n-Type or p-Type Backbones and Poly(3-hexylthiophene) Side Chains.* Macromolecules, 2013. **46**(5): p. 1783-1793.

134. Wang, J., M. Ueda, and T. Higashihara, *Synthesis of All-Conjugated Donor–Acceptor–Donor ABA-Type Triblock Copolymers via Kumada Catalyst-Transfer Polycondensation.* ACS Macro Letters, 2013. **2**(6): p. 506-510.

135. Wu, Z.-Q., et al., *One-pot synthesis of conjugated poly(3-hexylthiophene)-b-poly(phenyl isocyanide) hybrid rod–rod block copolymers and its self-assembling properties.* Journal of Polymer Science Part A: Polymer Chemistry, 2013. **51**(13): p. 2939-2947.

136. Yokozawa, T., et al., *Precision Synthesis of Poly(3-hexylthiophene) from Catalyst-Transfer Suzuki−Miyaura Coupling Polymerization.* Macromolecular Rapid Communications, 2011. **32**(11): p. 801-806.

137. Yokozawa, T.N., Y.; Kohno, H.; Suzuki, R.; Nojima, M.; Ohta, Y, *Catalyst-transfer condensation polymerization for precision synthesis of pi-conjugated polymers.* Pure and Applied Chemistry, 2013. **85**(3): p. 573-587.

138. Yu, D., et al., *Soluble P3HT-Grafted Graphene for Efficient Bilayer−Heterojunction Photovoltaic Devices.* ACS Nano, 2010. **4**(10): p. 5633-5640.

139. Yuan, M., et al., *Constructing Regioregular Star Poly(3-hexylthiophene) via Externally Initiated Kumada Catalyst-Transfer Polycondensation.* ACS Macro Letters, 2012. **1**(3): p. 392-395.

140. Enders, C., S. Tanner, and W.H. Binder, *End-Group Telechelic Oligo- and Polythiophenes by "Click" Reactions: Synthesis and Analysis via LC-ESI-TOF MS.* Macromolecules, 2010. **43**(20): p. 8436-8446.

141. Miyaura, N.S., A., *Stereoselective synthesis of arylated (E)-alkenes by the reaction of alk-1-enylboranes with aryl halides in the presence of palladium catalyst.* Chemical Communications, 1979. **19**: p. 866-867.

142. Miyaura, N.Y., K.; Suzuki, A., *A new stereospecific cross-coupling by the palladium-catalyzed reaction of 1-alkenylboranes with 1-alkenyl or 1-alkynyl halides.* Tetrahedron Letters, 1979. **20**(36): p. 3437-3440.

143. Li, W., et al., *Tris[tri(2-thienyl)phosphine]palladium as the catalyst precursor for thiophene-based Suzuki-Miyaura crosscoupling and polycondensation.* Journal of Polymer Science Part A: Polymer Chemistry, 2008. **46**(13): p. 4556-4563.

144. Sommer, M., et al., *Synthesis, Purification, and Characterization of Well-Defined All-Conjugated Diblock Copolymers PF8TBT-b-P3HT.* Macromolecules, 2012. **45**(10): p. 4142-4151.

145. Janietz, S., et al., *Tailoring of Low Bandgap Polymer and its Performance Analysis in Organic Solar Cells.* Macromolecular Chemistry and Physics, 2009. **210**(18): p. 1493-1503.

146. Gu, Z., et al., *Annealing effect on performance and morphology of photovoltaic devices based on poly(3-hexylthiophene)-b-poly(ethylene oxide).* Journal of Polymer Science Part A: Polymer Chemistry, 2011. **49**(12): p. 2645-2652.

147. Gu, Z.T., Y.; Tsuchiya, K.; Shimomura, T.; Ogino, K., *Synthesis and characterization of poly(3-hexylthiophene)-b-polystyrene for photovoltaic application.* Polymers, 2011. **3**(1): p. 558-570.

148. Nehls, B.S., et al., *Semiconducting Polymers via Microwave-Assisted Suzuki and Stille Cross-Coupling Reactions.* Advanced Functional Materials, 2004. **14**(4): p. 352-356.

149. Wang, C., et al., *Oligo(3-hexylthiophene)-functionalized dicyano-ethylene substituted quinacridone derivatives: synthesis, characterizations and applications as acceptors in photovoltaic devices.* New Journal of Chemistry, 2012. **36**(9): p. 1788-1797.

150. Beyer, F.L., et al., *Morphological behavior of A2B2 star block copolymers.* Journal of Polymer Science Part B: Polymer Physics, 1999. **37**(24): p. 3392-3400.

151. Dyer, C., et al., *Effect of Macromolecular Architecture on the Morphology of Polystyrene–Polyisoprene Block Copolymers.* Macromolecules, 2013. **46**(5): p. 2023-2031.

152. Lee, C., et al., *Asymmetric Single Graft Block Copolymers: Effect of Molecular Architecture on Morphology.* Macromolecules, 1997. **30**(13): p. 3732-3738.

153. Milner, S.T., *Chain architecture and asymmetry in copolymer microphases.* Macromolecules, 1994. **27**: p. 2333-2335.

154. Adhikari, R. and G.H. Michler, *Influence of molecular architecture on morphology and micromechanical behavior of styrene/butadiene block copolymer systems.* Progress in Polymer Science, 2004. **29**(9): p. 949-986.

155. Rajeev, K., et al., *Morphology diagrams for A 2 B copolymer melts: real-space self-consistent field theory*. Journal of Physics: Conference Series, 2012. **402**(1): p. 012042.

156. Zhu, Y., et al., *Morphology and Tensile Properties of Multigraft Copolymers with Regularly Spaced Tri-, Tetra-, and Hexafunctional Junction Points.* Macromolecules, 2006. **39**(13): p. 4428-4436.

157. Matsen, M.W. and F.S. Bates, *Unifying Weak- and Strong-Segregation Block Copolymer Theories*. Macromolecules, 1996. **29**(4): p. 1091-1098.

158. Bates, F.S.F., G. H., *Block Copolymers - Designer Soft Materials.* Physics Today, 1999. **52**(2): p. 32-38.

159. Khandpur, A.K., et al., *Polyisoprene-Polystyrene Diblock Copolymer Phase Diagram near the Order-Disorder Transition.* Macromolecules, 1995. **28**(26): p. 8796-8806.

VITA

Justin Taylor Roop was born on May 2nd 1979 in Knoxville, Tennessee. He grew up just north of the city in the Claxton Community of Anderson County. In May of 1997 he graduated from Clinton High School. After several years in the "real world", he returned to the classroom in August of 2004 to pursue his Bachelor's degree in Chemistry. On October 16, 2004 he married his loving and supportive wife, Tiffani. In May of 2009 Justin graduated with an ACS-certified B.S. in Chemistry from the University of Tennessee. After an internship at the National Transportation Research Center under the mentorship of Dr. Todd Toops, Justin joined the graduate program at UT to pursue his doctorate in Polymer Chemistry under the direction of Dr. Jimmy Mays. The following year, in May 2010, Justin and Tiffani welcomed their firstborn son, Nathaniel. They would welcome another son, Samuel, in September of 2012. On April 1, 2014 Justin successfully defended his Ph.D. dissertation